

UNIVERSITÀ DEGLI STUDI DI MILANO

**Scuola di Dottorato in Medicina Molecolare
Curriculum in Genomica, Proteomica e Tecnologie Correlate**

Ciclo XXIV

Anno Accademico: 2010/2011



Dottorando: Elisa FASSONE

**BIOCHEMICAL AND GENETIC
APPROACHES TO UNRAVEL
MITOCHONDRIAL COMPLEX I DEFICIENCY**

Direttore della Scuola: Ch.mo Prof. Mario CLERICI

Tutore: Ch.mo Prof. Giacomo Pietro COMI

Co-Tutore: Ch.ma Dott.ssa Shamima RAHMAN

SOMMARIO

Utilizzando un approccio biochimico e genetico combinato, siamo riusciti ad identificare il difetto genetico alla base del deficit di complesso I mitocondriale in 3 di 12 pazienti nella nostra coorte. I soggetti indagati in questo studio provengono da differenti aree geografiche: Inghilterra, Francia, Medio Oriente, Israele, India e Pakistan. Clinicamente presentano fenotipi differenti: sindrome di Leigh, acidosi lattica congenita, cardiomiopatia ipertrofica, encefalopatia, ritardo dello sviluppo, malattia di Alpers.

Dopo aver escluso la presenza di mutazioni nel DNA mitocondriale estratto da muscolo (analisi effettuata dal laboratorio diagnostico al National Hospital for Neurology, Queen Square, London), i fibroblasti dei pazienti sono stati sottoposti a indagine biochimica che ha confermato il difetto nell'attività del complesso I in tutti i pazienti anche in questo tessuto, inoltre sono state effettuate analisi in Blue Nativo. L'uso di anticorpi diretti verso diverse subunità del complesso I ha evidenziato la presenza di sub-complessi dell'oloenzima da ~1MDa in alcuni pazienti; mentre in altri, sono stati osservati vari livelli di riduzione dell'oloenzima. L'analisi del profilo di migrazione del complesso I su gel Blue Nativi ha indirizzato lo screening genetico verso un gruppo selezionato di geni, già associati a deficit di complesso I. Due pedigree sono stati analizzati su un Affymetrix 10K SNP chip array e analizzati con l'approccio del mappaggio dell'omozigosi, basato sull'ipotesi che gli individui affetti avessero ereditato due copie dello stesso allele ancestrale mutato (autozigosi). Successivamente, un'analisi bioinformatica (con l'implementazione dei database Maestro e MitoCarta) ha permesso la selezione di un gruppo di geni candidati che potessero contenere il difetto genetico, tenendo in considerazione anche i risultati ottenuti dallo studio in Blue Nativo.

Lo screening genetico ha identificato una nuova delezione frameshift di 8bp (c.377_384del; Q126fsX2) nel gene *NDUFS4*, come causa della malattia in un paziente proveniente da una famiglia analizzata mediante mappaggio dell'omozigosi. Sua cugina si è rivelata essere eterozigote per la stessa mutazione, ma nessun altro difetto venne identificato, lasciando questo caso di deficit di complesso I irrisolto. Nel secondo pedigree analizzato mediante mappaggio dell'omozigosi, è stata individuata una mutazione omozigote in un nuovo fattore di assemblaggio del complesso I mai associato in precedenza con malattie nell'uomo. La mutazione c.1054C>T; R352W in *FOXRED1* segregava con il fenotipo nella famiglia e non è stata riscontrata in 268 alleli controllo. L'analisi Western blot ha mostrato una riduzione dei livelli proteici di *FOXRED1* in fibroblasti del paziente e il ripristino dell'attività del complesso I dopo trasduzione con vettori lentivirali mediante il cDNA wild-type di *FOXRED1*. Infine, mediante sequenziamento dei geni candidati, due nuove mutazioni in eterozigosi composta sono state identificate in *NDUFAF1*: c.631C>T; R211C e c.733G>A; G245R.

In sintesi, lo studio ha consentito di identificare difetti genetici in (i) una subunità del complesso I: *NDUFS4*, già associata con deficit di complesso I; (ii) un nuovo fattore di assemblaggio del complesso I: *FOXRED1*; (iii) e di identificare due nuove mutazioni in un altro fattore di assemblaggio: *NDUFAF1*. In conclusione, il nostro approccio combinato si è rivelato efficiente nell'identificazione del difetto genetico in pazienti affetti da deficit di complesso I.

ABSTRACT

Using biochemical and genetic approaches we have been able to identify the genetic defect underlying mitochondrial complex I deficiency in 3 patients out of the 12 patients in the cohort. The patient cohort investigated in this study is genetically heterogeneous, originating from several different geographical areas: England, France, the Middle East, Israel, India and Pakistan. They presented with different clinical phenotypes: Leigh syndrome, congenital lactic acidosis, hypertrophic cardiomyopathy, encephalopathy, developmental delay, Alpers' disease.

After having excluded the mitochondrial DNA molecule for carrying mutations in muscle (analysis carried out by the diagnostic laboratories' staff, at the National Hospital for Neurology, Queen Square, London), a biochemical investigation was undertaken in patients' fibroblasts: the complex I activity defect was confirmed in this tissue as well for all the patients, and Blue Native studies were carried out. Antibodies against several subunits of complex I identified various subassemblies of the ~1MDa holoenzyme in several patients; in some others various degrees of reduction in holo-complex I content were observed. Analysis of the complex I pattern on Blue Native gels led the genetic screening towards a subset of genes, already known to be involved in complex I deficiency.

Two families were also run on the Affymetrix 10K SNP chip array and then a homozygosity mapping approach was undertaken on the assumption that the affected individuals inherited two copies of the same ancestral mutated allele from a common ancestor (autozygosity). A subsequent bioinformatics analysis (also involving the implementation of the Maestro and MitoCarta databases) allowed the selection of a subgroup of genes that could possibly bear the genetic defect; this was done taking into account the Blue Native complex I pattern as well.

Genetic screening identified a novel 8bp frameshift deletion (c.377_384del; Q126fsX2) in the *NDUFS4* gene as cause of the disease in a patient from the first pedigree analyzed by homozygosity mapping. Her cousin was heterozygous for the same defect, but no other mutation has been identified, leaving this complex I deficiency case unsolved. In the second pedigree analyzed by homozygosity mapping approach, a homozygous mutation in a novel complex I assembly factor never previously linked to human disease has been identified. The c.1054C>T; R352W mutation in *FOXRED1* segregated with disease in the family and was not found in 268 healthy control alleles. Western blot analysis showed a reduced steady-state level of FOXRED1 in patient fibroblasts and restoration of complex I activity after lentiviral transduction of patient fibroblasts with wild-type *FOXRED1* cDNA. Finally, by candidate gene sequencing, two novel compound heterozygous mutations in *NDUFAB1* were identified in a third patient: c.631C>T; R211C and c.733G>A; G245R.

In summary, this study allowed the identification of mutations in (i) one complex I subunit, *NDUFS4*, already associated with complex I deficiency; (ii) one novel complex I assembly factor: FOXRED1; (iii) and *NDUFAB1*, a known complex I assembly factor whose mutations give a similar complex I Blue Native pattern to the one observed in our patient. In conclusion our combined approach proved to be efficient in the identification of the genetic defect in patients affected with complex I deficiency.

TABLE of CONTENTS

SOMMARIO..... I

ABSTRACT III

TABLE of CONTENTS..... V

ABBREVIATIONS VIII

1 INTRODUCTION..... 1

1.1 *Mitochondria and Mitochondrial Proteome* 1

1.2 *Mitochondrial Respiratory Chain and Oxidative Phosphorylation System* 1

1.2.1 Complex I: NADH:ubiquinone oxidoreductase..... 2

1.2.2 Complex II: Succinate CoQ Reductase 3

1.2.3 Complex III: Ubiquinol-Cytochrome c Reductase 3

1.2.4 Complex IV: Cytochrome c Oxidase..... 3

1.2.5 Complex V: ATP Synthase 3

1.3 *Biochemical Assessment of Complex I Deficiency*..... 4

1.4 *Complex I Function, Structure and Assembly*..... 4

1.5 *Mitochondrial Disease* 12

1.6 *Genetics of Complex I Deficiency*..... 14

1.6.1 mtDNA mutations 14

1.6.2 Nuclear DNA Subunit Mutations 15

1.6.3 Assembly Factor Mutations..... 15

1.7 *Mouse Models for Nuclear DNA-encoded Mitochondrial Complex I Deficiency* 23

1.7.1 The Harlequin mouse..... 23

1.7.2 The NDUFS4-knock out mouse..... 24

1.8 *Approaches to Treatment of Complex I Deficiency* 25

2 AIM OF THE THESIS 29

3 MATERIALS and METHODS..... 32

3.1 *Patient Cohort*..... 32

3.2 *Cell culture methods*..... 35

3.3 *Biochemical studies*..... 35

3.3.1 Complex I/Complex IV microplate and dipstick assays..... 35

3.3.2 Preparation of crude mitochondrial pellets with digitonin (mitoplasts) 36

3.3.3 Blue Native studies..... 37

3.3.4 Western blot studies 38

3.3.5 Submitochondrial fractionation 38

3.4 Genetic studies	40
3.4.1 DNA and RNA extraction.....	40
3.4.2 Homozygosity Mapping and Bioinformatics analysis.....	41
3.4.3 Sequencing of candidate genes.....	43
3.5 Functional studies	48
3.5.1 Preparation of lentiviral vectors.....	48
3.5.2 Complementation and RNA interference studies.....	49
4 RESULTS	51
4.1 Biochemistry	51
4.1.1 Complex I activity.....	51
4.1.2 Blue Native studies.....	52
4.2 Genetics studies	56
4.2.1 Homozygosity Mapping and Bioinformatics Analysis.....	56
4.2.2 Candidate Gene Approach.....	59
4.3 Functional studies	62
4.3.1 Family 1, Patients 1 and 2: NDUFS4.....	62
4.3.2 Family 4, Patient 5: FOXRED1.....	62
4.3.2.1 <i>Lentiviral-mediated complementation and silencing studies</i> ...	62
4.3.2.2 <i>Western blot analysis</i>	63
4.3.2.3 <i>Subcellular and submitochondrial localization</i>	64
4.3.3 Patient 6: NDUF AF1.....	65
4.3.3.1 <i>Western blot</i>	66
5 DISCUSSION	69
5.1 <i>NDUFS4</i>	69
5.2 <i>FOXRED1</i>	70
5.3 <i>NDUF AF1</i>	72
5.4 <i>Other Patients in the cohort</i>	73
5.5 <i>Complex I assembly</i>	73
6 CONCLUSIONS	79
REFERENCES	82
APPENDIX	102

ABBREVIATIONS

ADP: Adenosine Diphosphate

ATP: Adenosine Triphosphate

BN-PAGE: Blue Native Polyacrylamide Gel Electrophoresis

cAMP: Cyclic Adenosine Monophosphate

cDNA: Complementary Deoxyribonucleic Acid

CI: Complex I

COPP: Complex One Phylogenetic Profile

COX: Cytochrome c Oxidase

CSF: Cerebrospinal Fluid

DD: Developmental Delay

DMEM: Dulbecco's Modified Eagle Medium

ECMO: Extracorporeal Membrane Oxygenation

FAD: Flavin Adenine Dinucleotide

FBS: Fetal Bovine Serum

FMN: Flavin Mononucleotide

GFP: Green Fluorescent Protein

HCM: Hypertrophic Cardiomyopathy

IM: Inner Membrane

IMM: Inner Mitochondrial Membrane

IMS: Intermembrane Space

KO: Knock Out

LA: Lactic Acidosis

LS: Leigh Syndrome

LV: Left Ventricular

M: Matrix

MRI: Magnetic Resonance Imaging

mtDNA: mitochondrial DNA

NADH: Reduced form of the Nicotinamide Adenine Dinucleotide

NADPH: Reduced form of the Nicotinamide Adenine Dinucleotide Phosphate

NCLV: Noncompaction of the Left Ventricle

OM: Outer Membrane

OXPHOS: Oxidative Phosphorylation

PBS: Phosphate Buffered Saline

PCR: Polymerase Chain Reaction

PDHc: Pyruvate Dehydrogenase complex

RC: Respiratory Chain

ROS: Reactive Oxygen Species

RRF: Ragged Red Fibre

SAM: S-Adenosylmethionine

SNP: Single Nucleotide Polymorphism

TIM: Translocase of Inner Membrane

TOM: Translocase of Outer Membrane

1 INTRODUCTION

1.1 Mitochondria and Mitochondrial Proteome

Mitochondria are ubiquitous, essential-for-survival organelles that provide energy substrates (such as ATP) for intracellular metabolic pathways. They are characterised by the presence of two membranes, an outer and an inner, which delimit two aqueous compartments: the inter membrane space, in between the two membranes, and the matrix, enclosed by the inner membrane which also forms cristae protruding into it. Several metabolic pathways are hosted in mitochondria, including the Krebs cycle, β -oxidation, lipid and cholesterol biosynthesis and oxidative phosphorylation. They also play an important role in cell signalling, particularly in signalling for apoptotic cell death. Given its fundamental role in the human body, defects of mitochondrial function can have disastrous consequences.

Mitochondrial DNA (mtDNA) is a maternally inherited circular genome of approximately 16 kb with a copy number of about 100 per cell [1,2]. Typically, an individual or cell contains only one variant or haplotype of the mitochondrial genome, a state known as homoplasmy. Somatic and germ line mutations can cause two or more variants to co-exist (heteroplasmy) and can impair mitochondrial oxidative phosphorylation (OXPHOS) when they exceed a threshold. Segregation of heteroplasmic mtDNA variants is usually a random process in both the germline and in somatic cells, dependent on mtDNA turnover and copy number [3]. However, some pathogenic mtDNA mutations can have skewed segregation patterns affecting the onset and severity of disease. These segregation patterns are mutation and tissue-specific but independent of the biochemical defect. The human mitochondrial proteome is thought to contain more than 1500 proteins [4,5]; but only about 1% are synthesized inside the organelle, the vast majority are synthesized in the cytosol. The mitochondrial DNA codes for 13 OXPHOS subunits (assembled into complexes I, III, IV and V), 22 transfer RNA and specific ribosomal RNAs, necessary for endogenous mitochondrial protein synthesis. All the other proteins involved in the structure and assembly of the OXPHOS complexes, enzymes involved in catabolism and anabolism of energetic substrates, transporters and proteins for mitochondrial fusion and fission are encoded by the nuclear genome. Import mechanisms are then engaged to transfer these proteins inside the organelle, into the appropriate compartment.

1.2 Mitochondrial Respiratory Chain and Oxidative Phosphorylation System

Accommodated in the mitochondrial inner membrane there are the five OXPHOS complexes (complexes I–V), as shown in Fig. 1. The complexes I to IV are oxidoreductases which, with the exception of complex II, couple electron transport

1.2.2 Complex II: Succinate CoQ Reductase

It catalyses the oxidation of FADH_2 by transferring electrons to Coenzyme Q_{10} . It is comprised of succinate dehydrogenase and 3 other hydrophobic subunits and provides another entry point to transport high potential electrons in the mitochondrial respiratory chain besides complex I. So, mitochondrial complexes I and II do not operate in series but cooperate for the same result.

1.2.3 Complex III: Ubiquinol-Cytochrome c Reductase

Mitochondrial complex III catalyses the reduction of one molecule of Coenzyme Q_{10} with two molecules of cytochrome c. It contains 10 polypeptides, haem groups and iron-sulphur clusters. The electron flow is coupled to the transfer of 2 protons towards the inter membrane space.

1.2.4 Complex IV: Cytochrome c Oxidase

It is composed of 13 subunits and transfers electrons from cytochrome c to oxygen, coupled to the transfer of two protons across the inner membrane. During this step molecular oxygen is reduced, forming two molecules of water.

1.2.5 Complex V: ATP Synthase

Complex V (ATP synthase) of the mitochondrion comprises 17 subunits encoded by nuclear DNA and two subunits (ATPase 6 and ATPase 8) encoded by mtDNA. It is a highly conserved enzyme and is powered by the transmembrane proton electrochemical gradient generated by the redox reactions of complexes I-IV.

The efflux of protons from the mitochondrial matrix to the inter membrane space creates an electrochemical gradient (proton gradient) across the membrane, which is often called the proton-motive force. This gradient has two components: a difference in proton concentration (an H^+ gradient) and a difference in electric potential, with the matrix side having a negative charge. The energy is stored largely as the difference of electric potentials in mitochondria [10].

ATP synthase releases this stored energy by completing the circuit and allowing protons to flow down the electrochemical gradient, back to the mitochondrial matrix [11]. This enzyme is like an electric motor as it uses the proton-motive force to drive the rotation of part of its structure and couples this motion to the synthesis of ATP. The amount of energy released by oxidative phosphorylation is high, compared with the amount produced by anaerobic fermentation. Glycolysis produces only 2 ATP molecules, but between 30 and 36 ATPs are produced by the oxidative phosphorylation of the 10 NADH and 2 succinate molecules made by converting one molecule of glucose to carbon dioxide and water, while each cycle of beta oxidation of a fatty acid yields about 14 ATPs. These ATP yields are theoretical maximum values; in practice, some protons leak across the membrane, lowering the yield of ATP [12].

1.3 Biochemical Assessment of Complex I Deficiency

The most common defect of the mitochondrial OXPHOS system is complex I deficiency, which accounts for ~1/3 of all cases of OXPHOS disorders [13]. Complex I deficiency like all OXPHOS disorders can cause almost any symptom in any tissue or organ, with any age of onset, and showing any mode of inheritance [14]. Therefore the diagnosis of such a disorder should rely on many different parameters, first of all the multi-organ involvement, typical of a metabolic disease manifestation. The starting point for an accurate diagnosis is the biochemical examination, which is typically achieved by spectrophotometric assay of tissue biopsy material or cultured patient fibroblasts.

For a diagnosis of isolated complex I deficiency, the activity of complex I relative to the activity of either citrate synthase, an enzyme involved in the Krebs cycle, or mitochondrial complex II should be markedly reduced compared to controls (e.g. <30%) while the activity of the other complexes should be within or close to their reference range [15,16]. It is good practice to express the results in ratios because the activity values have to be normalised by an indicator of the mitochondrial content: either the number of OXPHOS systems by normalising to complex II activity, or the Krebs cycle activity by normalising to citrate synthase; these two enzymes are the commonest used for these purposes. Furthermore, the enzyme assay measures the redox activity of the peripheral arm of complex I, meaning that mutations that affect the proton pumping function of the membrane arm may show “normal” activity. A normal enzymatic result, therefore, does not eliminate the possibility of complex I deficiency. A clear complex I deficiency by biochemical analysis, however, guides future molecular studies.

1.4 Complex I Function, Structure and Assembly

Electron microscopy studies of purified complex I revealed the L-shaped structure of the enzyme consisting of a hydrophobic membrane arm and a peripheral arm that protrudes into the mitochondrial matrix [17] (Fig. 2). The membrane arm houses the hydrophobic mtDNA encoded subunits whereas the core nuclear encoded subunits all reside in the peripheral arm. NADH is oxidized at a site near the tip of the peripheral arm and electrons are transferred via flavin mononucleotide (FMN) and a chain of iron–sulphur clusters to the ubiquinone reduction site near the base of the peripheral arm. The membrane domain utilizes the energy released by the redox reactions within the peripheral arm to pump hydrogen ions into the intermembrane space to contribute to the electrochemical gradient that drives ATP synthesis [18,19]. Homologues of mammalian complex I can be found in bacteria, with the bacterial complex formed from three evolutionarily conserved modules; the electron input module (N), electron output module (Q), and the proton translocation module (P).

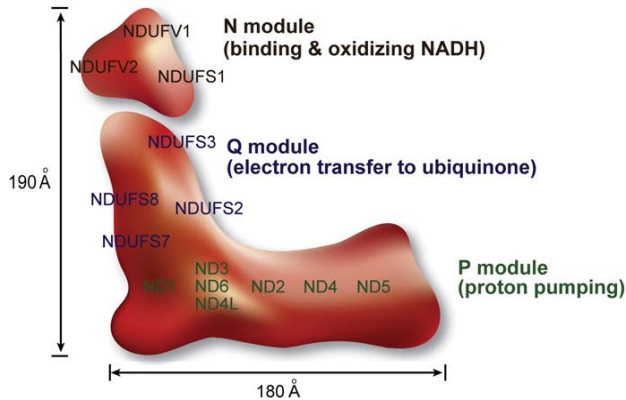


FIGURE 2: Schematic graph of mammalian mitochondrial complex I structure. The matrix arm and the membrane arm form an L-shaped structure. It is composed of three conserved functional modules: the NADH dehydrogenase module (N module), the electron transfer module (Q module) and the proton translocation module (P module). The positions of 14 core subunits are indicated, all of which are highly conserved from prokaryotes to eukaryotes (picture taken from Mimaki M. et al. *Biochim Biophys Acta* 2011 Sep 2).

The exact positions of each subunit within this structure have not yet been fully defined; however, treatment with mild chaotropic agents can dissociate the complex into four subcomplexes ($I\alpha$, $I\beta$, $I\lambda$, and $I\gamma$), allowing for the identification of subunits within each subcomplex [20-22]. In addition, the crystal structure from the bacterium *Thermus thermophilus* has defined the relative positions of the eight subunits that comprise the peripheral arm of complex I in this organism [18,23]. Although it is not known exactly how each subunit is assembled to form mature complex I in humans, in the last few years a model for its assembly has developed [24,25]. In addition, a number of assembly factors are required for assembly to proceed effectively.

Human complex I consists of 45 different subunits (Fig. 3), 14 of which are crucial for its catalytic function and are conserved in all species that have a complex I, including bacteria [26]. Seven of these “core” subunits are hydrophobic and encoded by the mtDNA (ND1, ND2, ND3, ND4, ND4L, ND5 and ND6), whereas the other seven are hydrophilic and encoded by the nuclear DNA (nDNA) (NDUFV1, NDUFV2, NDUFS1, NDUFS2, NDUFS3, NDUFS7, NDUFS8). They have been defined as the “minimal enzyme”, while other subunits are often referred to as “supernumerary”. The minimal enzyme includes the core subunits of complex I considered essential for catalysing electron transfer from NADH to ubiquinone, and for the generation of the proton motive force.

separate intermediates forming the membrane arm [28], in humans both matrix and membrane arm subunits are found together in early-stage intermediates. In a separate study, by using radiolabelling techniques it was found that the hydrophobic mtDNA-encoded subunits assembled into different intermediates and their subsequent integration into complex I required relatively long chase times [29]. Furthermore, a number of nuclear-encoded subunits appeared to assemble directly into mature pre-existing complex I (and its supercomplex forms) [29]. The observation that newly synthesized subunits can be interchanged with pre-existing counterparts in the mature complex I suggests that a subunit exchange mechanism model is preferable to a static model to explain the complex I assembly and homeostasis [24].

In addition to the structural components of complex I, there are a number of known and putative assembly factors, which gather 45 subunit proteins, one flavin mononucleotide and 8 iron-sulphur clusters through the intricate process of assembling the final ~980kDa holoenzyme [30]. To date, 9 known complex I assembly factors have been described and associated with mutations (NDUFAF1, NDUFAF2, NDUFAF3, NDUFAF4, C20ORF7, C8ORF38, NUBPL, FOXRED1, and ACAD9). It is likely that many more assembly factors of complex I will be identified, bearing in mind that the much smaller complex IV, which has only 13 subunits, requires more than 15 assembly factors for its assembly. Studies in *S. cerevisiae* led to the identification of over 20 factors [31,32] for complexes IV and V. However, the absence of complex I in *S. cerevisiae* has impeded similar studies and, to date, only three complex I assembly and maturation factors have been identified by using this comparison approach in either *Neurospora crassa* or *Yarrowia lipolytica* which have conserved mitochondrial complex I through evolution: NDUFAF1/CIA30 [33], NDUFAF2/B17.2L [34], NUBPL/Ind1 [35].

Assembly of complex I has been extensively studied in both the fungus *N. crassa* and in human cells [36,30,33,37] and these studies, together with the phylogenetic profiling work of Mootha and colleagues [4], have led to the identification of 25 complex I assembly factors (Table 2). Sixteen of these have already been associated with human disease, including 9 complex I deficiency syndromes and one mitochondrial disorder with multiple respiratory chain deficiencies [38-40]. Interestingly, mutations in 7 of these putative complex I assembly factors have been linked to non-mitochondrial diseases, such as peroxisomal disorders, organic acidaemias and a ketone body utilisation defect (Table 2). It is not clear whether reduced complex I activity may be involved in the pathogenesis of any of these disorders. In contrast to the assembly chaperones described for complex IV, which play a role in the incorporation of prosthetic groups (e.g. COX10, COX11, SCO1, SCO2) or the maturation and membrane insertion of subunits encoded by mitochondrial DNA (e.g. SURF1 and OXA1), the molecular role of the complex I chaperones is still not clear. Whilst the precise mechanism of complex I assembly is still debated, a consensus view has recently been proposed of a dynamic multidirectional process that includes the possibility of direct subunit exchange into pre-existing mature complex I [30].

The role of only some of these assembly factors has been elucidated. NDUFAF1 appears to be involved at an intermediate stage of complex I assembly, in contrast to C20ORF7, NDUFAF3 and NDUFAF4 which are needed early in the assembly process, and NDUFAF2 which has a role in the late stages [30]. Tandem affinity purification experiments demonstrated that NDUFAF1 co-purifies with two other putative complex I assembly factors ECSIT and ACAD9 [40,37]. Possible functions of the various putative complex I assembly factors/chaperones include assembly of iron–sulphur clusters that are important complex I prosthetic groups (e.g. NUBPL, also called huInd1) [41], translational co-activation of complex I subunits (as has been suggested for C20ORF7 for ND1) and direction of nuclear-encoded complex I subunits to the correct intramitochondrial compartment (i.e. to the matrix side of the enzyme or to the intermembrane space) [30]. However, full understanding of complex I assembly is far from achieved and there are likely to be many additional assembly factors involved in the process that are yet to be discovered.

At the early stages of complex I assembly, newly translated mtDNA-encoded subunits assemble into a number of distinct membrane arm intermediates [29]. This step is chaperoned by C20ORF7, which has been proposed to be a translational activator of ND1, also involved in the insertion of ND1 into the membrane, or to aid the assembly of ND1 into an early membrane arm intermediate. C20ORF7 also has a predicted SAM-dependent fold and it may methylate proteins, RNA, or DNA within mitochondria [42,43]. As far as protein methylation is concerned, only 2 complex I methylated subunits have been detected [44]. One of them is NDUFS2, which harbours a methylated arginine, and the other is NDUFB3. At least two highly conserved histidines (possibly 3) are methylated in NDUFB3 [45], and this subunit is located in the membrane arm of complex I containing ND1. Although the interaction of C20ORF7 with NDUFB3 and its subsequent methylation remain to be investigated further, it is possible that this post-translational modification of the subunit plays a role in the assembly or stability of the mature complex I. However, a patient with combined complex I and IV deficiency was recently described to bear a C20ORF7 defect; notably decreased complex IV was also observed by knockdown of C20ORF7 expression in control cells using lentiviral-mediated RNAi [46]. These findings raise the possibility that C20ORF7 may play a role in the post transcriptional modification of one or several proteins of importance for complex I and IV function and/or assembly [46,47].

The formation of the peripheral matrix arm begins with the assembly of NDUFS3 together with NDUFS2 and the subsequent integration of subunits NDUFS7 and NDUFS8 to form intermediate 2 (Fig. 4). These four subunits are part of the 14 “core” mammalian subunits (each of which has a homologue in complex I from *Escherichia coli*) and form part of the evolutionarily conserved hydrogenase module. The crystal structure of the peripheral arm of complex I from *Thermus thermophilus* revealed that the orthologues of NDUFS2 (Nqo4), NDUFS3 (Nqo5), NDUFS7 (Nqo6), and NDUFS8 (Nqo9) lie adjacent to one another [23], consistent with their proposed early assembly into intermediate 2.

It has been shown that pathogenic mutations in the genes encoding either NDUFAF3 (C3ORF60) or NDUFAF4 (C6ORF66) result in fatal neonatal mitochondrial disease with severe complex I enzymatic deficiency and the accumulation of two sub-complexes of undetermined size that may be stalled early assembly intermediates [36,48]. Further studies proved that both proteins tightly associate with each other [36] and to the subunits that form intermediate 2. Their membrane localisation also suggests that NDUFAF3 and NDUFAF4 may be involved in membrane anchoring of an early intermediate complex, which contains the complex I subunits NDUFS2, NDUFS3, NDUFS7 and NDUFS8. With the addition of further subunits, including possibly NDUFA9 [27,49], NDUFAF3 and NDUFAF4 promote the maturation of intermediate 2 to form intermediate 3, which is then anchored to the membrane (Fig. 4). Both NDUFAF3 and NDUFAF4 appear to remain associated with intermediates 4 (~400kDa), 5 (~650kDa), and 6 (~830kDa) as complex I is assembled, but are dissociated just before the formation of the mature holo-complex (Fig. 4) [36].

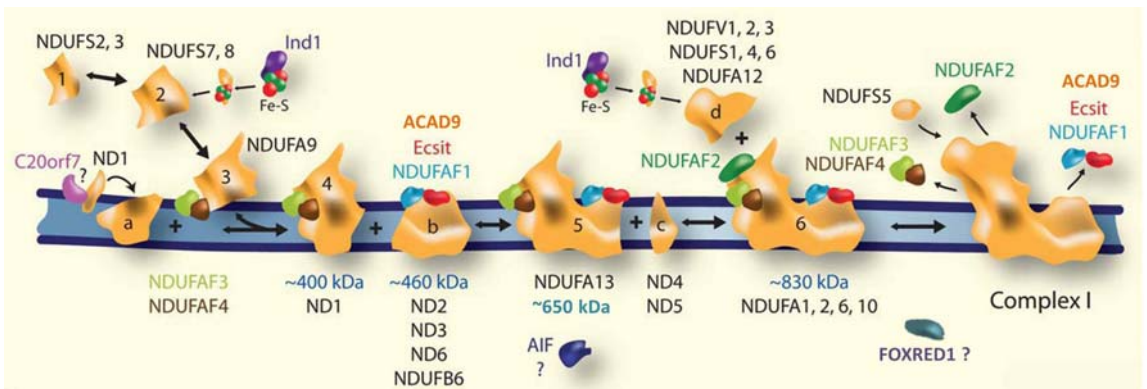


FIGURE 4: Current model of human complex I assembly. Intermediates 1-6 correspond to the NDUFS3 containing intermediates described by Vogel and colleagues [50]. Entry points of structural subunits (black) are indicated. During the early stages of assembly, subunits NDUFS2, 3, 7, and 8 form an evolutionarily conserved hydrogenase module (Q module) as part of intermediate 2. With the addition of NDUFA9 (and possibly other subunits), intermediate 3 is assembled and subsequently anchored to the membrane by the assembly factors NDUFAF3 (C3ORF60) and NDUFAF4 (C6ORF66). The Fe-S clusters are then added by IND1 (NUBPL) at this stage and during the formation of the ~830 kDa assembly. Intermediate 3 is assembled with intermediate “a” (which contains ND1) to form the ~400 kDa intermediate 4. The ~460 kDa intermediate “b” is assembled from the membrane arm subunits ND2, ND3, ND6, and NDUFB6 and is associated with the assembly factors NDUFAF1 (CIA30) and ECSIT and possibly ACAD9. Intermediate 4 and “b” assemble together, with the addition of ND4 and ND5 resulting in the formation of the ~830 kDa intermediate 6. The assembly factors

NDUFAF1, NDUFAF2 (B17.2L), ECSIT, NDUFAF3, NDUFAF4 and ACAD9 remain associated with this intermediate until the last stage of assembly, where intermediate "d" (which contains the N module) is assembled to form mature complex I. AIF and FOXRED1 entry points are yet to be defined. (picture amended from McKenzie M. and Ryan MT. IUBMB Life 2010 Jul;62(7):497-502 Review).

The next step in the complex I assembly is the joining of intermediate 4 (a ~400 kDa sub-complex containing at least NDUFS2, NDUFS3, NDUFS7, NDUFS8, and ND1) with a second membrane arm intermediate of ~460 kDa containing at least ND2, ND3, and ND6 [29]. Two assembly factors, NDUFAF1 (CIA30) and ECSIT (Evolutionary conserved signalling intermediate in Toll pathways), are involved at this stage of assembly (Fig. 4). The complex I intermediate associated protein CIA30 was originally isolated with a membrane arm intermediate from the fungus *N. crassa* [33]. Pathogenic mutations in the gene encoding NDUFAF1, which result in isolated complex I deficiency and cardiomyopathy in 2 patients, result in the loss of ND2 and stall the holo-complex I formation at the ~400 kDa and ~460 kDa intermediates, highlighting the importance of NDUFAF1 for the assembly/stability of these intermediates [51,52]. Recently, the mRNA level and the protein expression of NDUFAF1 were found to decrease in muscles from mice lacking testicular nuclear receptor 4 (TR4) [53]. A chromatin immunoprecipitation assay indicated that TR4 directly binds to *NDUFAF1* promoter. Since TR4 is a key transcriptional regulator of many signalling pathways, TR4 could modulate complex I activity via transcriptionally regulating *NDUFAF1* [53]. On the other hand, ECSIT was originally identified as a cytosolic protein involved in the inflammatory response and embryonic development [54,55], but was later found in complexes of similar size to the NDUFAF1 intermediates [56]. Furthermore, knock-down of ECSIT using RNA interference reduced the levels of both mature complex I and NDUFAF1 protein [56]. However, *NDUFAF1* knock-down has only a minor effect on the levels of ECSIT-associated complexes [56], suggesting that although NDUFAF1 and ECSIT are found in the same intermediates, they may have independent functions in complex I biogenesis.

Together with NDUFAF1 and ECSIT, ACAD9 has also been shown to be associated with these two assembly factors and the ~460kDa and ~850kDa subassemblies of complex I. Acyl-CoA dehydrogenase 9 (ACAD9) was initially cloned and identified as a member of the acyl-CoA dehydrogenase family [57]. Contrary to its previously proposed involvement in fatty acid oxidation, a new role for ACAD9 in OXPHOS was recently discovered: quite a few complex I deficient patients have been recently described to bear ACAD9 defects [40,58,59] but no biochemical evidence of disturbed fatty acid oxidation, suggesting that the primary *in vivo* role of ACAD9 is in the assembly of complex I.

As complex I assembly proceeds, the two main membrane arm intermediates previously described, are assembled together to form intermediate 5, at which stage NDUFA13 is incorporated [50]. The subunits ND4 and ND5 are then

assembled into the growing complex, possibly together with other subunits in a small membrane arm intermediate [24]. The resulting ~830 kDa intermediate 6 remains associated with NDUFAF1 and has been shown by coimmunoprecipitation to contain ND1, ND2, ND3, ND6, NDUFB6, NDUFA6, NDUFA9, NDUFS3, and NDUFS7 (but not NDUFS5) [51]. In addition, studies suggest that NDUFA1, NDUFA2, NDUFA6 [50], NDUFB8, and NDUFA10 [29] are assembled into intermediate 6 at this stage.

Studies such as whole genome subtraction, carried out in the aerobic yeasts *Yarrowia lipolytica* and *Debaryomyces hansenii* (which both contain complex I), identified NDUFAF2 (B17.2L) as a putative complex I assembly protein [34]. NDUFAF2 shares 17% identity with NDUFA12/B17.2, a structural subunit of complex I, and null mutations in NDUFAF2 cause progressive encephalopathy in patients with a dramatic loss of mature complex I and the accumulation of intermediates of ~830 kDa containing the subunits NDUFS2 and NDUFS3 [60,34]. Notably, the stability of this intermediate appears crucial, with the assembly factors NDUFAF1, ECSIT, NDUFAF2, NDUFAF3, and NDUFAF4 all associated with this complex (Fig. 4). These findings suggest that NDUFAF2 is associated with the ~830kDa complex and required in the late stage of complex I assembly.

The last step for the completion of a fully assembled complex I is the final insertion of the N module, which by in vitro import studies has been shown to contain the subunits NDUFS1, NDUFV1, NDUFV2, NDUFV3, NDUFS4, NDUFS6, and NDUFA12 and a flavin mononucleotide (FMN) [29]. This last module is a ~300 kDa intermediate and provides the entry point for electrons into complex I [61]. During the final stages of assembly, this small intermediate assembles with intermediate 6 to form mature complex I (Fig. 4). At this point, the assembly factors NDUFAF1, ECSIT, NDUFAF2, NDUFAF3, and NDUFAF4 are dissociated from the nascent holoenzyme (these proteins are not found associated with the mature holoenzyme). The subunit NDUFS5 is also incorporated into (the near) mature complex I at this stage (Fig. 4); the fact that this subunit is not present in any assembly intermediates suggests that it is assembled at a very late stage [49].

Complex I also requires the incorporation of iron–sulphur (Fe–S) clusters to exert its function. This step is most likely carried out by at least one assembly factor: NUBPL/Hulnd1 (iron–sulphur protein required for NADH dehydrogenase), also known as NUBPL (Nucleotide-binding protein-like protein). Complex I contains eight Fe–S clusters, and NUBPL is a mitochondrial protein which binds Fe–S clusters via a conserved CxxC motif [35]; NUBPL is important for the assembly of these clusters into various subunits of the holoenzyme [35,41]. NDUFS7 and NDUFS8 contain Fe–S clusters and are assembled in intermediate 2; NDUFS1 and NDUFV1 also contain Fe–S clusters and are found in intermediate 4. NUBPL is important for delivering Fe–S clusters to complex I subunits during their assembly into intermediate complexes, in particular intermediate 2 and intermediate 4 (Fig. 4).

In recent years, many new assembly factors have been discovered, including in patients with pathogenic mutations in assembly factor genes. These studies have helped to define the different roles of the assembly factors in complex I biogenesis; however, in most cases, their exact biochemical function remains unclear. AIF (apoptosis-inducing factor), for example, was recently identified as a mitochondrial pro-apoptotic protein and in mice with a partial AIF deficiency, Harlequin (Hq) mice, the levels of AIF are reduced by ~80% due to a fortuitous retroviral insertion in the first intron of the X-chromosomal AIF gene encoding AIF. These mice display reduced levels of complex I and complex I subunits along with defects in complex I-driven mitochondrial respiration [62-64]. Recently, a pathological mutation in the human X-linked *AIFM1* gene encoding AIF was identified in 2 infant male patients with progressive mitochondrial encephalopathy [65]. Surprisingly, fibroblasts from the patients showed a reduction of respiratory chain complex III and complex IV activity, but not of complex I activity.

Furthermore, AIF has never been associated with any complex I subunits; however it exhibits NADH and NADPH oxidase activity [66] and can form stable NADH-associated dimers [67], suggesting a possible role in redox-dependent substrate delivery to complex I. The findings in the patient's cells will require the interpretation of the role of AIF in complex I biogenesis.

1.5 Mitochondrial Disease

Mitochondrial diseases are a heterogeneous group of diseases displaying a variable degree of dysfunction of the mitochondrial OXPHOS system, which is demonstrated by rigorous morphologic investigations, and biochemical and genetic methods. The birth prevalence of mitochondrial diseases is ~1/5000 [13], and they cause a wide spectrum of clinical phenotypes. Usually, organs with high energy demand, such as brain, muscle and heart are the most affected, together or in isolation, and symptoms generally arise at birth, infancy or adulthood, less often *in utero*.

Isolated deficiency of complex I is the most commonly identified biochemical defect in childhood-onset mitochondrial disease [15], and accounts for ~1/3 of all cases of OXPHOS disorders [13]. Despite the existence of some mitochondrial myopathies, characterised by the isolated defect of the skeletal muscles, the ubiquitous nature of the mitochondria, as well as the high metabolic demand of the tissues that most rely on the OXPHOS activity, convey the multisystem nature of mitochondrial disease, with impairment of the central nervous system, neurosensory organs, endocrine apparatus, heart, liver and gastrointestinal and hematopoietic systems. Patients with a defect in a nuclear DNA (nDNA)-encoded complex I structural gene may display basal ganglia and/or brainstem lesions, respiratory abnormalities, muscular hypotonia, failure to thrive, seizures, cardiomyopathy and lactic acidemia [68]. In general, prenatal development is normal and children are born at term with no obvious organ anomalies or dysmorphic features. However, most children develop symptoms during the first year of life and then suffer from rapid disease

deterioration, resulting in a fatal outcome [69]. The clinical presentations may vary, from infantile Leigh syndrome, to childhood MELAS (Mitochondrial Encephalomyopathy, Lactic Acidosis, and Stroke-like episodes), to adult-onset encephalomyopathic syndromes of variable severity.

Inherited isolated complex I deficiency can result from mutations in either mtDNA- or nDNA-encoded complex I structural subunits or nDNA-encoded complex I assembly factors [26]. To date, genetic defects causing inherited isolated complex I deficiency have been reported for all seven mtDNA-encoded complex I subunits [70]. Mutations in nDNA-encoded complex I subunits are frequently inherited in an autosomal recessive fashion, meaning that both parents have to be heterozygous carriers, and thus far disease-causing mutations have been demonstrated in genes encoding 13 complex I subunits [71-83]. Finally, inherited isolated complex I deficiency can be caused by mutations in nDNA-encoded proteins involved in complex I assembly and/or stabilization. Mutations have been found in: *NDUFAF1* [51,52], *NDUFAF2* [60], *NDUFAF3* [36], *NDUFAF4* [48], *C8ORF38* [4], *C20ORF7* [46], *FOXRED1* [38], *NUBPL* [39] and *ACAD9* [40].

Up to now, most of the mutations in nuclear genes encoding complex I subunits (*NDUFV1*, *NDUFA1*, *NDUFA10*, *NDUFS1*, *NDUFS2*, *NDUFS3*, *NDUFS4*, *NDUFS7*, *NDUFS8*, *NDUFAF2*) have been shown to cause neurological disease (Leigh or Leigh-like syndrome), together with some assembly factor genes (*C20ORF7*, *C8ORF38* and *FOXRED1*); while heart involvement has been reported in patients harbouring mutations in three other nuclear genes encoding complex I subunits (*NDUFS2* and *NDUFV2*, *NDUFA11*) and three assembly factor genes (*NDUFAF1*, *ACAD9* and *FOXRED1*) (see Table 1 for full phenotypes and references). To date, no simple explanation accounts for this clinical variability. The *NDUFV1*, *NDUFV2*, *NDUFS1*, *NDUFS2*, and *NDUFS3* genes all encode subunits that are presumably involved in the catalysis of electron transfer from NADH to ubiquinone. The possibility that only part of these mutations results in superoxide overproduction has been proposed to explain specific cardiac involvement, since superoxide overproduction is known to readily trigger cardiomyocyte hypertrophy. On the other hand, differences in residual complex I activity compromising cell specific functions should be also considered [75].

Gene (complex I subunits)	References	Genetic changes	AA changes	C1 heterozygote levels	C1 heterozygote substrates	Patients and Families	C1 residual activity in muscles (relative to control mean)	C1 residual activity in fibroblasts (relative to control mean)	Age of onset	Age at death	Vomiting	Flapping	Lethargy	Anemia	HCM / Cardiac Implant	Hepatosplenomegaly	Respiratory failure	Ocular involvement	Sensorineural deafness	Muscular hypotonia	Spasticity	Pyramidal syndrome	Dystonia	Myoclonic epilepsy	Seizures	Cerebellar Ataxia	Psychomotor development	Developmental delay	Microcephaly / Macrocephaly	Encephalopathy	Cranial MRI / Post-mortem reports	Blood lactate (normal <2.8 mM)	CSF lactate (normal <2.2 mM)	Metabolic acidosis
NDUFV1	Schuelke M et al. Nat Genet. 1999 Mar	compound heterozygous c.175C>T + c.1268C>T	R59K + T423M			2 brothers	deficiency	deficiency	5 months	14 and 17 months																				brain atrophy	elevated	elevated		
		homozygous 1022 C>T	A341V			1 girl	deficiency	deficiency	6 months	alive at 10 years																			brain atrophy	normal	elevated			
		compound heterozygous c.642G>A + A>C intron 8 splice site	E214K + exon 8 skipping -> unstable mRNA			1 boy French unrelated parents	deficiency	normal	1 year	3 years, of metabolic acidosis																				brain atrophy + gray matter degeneration	2.6 mM		yes	
	Bénit P et al. Am J Hum Genet. 2001 Jun	compound heterozygous 1294 G>C del nt 989-990 2bp deletion in exon 7	A432P + premature stop codon -> unstable mRNA			1 girl French unrelated parents	deficiency	normal	6 months	18 months, of metabolic acidosis																				areas of hyperintensity in the basal ganglia	4 mM		pH 7.24	
		heterozygous c.611A>G + c.616T>G	Y204C + C206G			1 boy French unrelated parents	deficiency	normal	5 months	alive at 3 years; unable to walk unaided and still mentally retarded																				areas of hyperintensity of the locus niger	2.3 mM			
	Bugiani M et al. Biochim Biophys Acta. 2004 Dec	c.1022C>T	A341V			1 baby	36%	normal	first months of life																					ventricular enlargement, early-onset leukoencephalopathy	elevated	elevated		
	Laugel V et al. Pediatr Neurol. 2007 Jan	compound heterozygous c.611A>G + c.616T>G	Y204C + C206G			1 boy Caucasian unrelated parents	13%	normal	7 months	Independent walking is still impossible and hardly intelligible at 7 years																				bilateral hyperintensities in the putamina, red nuclei, and substantia nigrae	3.7 + 8.0 mM	4.8 mM	severe	
	Calvo SE et al. Nat Genet. 2010 Oct	homozygous c.1129G>A	E377K			1 girl first cousin Lebanese parents			2 weeks	4 months, from respiratory failure																								persistent
Vilain C et al. Clin Genet. 2011 Jun	homozygous c.1156G>A	R386H			1 brother and 1 sister first cousin Moroccan parents			3.5 months	4.5 months																				T2 hypersignal and T1 hyposignal in the medulla, the pons and in the mesencephalon	1.7 mM; 5.2 mM	2.3 mM; 2.8 mM			
NDUFV2	Bénit P et al. Hum Mutat. 2003 Jun	homozygous 4bp deletion of intron 2 IVS2:5-8delGTTA	skipping of exon 2			2 brothers first cousin African parents	45%		5 days of life	3 months																					>5 mM			
	Nishioka K et al. Parkinsonism Relat Disord. 2010 Oct	c.625AG	K209R																															
NDUFA1	Fernandez-Moreira D et al. Ann Neurol. 2007 Jan	homozygous c.222C>C	GBR			2 brothers In vitro fertilization, 2+ anonymous fathers	20% of the lowest CTR value	17% of the lowest CTR value	4 months	14 months, of cardiorespiratory arrest																				bilateral lesions affecting the thalamus, cerebral peduncles, and brainstem	Increased			
		homozygous c.251G>C	R375			1 boy nonconsanguineous parents	30% of the lowest CTR value	70% of the lowest CTR value	6 months	He is now 10 years old and his clinical evolution remains stable																				cerebellar atrophy with alterations of signal in the dentatus nuclei	normal		normal	
	Pottluri P et al. Mol Genet Metab. 2009 Apr	homozygous c.94G>C	G32R			1 boy nonconsanguineous parents	7%		4 years	Alive at 35 years of age																			mild cerebellar atrophy	normal		normal		
		homozygous c.94G>C	G32R			1 boy nonconsanguineous parents	7%		5 years	Alive at 30 years of age																						3 mM	1.98 mM	
	Máyr A et al. Mol Genet Metab. 2011 May	heterozygous c.94G>C	G32R			1 girl nonconsanguineous Caucasian parents	2%		11 months	at 5 years of age her psychomotor and speech development is within age appropriate limits																					3 < 4 mM			
NDUFA2	Hoefs SJ et al. Am J Hum Genet. 2008 Jun	homozygous c.208+5G>A	impaired splicing of exon 2 -> almost complete lack of exon 2 -> frame-shift resulting in a truncated protein -> unstable and degraded		~830kDa	1 boy first cousins Turkish parents	20% of the lowest CTR value	36% of the lowest CTR value	5 days of life	at 11 months, of cardiovascular arrest, after further episodes of apnea and asystolia																				Leigh syndrome			severe	
NDUFA9	2011	homozygous c.962G>C	R321P			1 boy second cousins Kurdish parents	29%	11%	soon after birth	1 month after birth due to respiratory insufficiency																			Leigh syndrome	10 mM		yes		

Gene (complex subunits)	References	Genetic changes	AA changes	Cholesterolemia levels	Cholesterolemia subfamilies	Patient sex/families	Clinical activity in males (relative to control mean)	Clinical activity in fibroblasts (relative to control mean)	Age of onset	Age at death	Vomiting	Flapping	Lethargy	Anemia	HCM/ Cardiac Impairment	Hepatoenlargy	Respiratory failure	Ocular involvement	Sensorineural deafness	Muscular hypotonia	Spasticity	Pyramidal syndrome	Dystonia	Myoclonic epilepsy	Seizures	Cerebellar Ataxia	Psychomotor development	Developmental delay	Microcephaly / Macrocephaly	Encephalopathy	Coronal MRI / Post-necropsy reports	Blood lactate (normal <2.0 mM)	CSF lactate (normal <2.2 mM)	Metabolic acidosis		
NDUFA10	Hoefs SJ et al. Eur J Hum Genet. 2011 Mar	compound heterozygous c.1A>G + c.425A>G	M17 + Q142R			1 boy	19%	3% + 34% CIII		23 months. At autopsy, besides the already known cardiomyopathy, degenerative abnormalities were reported in the liver, spleen, kidneys, and pancreas.																			Leigh syndrome	8.6 mM	4.9 mM	pH 7.12				
NDUFA11	Berger I et al Ann Neurol. 2008 Mar	homozygous IVS1-5 G>A	leaky splicing with the consequent activation of a cryptic splice site at 19 to 20bp of exon 1, lacking the 3' end 78bp of exon 1			2 brothers + 1 boy first cousin parents	7%; 20%	45%	at 10 to 24 hours of age	patients died at 6 to 40 days of age because of intractable acidosis																					10 < 15 mM		pH 6.8 < 6.9			
		homozygous IVS1-5 G>A				2 brothers and 1 sister first cousins Israeli-Bedouin parents	29%	45%	at 10 to 24 hours of age	2 patients died at 18 months and 4 years of age during an intercurrent infection. One patient was alive at 6 months at the time of writing this report																			generalized brain atrophy	3.2 < 10mM		yes				
NDUFS1	Bénit P et al. Am J Hum Genet. 2001 Jun	compound heterozygous 3bp deletion at c.664-6 + c.755 A>G	in-frame codon 222 deletion + D252G			2 brothers 1 sister nonconsanguineous parents	deficiency	deficiency	2 years; 4 months	10 months, of bradycardia; 7 months																						4.4 mM				
		compound heterozygous c.224 C>T + compound heterozygous 2119 A>G + de novo deletion of the paternal NDUFS1 allele	R241W + R557X -> unstable mRNA		1 brother; 1 sister nonconsanguineous parents	deficiency	deficiency	2 months	5 months																								5 mM		yes	
	Bugiani M et al Biochim Biophys Acta. 2004 Dec	homozygous c.1564C>A	Q522K			2 siblings consanguineous parents	45%	45%	6 months																					diffuse leukoencephalopathy with no cavitations	increased					
	Martin MA et al. Arch Neurol. 2005 Apr	homozygous c.691C>G	L231V			1 sister 1 brother nonconsanguineous Spanish parents	25%		8.5 months	14 months the sister; 8 months the brother after an acute episode of respiratory failure																				bilateral lesions affecting the substantia nigra and midbrain	increased	increased				
	Liso A et al. J Biol Chem. 2006 Apr	homozygous c.1564 C>A	Q522K			2 brothers		90%	6 months	progressive disease course																				leukodystrophy	elevated					
	Scacco S et al Ital J Biochem. 2006 Sep-Dec																																			
	Hoefs SJ et al Mol Genet Metab. 2010 Jul	compound heterozygous c.1669C>T + c.1855G>A	R557X + D619N			1 girl nonconsanguineous parents	63% of the lowest CTR value	27% of the lowest CTR value		pregnancy complicated by gestational diabetes with a modest intrauterine	12 years																									
		homozygous c.1222C>T	R408C		~830kDa	2 brothers first cousins parents	10% + 70% of the lowest CTR value in CIII	20% of the lowest CTR value	4 months	8 months																					leukoencephalopathy	high	high			
		compound heterozygous c.631-633del-GAA + c.692C>C	211delGlu + V28A		~830kDa	1 girl nonconsanguineous parents		24% of the lowest CTR value	5 months	2 years																					changes in the frontal and parietal lobes + periventricular areas in the temporal lobes					
	Tuppen HA et al Brain. 2010 Oct	homozygous c.1222C>T	R408C		~830kDa	2 sisters first cousins parents	23%		4 months	after 24 hours since the encephalopathy at 10.5 months																				extensive symmetrical abnormalities in the cerebral peduncles, anterior horns, internal capsules	3.3 mM	4.7 mM				
Ferreira M et al. Neurogenetics 2011 Feb	homozygous c.1783A>G	T595A			1 sister + 1 brother first cousins parents	45%, 98% of the lowest control	146%, 53% of the lowest control	11 months																					white matter abnormalities + cystic lesions involving the white matter, the corpus callosum, and the brainstem	2.42 mM; 5.1 mM	2.86 mM					

Gene (complex / subunits)	References	Genetic changes	AA changes	G homomyme levels	Chomomyme substrabilities	Patients and families	C residual activity in muscles (relative to control mean)	G residual activity in fibroblasts (relative to control mean)	Age of onset	Age at death	Nystagmus	Flapping	Lethargy	Areflexia	HCN / Cardiac Impairment	Hepatosplenomegaly	Respiratory failure	Ocular involvement	Sensorimotor deafness	Muscular hypotonia	Spasticity	Pyramidal syndrome	Dystonia	Myoclonic epilepsy	Seizures	Cerebellar Ataxia	Psychomotor development	Developmental delay	Microcephaly / Macrocephaly	Encephalopathy	Cranial MR / Post-mortem reports	Blood lactate (normal <2.0 mM)	CSF lactate (normal <2.2 mM)	Metabolic cascades
NDUFS2	Loeffen J et al Ann Neurol. 2001 Feb	homozygous c.683G>A	R228Q			1 brother + 1 sister consanguineous parents	20%	him 22%, her 30%	after 6 months neurological regression was noted	24 months, due to episodes of apnea																				marked generalized atrophy with ventriculomegaly	12 mM			
		homozygous c.686C>A	P229Q			1 boy nonconsanguineous us parents	8%	20%	respiratory insufficiency during the first day of life.	4 days, due to cardiorespiratory failure.																						24 mM		pH 6.9
		homozygous c.1237T>C	S413P			3 brothers consanguineous parents	24%	23%	7 months and 10 months with a phenotype strongly similar	18 months, 3 years, 2 years																					areas of white-matter hypodensities, progressive hypodensity of basal ganglia and midbrain	4.2 mM, 5.0 mM, 12.5 mM	3.3 mM	
	Buglani M et al Biochim Biophys Acta. 2004 Dec	compound heterozygous c.671C>T + c.305G>A in NDUFA8	A224V + E109K in NDUFA8 -> degraded transcript			1 baby first cousins Italian parents	13%	normal	soon after birth	2 months																						intermittently high		
	Tuppen HA et al Brain. 2010 Oct	compound heterozygous c.413G>A + c.598G>A	R138Q + R333Q			1 girl nonconsanguineous us parents	16%		2 hours after birth	3.5 months of age, of respiratory arrest																					6 < 9 mM	18 mM		mild
NDUFS3	Bénil P et al J Med Genet. 2004 Jan	single heterozygous c.422A>G	Y141C																															
		single heterozygous c.875T>C	M292T			3 girls nonconsanguineous us parents	20%		8 months	22 months, of central hypopnoea. One did not walk independently until 3 years and remains unsteady at 5 years.																						11.66 mM	5.56 mM	severe
	Pagites-Mannes H et al Mol Genet Metab. 2009 Aug	unique heterozygous c.668C>T	P223L			1 baby	11%																											
NDUFS4	van den Heuvel L et al Am J Hum Genet. 1998 Feb	homozygous 5-bp duplication c.466_470dupl AAGTC	frame shift resulting in K158fsX31			1 boy nonconsanguineous us Caucasian parents	9%	42%	8 months	16 months, of cardiorespiratory failure																				generalized brain atrophy and symmetrical basal ganglia abnormalities	normal	normal		
	Budde SM et al Biochem Biophys Res Commun. 2000 Aug	homozygous 1bp deletion c.289delG	W96X			1 girl consanguineous parents	22%	47% + 87% CIII of the lowest CTR value	1 week	3 months, in the course of a progressive respiratory insufficiency																				bilateral basal ganglia hypodensities	5.5 mM	7.6 mM		
	Petruzzella V et al Hum Mol Genet. 2001 Mar	homozygous c.C316T	A106X			1 boy first cousins parents	14% + 57% CIII of the lowest control	60% + 67% CIII of the lowest CTR value	7 weeks	3 months, of cardiorespiratory insufficiency despite continued mechanical ventilation																					Leigh syndrome	3.0 mM	3.4 mM	
		homozygous c.446>A	W15X		~830Da	1 girl, pregnancy complicated by pre-eclampsic syndrome nonconsanguineous us parents	35%	16%	2 weeks	7 months, after a persistent comatose status																					Leigh Syndrome	severe		
		homozygous IVS1nt-1, G>A	Exon 2 skipping			2 sisters first cousin Moroccan parents	48%		2 months	4 months, of major swallowing difficulties, hypoventilation and severe brainstem involvement																					Leigh syndrome	6 < 7 mM	3.9 mM	
Rötig et al., Biochim Biophys Acta 2004	Exon 3,5 deletion	no protein product?			not specified																													
Andersen SL et al J Inherit Metab Dis. 2008 Dec	homozygous c.462delA	N154fsX33			1 boy Ashkenazi Jews parents	88%		3.5 months	10 months																					Leigh Syndrome	1.0 < 9.5 mM	4.5 mM		
Lehinsky-Silver E et al Mol Genet Metab. 2009 Jul	compound heterozygous c.115G>A + c.462delA	N119H + K154fs		~830Da	1 boy non-consanguineous Ashkenazi and Sephardic Jews	54%		8 months	2.4 years, of respiratory insufficiency																					bilateral bright lesions in the medulla, midbrain, and dorsal pons extending into the medulla				
Fassone et al manuscript in preparation	homozygous c.377_384del TAACCTC	Q126fsX2		~830Da	1 girl consanguineous Qatari parents		55%		5 months																					Leigh syndrome	normal	2.8 mM		

TABLE 1: All complex I subunits and assembly factor mutations reported so far. For each mutation, the genetic/proteic defect and the clinical phenotype including the biochemical values are reported. Unless differently specified, the values are referred to the control mean.

1.6 Genetics of Complex I Deficiency

The many causes of complex I deficiency mean that it may potentially be transmitted by any mode of inheritance, including autosomal dominant, autosomal recessive, and X-linked as well as maternal inheritance. The molecular diagnosis of patients with human complex I deficiency is challenging, owing to the large number of potential disease-causing genes, the large degree of clinical heterogeneity among patients and the paucity of genotype:phenotype correlations. The range of clinical presentations in complex I deficiency due to nuclear DNA mutations have been reviewed elsewhere [15,68] and are summarized in Table 1. For a complete list of all the mtDNA mutations associated with complex I deficiency see online: <http://www.mitomap.org/MITOMAP>.

One of the classical presentations is Leigh syndrome, a fatal progressive encephalopathy characterized by bilateral brain lesions affecting the brain stem and/or basal ganglia. Despite being a distinct clinical presentation, Leigh syndrome associated with isolated complex I deficiency can result from mutations in at least 14 different genes (see Table 1). Furthermore, mutations in the same gene can present with very different clinical phenotypes. For example, the first patient with pathogenic mutations in *C20ORF7* presented with lethal infantile mitochondrial disease and died within the first week of life [46]. In contrast, patients have since been reported with mutations in this gene causing mild Leigh syndrome with survival beyond 20 years of age [84]. Likewise, mutations found in *NDUFAF1* led to fatal infantile cardiomyopathy in a young infant [52], but an initially severe hypertrophic cardiomyopathy later improved in a 20-year-old man who first presented at 15 months [51]. A limited number of complex I related genes may be associated with a specific clinical phenotype. For example, most patients reported with mutations in *ACAD9* present with cardiomyopathy and/or exercise intolerance [40,58,59], and patients with mutations in *NDUFAF2* present a particular MRI pattern, with brainstem lesions without changes in thalami and basal ganglia on T2-weighted images [85]. Given the small number of patients reported with mutations in each gene, however, it is difficult to draw definitive conclusions about any genotype:phenotype correlations.

1.6.1 mtDNA mutations

Mutation pathogenicity can be difficult to prove, especially for mutations found in mtDNA since they are often present in heteroplasmic state, and cause disease only when they exceed a certain threshold. Interestingly, recent studies report that

the prevalence of pathogenic mtDNA mutations is 1/200 individuals in the general population, much higher than expected, although not all mtDNA mutations are common, most are rare or even private to individual families [86]. It is likely that some of these individuals may develop milder forms of mitochondrial disease later in life that do not meet the clinical picture for mitochondrial disease diagnosis. Despite the maternal inheritance of the mtDNA, pathogenic mtDNA mutations often arise sporadically and can cause complex I deficiency in families with no suspicion of maternal inheritance [87,88]. Recently, published next generation sequencing and cohort studies found causative mtDNA mutations in 20–30% of patients [39,88,89]. These studies suggest that although the small mtDNA molecule accounts for the complex I deficiency in a substantial number of cases, the majority of cases still have a nuclear genetic basis.

1.6.2 Nuclear DNA Subunit Mutations

Thus far, mutations in 13 of the 38 nuclear-encoded complex I subunits have been described to cause complex I deficiency, including all the seven core nuclear encoded subunits and six of the supernumerary subunits. The first cases of nuclear gene defects underlying complex I deficiency were reported in 1998, in the genes encoding the core subunit NDUFS8 and the supernumerary subunit NDUFS4 [78,77]. To date, a total of about 100 individuals have been reported with causative genetic defects in nuclear-encoded complex I subunits. Among them, ~60% had mutations in core complex I subunits and ~40% had mutations in supernumerary subunits. The fact that most defects are detected in core subunits may reflect a bias in selecting core subunits for sequencing, or that mutations within these genes have more severe consequences. Indeed, it is conceivable that “null mutations”, including nonsense, frameshift and splice site mutations and large gene rearrangements, that cause very little, if any, protein to be expressed, are rare in the core complex I subunit genes and may not be compatible with life. Furthermore, 80% of the mutations identified in core complex I subunit genes were missense mutations and 29% of the mutations identified within supernumerary complex I subunits were missense mutations. This indicates that missense mutations in supernumerary subunits are more likely to be tolerated and may not manifest as clinical disease, in contrast to missense mutations in core subunits.

1.6.3 Assembly Factor Mutations

The first patient with pathogenic mutations in a complex I assembly factor was identified in 2005 [34]. Since this initial report, a total of 47 patients from 27 different families have been described with mutations in complex I assembly factors and there are now nine complex I assembly factors in which mutations are known to cause disease. The most common mutation type found in complex I assembly factors is missense, being 60%, however there seem to be a distribution by type in different genes: for example, there are now 11 pathogenic mutations

described within the *ACAD9* gene, 10 of which are missense mutations; in contrast, there are 8 different pathogenic mutations now described in *NDUFAF2*, all of which are null-type mutations. This may suggest that defects in some proteins that leave them partially functional, such as *ACAD9*, are not as tolerable as perturbations to some others, like *NDUFAF2*. As more diagnoses are made and more data become available, it is likely to become clear which of the complex I assembly factors play the most critical roles in complex I assembly. Table 2 lists all the known and putative complex I assembly factors reported so far. Most of the genes reported in the table have been proposed to have a role in complex I assembly as a result of the studies carried out by Pagliarini and colleagues, who did a phylogenetic profiling, which uses shared evolutionary history to identify functionally related proteins [90].

TABLE 2: *List of the 26 genes that have already been associated with complex I assembly or that have been inferred to be linked with the complex I assembly process. COPP = Complex One Phylogenetic Profile, these proteins were listed in the MitoCarta catalogue and are categorized as COPP Tier 1: 17 MitoCarta genes following phylogenetic signature with known complex I genes: absent in 11 species (*S. pombe*, *A. gossypii*, *C. glabrata*, *S. cerevisiae*, *C. hominis*, *C. parvum*, *P. falciparum* 3D7, *T. annulata*, *T. parva*, *G. lamblia*, *E. cuniculi*), present in a bacterial genome, present in ≥ 1 plant-like species (*A. thaliana*, *O. sativa*, *D. discoideum*, *C. merolae*) and present in ≥ 2 other yeasts (*Y. lipolytica*, *C. albicans*, *P. stipitis*, *D. Hansenii*). Other genes have been linked to complex I assembly because of one or more cases of human disease, or there is a homologue in another species or a mouse model displays a complex I deficiency phenotype.*

INTRODUCTION

Human Genes	Mouse Genes	Aliases	Protein Name	Human Chr	Protein Isoforms	Maestro Score	Function	Evidence	Disease (OMIM)	Number of Patients (Families)	References
<i>NDUFAF1</i>	<i>Ndufaf1</i>	<i>CIA30</i>	NADH dehydrogenase (ubiquinone) 1 alpha subcomplex, assembly factor 1	15	1	7.2636	Complex I assembly factor (mid stage)	Homologue of <i>N. crassa</i> complex I assembly factor; causes human complex I deficiency	Mitochondrial complex I deficiency (252010)	2 (2)	Dunning <i>et al.</i> (2007) [51]; Fassone <i>et al.</i> (2011) [52]
<i>NDUFAF2</i>	<i>Ndufaf2</i>	<i>B17.2, NDUFA12 mimitin</i>	NADH dehydrogenase (ubiquinone) 1 alpha subcomplex, assembly factor 2	5	3	8.3464 – –	Complex I assembly factor (late stage)	Genetic subtraction studies; causes human complex I deficiency	Mitochondrial complex I deficiency (252010)	10 (9)	Ogilvie <i>et al.</i> (2005) [34]; Calvo <i>et al.</i> (2010) [39];
<i>NDUFAF3</i>	<i>4733401H1 8Rik</i>	<i>C3orf60</i>	NADH dehydrogenase (ubiquinone) 1 alpha subcomplex, assembly factor 3	3	4	6.3325 4.1386 4.1386 –	Complex I assembly factor (early stage)	COPP Tier 1; causes human complex I deficiency	Neonatal complex I deficiency (252010)	5 (3)	Saada <i>et al.</i> (2009) [36]
<i>NDUFAF4</i>	<i>1110007M 04Rik</i>	<i>C6orf66</i>	NADH dehydrogenase (ubiquinone) 1 alpha subcomplex, assembly factor 4	6	1	2.6658	Complex I assembly factor	Causes human complex I deficiency	Mitochondrial complex I deficiency (252010)	1 (1)	Saada <i>et al.</i> (2008) [48]
<i>C8ORF38</i>	<i>2310030N0 2Rik</i>	<i>MGC40214</i>	chromosome 8 open reading frame 38	8	8	3.8034	Complex I assembly factor; putative phytoene synthase	COPP Tier 1; causes human complex I deficiency	Leigh syndrome + complex I deficiency (256000)	2 (1)	Pagliarini <i>et al.</i> (2008) [4]

INTRODUCTION

Human Genes	Mouse Genes	Aliases	Protein Name	Human Chr	Protein Isoforms	Maestro Score	Function	Evidence	Disease (OMIM)	Number of Patients (Families)	References
C20ORF7	2310003L2 2Rik	FLJ22324	chromosome 20 open reading frame 7	20	3	7.9214 5.8411 –	Putative methyl-transferase; possible ND1 translational coactivator	COPP Tier 1; causes human complex I deficiency	Neonatal complex I deficiency (252010) and Leigh syndrome (256000)	5 (2)	Sugiana <i>et al.</i> (2008) [46]; Gerards <i>et al.</i> (2010) [84]
FOXRED1	<i>Foxred1</i>	<i>H17</i>	FAD-dependent oxidoreductase domain containing 1	11	3	– 7.9112 –	Probable chaperone protein required for complex I function	COPP Tier 1; causes human complex I deficiency	Mitochondrial complex I deficiency (252010) and Leigh syndrome (256000)	2 (2)	Calvo <i>et al.</i> (2010) [39]; Fassone <i>et al.</i> (2010) [38]
NUBPL	<i>Nubpl</i>	<i>IND1</i>	nucleotide binding protein-like	14	5	6.1646 5.1418 – – –	Needed for insertion of Fe-S clusters into Fe-S-containing complex I subunits	Homologue of <i>N. crassa</i> complex I assembly factor; causes human complex I deficiency	Mitochondrial complex I deficiency (252010)	1 (1)	Calvo <i>et al.</i> (2010) [39]
ACAD9	<i>Acad9</i>	<i>MGC14452</i>	acyl-CoA dehydrogenase family, member 9	3	4	6.6405 – 3.5026 –	Complex I assembly factor; some activity in fatty acid beta-oxidation	Causes human complex I deficiency	ACAD9 deficiency (611126) and Mitochondrial complex I deficiency (252010)	7 (7)	He <i>et al.</i> (2007) [91]; Nouws <i>et al.</i> (2010) [40]; Haack <i>et al.</i> (2010) [59]; Gerards <i>et al.</i> (2011) [58];

INTRODUCTION

Human Genes	Mouse Genes	Aliases	Protein Name	Human Chr	Protein Isoforms	Maestro Score	Function	Evidence	Disease (OMIM)	Number of Patients (Families)	References
ECSIT	<i>Ecsit</i>	<i>SITPEC</i>	ECSIT homolog (Drosophila)	19	3	6.0053 6.0053 -	Cytosolic signalling protein involved in immune response pathways	Co-purifies with NDUFAF1; Mouse model: embryonic lethal (day 7.5)	None known	-	-
C2ORF56	<i>2410091C18Rik</i>	<i>MidA</i>	chromosome 2 open reading frame 56	2	6	10.0319 7.9516 - - -	Putative methyl-transferase required for complex I function	COPP Tier 1	None known	-	-
DHDPSL	<i>0610010D20Rik</i>	<i>HOGA1</i>	4-hydroxy-2-oxoglutarate aldolase 1	10	3	Not in Maestro	Catalyzes final step in metabolic pathway of hydroxyproline	COPP Tier 1	Primary hyperoxaluria type III, HP3 (613616)	4 (4)	Belostotsky <i>et al.</i> (2010) [92]
OXCT2	<i>Oxct2a/Oxct2b</i>	<i>SCOTT</i>	3-oxoacid CoA transferase 2	1	2	5.3157	Key enzyme for ketone body catabolism	COPP Tier 1	None known	-	-
OXCT1	<i>Oxct1</i>	<i>SCOT</i>	3-oxoacid CoA transferase 1	5	5	33.5145 - - - -	Key enzyme for ketone body catabolism (transfers CoA moiety from succinate to acetoacetate)	COPP Tier 1	Succinyl-CoA:3-oxoacid CoA transferase (SCOT) deficiency (245050)	14 patients	Kassovska-Bratinova <i>et al.</i> (1996) [93]

INTRODUCTION

Human Genes	Mouse Genes	Aliases	Protein Name	Human Chr	Protein Isoforms	Maestro Score	Function	Evidence	Disease (OMIM)	Number of Patients (Families)	References
IVD	<i>Ivd</i>	<i>ACAD2</i>	isovaleryl-CoA dehydrogenase	15	5	- - - 5.9903	Catalyzes third step in leucine catabolism	COPP Tier 1	Isovaleric acidemia (243500)	>70 subjects	Vockley <i>et al.</i> (1991) [94];
DCI	<i>Dci</i>	<i>ECI1</i>	enoyl-CoA delta isomerase 1	16	1	30.487	Involved in beta-oxidation of unsaturated fatty acids	COPP Tier 1	None known	-	-
MCCC2	<i>Mccc2</i>	<i>MCCB</i>	methylcrotonoyl-CoA carboxylase 2 (beta)	5	4	16.2556 - 16.2556	Catalyzes carboxylation of 3-methylcrotonyl-CoA to 3-methylglutaconyl-CoA	COPP Tier 1	MCC2 deficiency (609014)	7 (6)	Gallardo <i>et al.</i> (2001) [95];
GPAM	<i>Gpam</i>	<i>GPAT1</i>	glycerol-3-phosphate acyltransferase, mitochondrial	10	3	-4.3375 - -	Catalyzes initial and committing step in glycerolipid biosynthesis	COPP Tier 1	None known	-	-

INTRODUCTION

Human Genes	Mouse Genes	Aliases	Protein Name	Human Chr	Protein Isoforms	Maestro Score	Function	Evidence	Disease (OMIM)	Number of Patients (Families)	References
CTORF10	<i>AF397014</i>	<i>DERP13</i>	chromosome 7 open reading frame 10	7	6	-6.6155 - - -4.4216 -	Similar to members of CaiB/baiF CoA-transferase protein family	COPP Tier 1	Glutaric aciduria type III (GA III; 231690)	7 (5)	Sherman <i>et al.</i> (2008) [96]
AMACR	<i>Amacr</i>	<i>RACE</i>	alpha-methylacyl-CoA racemase	5	5	-5.659 - - - -	Peroxisomal enzyme: interconverts pristanoyl-CoA and C27-bile acylCoAs between their (R)-and (S)-stereoisomers.	COPP Tier 1	Alpha-methylacyl-CoA racemase deficiency (604489)	5 (5)	Ferdinandusse <i>et al.</i> (2000) [97];
PHYH	<i>Phyh</i>	<i>PAHX</i>	phytanoyl-CoA 2-hydroxylase	10	5	0.4795 - - - -	Peroxisomal enzyme: involved in alpha-oxidation of 3-methyl branched fatty acids	COPP Tier 1	Refsum disease (see 266500)	>100	Mihalik <i>et al.</i> (1997) [98];
LYRM5	<i>Lym5</i>	-	LYR motif containing 5	12	1	Not in Maestro	Unknown function	COPP Tier 1	None known	-	-

INTRODUCTION

Human Genes	Mouse Genes	Aliases	Protein Name	Human Chr	Protein Isoforms	Maestro Score	Function	Evidence	Disease (OMIM)	Number of Patients (Families)	References
LACTB	<i>Lactb</i>	<i>MRPL56</i>	lactamase, beta	15	2	-1.0143	Component of large (39S) subunit of mitochondrial ribosome	COPP Tier 1	None known	-	-
AIFM1	<i>Aifm1</i>	<i>AIF</i>	apoptosis-inducing factor, mitochondrion-associated, 1	X	6	41.2378 41.2378 31.3755 - - -	Probable oxidoreductase with dual proapoptotic/ antiapoptotic role	Harlequin mouse model has tissue-specific complex I deficiency	Combined OXPHOS deficiency resulting in a severe mitochondrial encephalomyopathy (COXPD6; 300816)	2 (1)	Ghezzi <i>et al.</i> (2010) [65]
NR2C2	<i>NR2C2</i>	TR4	nuclear receptor subfamily 2, group C, member 2	3	9	-6.9019 - - - - - -	Orphan nuclear receptor can act as a repressor or activator of transcriptional coactivator of NDUFAF1?	Mouse model	-	-	Liu <i>et al.</i> (2011) [53]

1.7 Mouse Models for Nuclear DNA-encoded Mitochondrial Complex I Deficiency

In order to study the effect of therapeutic compounds, many disease models have been described, both at the cell and organism level. Many attempts to create mouse models for OXPHOS deficiencies have failed because of embryonic lethality [99].

1.7.1 The Harlequin mouse

Attempts to create *Aif* (apoptosis inducing factor)-null mice by homologous recombination have been unsuccessful because *Aif*'s mitochondrial function is indispensable for cell survival during either early or advanced embryogenesis, depending on the knockout strategy and the genetic background [100]. This problem has been bypassed by producing the Harlequin (Hq) mice, which bear an ectopic proviral insertion in intron 1 of the X-linked *Aif* gene, leading to a 80% decrease in *Aif* expression and a substantial reduction in complex I activity [101]. This hypomorphic *Aif* mutation is tolerable and has no major effect on mouse development yet impacts severely on the aging organism [100]. Hq mice develop progressive ataxia and blindness due to the progressive loss of terminally differentiated cerebellar and retinal neurons. Moreover, signs of severe oxidative stress and degenerating mitochondria were detected in the brain of Hq mice [100]. Complex I dysfunction was revealed in the degenerating Hq tissues (retina, cerebellum, thalamus, cortex, optical nerves), less so in the skeletal muscle and not at all in other organs (heart, liver, testis) [100], unraveling a hitherto unexplained organ-dependent heterogeneity in the manifestation of genetically determined mitochondrial defects. Apoptosis-inducing factor (AIF) is a flavoprotein located in the mitochondrial intermembrane space [102] that contributes to apoptosis, but it also plays a role in neuronal cell survival by maintaining mitochondrial structure [103]. Although AIF itself is not part of complex I, it seems to play a crucial role in complex I biogenesis and/or maintenance [104].

Clinically, hemizygous males (Hq/Y) and homozygous females (Hq/Hq) exhibit a heterogeneous phenotype, with a wide intrapopulation variation in onset and severity of the symptoms [104]. These mice develop progressive cerebellar ataxia at 3 months of age, with loss of cerebellar neurons (interestingly readily evidenced at 15 days of age) occurring in all but 8% of the mice [104], in contrast to the human patients with *AIF* mutations, who presented with an early-onset progressive mitochondrial encephalomyopathy and neurological and psychomotor development abnormalities [65]. Hearts of Harlequin mice have a higher risk of hypertrophic cardiomyopathy and are highly sensitised to ischaemia-reperfusion injury [105,106]. Ocular pathology includes ocular hypoplasia in 20% and absence of the optic nerve in 40% of the mice [104,101]. Biochemical measurements show a reduction of complex I activity in cerebellum, cerebrum, skeletal muscle, retina and optic nerves and, to a lesser extent, in spinal cord and kidney, in contrast to the patients who displayed complex III and IV deficiency in fibroblasts and multiple RC deficiencies in muscle [65]. Normal complex I activity is observed in Hq mouse

heart, liver and testes. At the histology level, Hq mutant mice are normal until 3 months of age. At 4 months, hallmarks of early neuronal and retinal degeneration are noted [101], as well as astrocytosis with extensive vascular proliferation [64]. Retinal cell loss appears at 4 months of age, progressing to blindness at 10 months [101]. Heterozygous females are histologically and clinically normal until 26 months of age [101].

1.7.2 The *NDUFS4*-knock out mouse

In 2008 the Palmiter group created the first complex I deficient mouse, the “*Ndufs4*-knock out (KO) mouse”, by deleting the second exon of the gene using loxP flanking in embryonic stem cells, after which heterozygous mice were interbred to create the homozygous mutant KO mouse [107]. In humans, the *NDUFS4* gene localizes at chromosome 5 and encodes the complex I 18 kDa subunit (AQDQ) protein, located in the peripheral arm of the complex [108]. The *NDUFS4* gene is considered to be a mutational hotspot. KO mice show a significant failure to thrive and reversible hair loss, but there are no additional major clinical symptoms until about the fourth to fifth week of life. By postnatal day 30 (P30), the mice become lethargic and are unable to maintain body temperature (~2°C lower than that of wild type mice). By P35 they have become severely ataxic and show muscle weakness. Some of the older KO mice have defective vision, including the development of cataracts and the inability to open their eyes completely, and, by P35, the mice are deaf. Approximately 30% of the mice develop epilepsy. Between P35 and P50, KO mice stop grooming and gaining weight, display worsening of ataxia and eventually die. Mice heterozygous for the deleted *NDUFS4* gene are indistinguishable from wild type mice [107]. Complex I activity in the liver of mutant mice is approximately half that of controls, other complexes show normal activity, except for a minor decline in complex III activity. Blue native gel electrophoresis shows that the amount of intact complex I is reduced in mitochondria of KO mice.

Southern blot analysis indicates a normal mitochondrial genome number; histological evaluation of KO muscle fibers show normal mitochondrial ultrastructure, but large subsarcolemmal clusters are present in the soleus but not in the extensor digitorum longus. Mitochondrial morphology is normal, and there is no sign of ragged red fibres (RRFs), in keeping with the histological findings in human patients with *NDUFS4* mutations. Human patients with the *NDUFS4* mutations show failure to thrive, hypotonia, and basal ganglia abnormalities, and almost all patients have elevated lactate levels [109,110]. *NDUFS4* KO mice exhibit a clinical pattern of failure to thrive, lethargy, and elevated lactate and brainstem symptoms, such as hypothermia, deafness and blindness, which are commonly seen in Leigh syndrome. As in mice, in patients with *NDUFS4* mutations there is a failure of assembly of a normal, functional complex I in the inner mitochondrial membrane, which leads to reduced complex I content and activity [108].

1.8 Approaches to Treatment of Complex I Deficiency

Current strategies being developed to treat mitochondrial disease include (1) gene therapy (replacement or repair), (2) controlled regulation of specific transcriptional regulators, (3) metabolic manipulation (ROS scavenging, normalisation of the mitochondrial membrane potential ($\Delta\psi$), restoration of the endoplasmic reticulum Ca^{2+} content and/or normalisation of mitochondrial Ca^{2+} sequestration during hormonal stimulation) and (4), in the case of complex I deficiency of mtDNA origin, alteration of the balance between wild-type and mutated mtDNA (e.g. by exercise training) (Fig. 5). The effect of some of these interventions has already been explored in humans, while others are still at the level of single-cell research.

The risk of oxidative damage can be reduced by supplementation with scavenging enzymes or molecules to decrease mitochondrial ROS levels and downstream oxidative damage. This can be done by overexpression of naturally occurring scavenging enzymes such as SODs [111-113], supplementation with naturally occurring antioxidants such as glutathione [114,115] or treatment with scavenging compounds targeted to the mitochondria by lipophilic cation delivery. Examples of such compounds include MitoQ₁₀ [116], SkQs [117], and resveratrol [118]. Nutritional cofactor treatment by combined administration of multiple compounds (i.e., riboflavin + carnitine) has already been tested in patients with mitochondrial disease and proved to improve exercise capacity/tolerance and muscle tone and decrease serum lactate and pyruvate levels [119]. Unfortunately, high-dose vitamin and cofactor treatment and high-fat diet are well-tolerated with short-term application but ineffective in the longer-term [120].

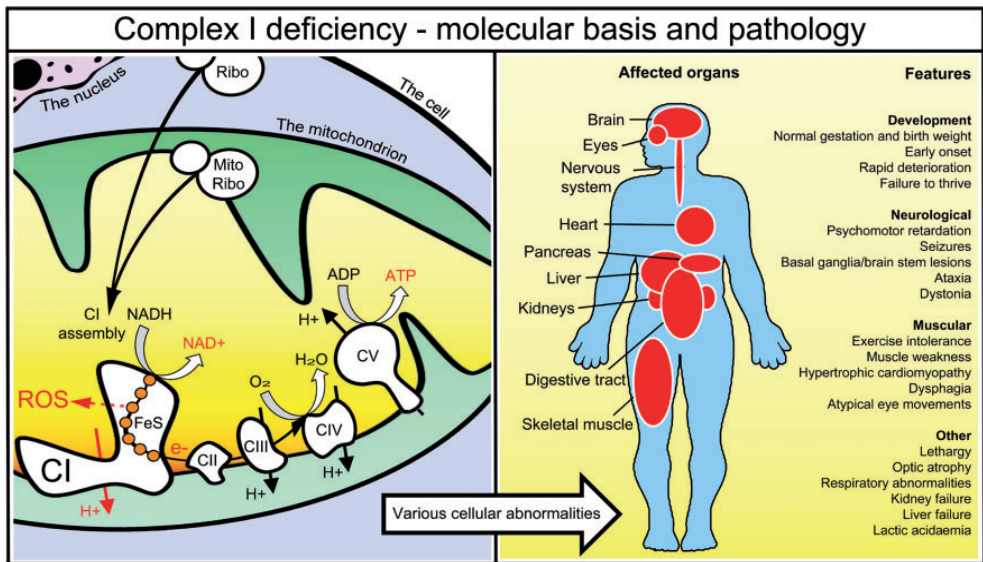


FIGURE 5: *The molecular basis and pathology of complex I deficiency. Left: complex I is part of a system of five enzyme complexes (CI–CV) embedded in the mitochondrial inner membrane, which together perform OXPHOS. In this system, complex I oxidizes NADH to transfer electrons to acceptor ubiquinone via a series of Fe-S clusters. In turn, this leads to proton translocation across the mitochondrial inner membrane to maintain a proton gradient required for complex V to produce ATP. Complex I is assembled from nuclear subunits translated by cytosolic ribosomes (Ribo) and mitochondrial subunits translated by the mitochondrial ribosome (MitoRibo). Disturbances in the assembly and/or stability of the complex can result in reduced conversion of NADH to NAD⁺, reduced proton translocation, increased release of ROS, and can ultimately lead to reduced ATP production and the accumulation of lactate. Deficiency of complex I can lead to various cellular abnormalities and apoptosis, which translates into a heterogeneous disease phenotype (right). Affected organs are primarily those with energy-demanding tissue, such as the nervous system, muscle, liver and kidneys. Complex I deficiency is generally an early onset, progressive multisystem disorder featuring severe neurological and muscular problems (picture taken from Nouws J et al. Brain. 2011 Oct).*

Notably, patients bearing mutations in ACAD9 are riboflavin responsive; this is a major breakthrough in the complex I deficiency field. After riboflavin treatment, complex I activity increased from 17 to 47% in the patient described by Gerards *et al.* [58]. However, riboflavin treatment has not extensively been documented. Previous reports showed clinical and biochemical improvements in small groups of patients with complex I deficiency [121,122], but not in a larger study of 16 patients [123]. Until now, riboflavin responsive complex I deficiency has only been described in patients with predominantly myopathic presentations. It is therefore unlikely that riboflavin will be beneficial for all patients with complex I deficiencies, but it may be for a well-defined subgroup. Riboflavin supplements are likely to increase intra-mitochondrial FAD concentration favouring FAD binding, which is important for the catalytic activity of flavoproteins as well as for their folding, assembly and/or stability [124,125]. It has been suggested that raising the intramitochondrial FAD concentration may compensate for a decreased folding capacity of mutant flavoproteins [126]. It is probable that the defect identified in the patients disturbs ACAD9 folding or its catalytic activity which may result in a reduction in FAD binding; riboflavin supplementation might compensate the defect by increasing the FAD binding and therefore contributing to an amelioration of the patient's complex I deficiency. An alternative or additional effect of riboflavin treatment in patients might be enhancement of the assembly of complex I and complex IV [127], which, together with complex III, are part of the respiratory chain supercomplexes.

Another treatment with CGP37157, a benzothiazepine drug inhibiting the mitochondrial sodium/calcium (Na⁺/Ca²⁺) exchanger, restored mitochondrial Ca²⁺ uptake and ensuing Ca²⁺-stimulated mitochondrial ATP production in cybrid cells

with the tRNALys mutation associated with MERRF syndrome (Myoclonic Epilepsy with Ragged Red Fibers) [128]. Similarly, this compound normalised the hormone-induced increase in mitochondrial Ca^{2+} concentration, Ca^{2+} -stimulated mitochondrial ATP production and ATP-dependent restoration of the resting Ca^{2+} concentration in fibroblasts of children with isolated complex I deficiency due to a mutation in the *NDUFS7* gene [129] or the *NDUFS4* gene [130,131].

In conclusion, theoretically interventions to mitigate or cure mitochondrial disorders can occur at the genetic, metabolic, or cell biological level and may include prevention of disease transmission from mother to child, gene therapy, exercise training, metabolic manipulation, and regulation of transcription [132]. However, a deeper understanding of complex I deficiency biology, along with more cellular, animal, and clinical studies is required to provide better clinical support and to develop efficient treatments.

2 AIM OF THE THESIS

Mitochondrial diseases are a heterogeneous group of diseases displaying a variable degree of dysfunction of the mitochondrial OXPHOS system, which is demonstrated by rigorous morphologic investigations, and biochemical and genetic methods. Isolated deficiency of complex I is the most commonly identified biochemical defect in childhood-onset mitochondrial disease [15], and accounts for ~1/3 of all cases of OXPHOS disorders [13]. This study aims to elucidate the genetic defect underlying the clinical phenotype and the biochemical impairment in a cohort of 12 complex I deficient patients.

The research project has been organised as follows:

- Collection of clinical data, patients' consent to study their tissues and DNA, biochemical analysis of the mitochondrial respiratory chain activity and mitochondrial DNA (mtDNA) sequencing on patients' muscles (carried out by the diagnostic laboratories' staff, at the National Hospital for Neurology, Queen Square, London). In this phase all the clinical information about the patients and their families and the grade of impairment of the respiratory chain activity via the analysis of the muscle tissue were gathered. The sequencing of the mtDNA excluded any pathogenic mutation in the molecule, leaving the search for the mutation focused on the nuclear genome only.
- Analysis of the holo-enzyme complex I in its native form via Blue native gel electrophoresis and enzymatic test of mitochondrial complex I activity in patients' fibroblasts. During this phase a few more clues regarding the biochemical defect were collected so that a first hypothesis regarding the underlying genetic defect in these patients could be made.
- Considering the pattern of the complex I assembly and the subassemblies, an initial screening was performed of nuclear genes that were considered good candidates, based on review of the literature and the patients' clinical/biochemical features. Also, homozygosity mapping analysis was carried out in suitable pedigrees to search for homozygous regions in the genome that were shared between the affected subjects. This was followed by bioinformatics analysis to prioritise the genetic screening by ranking the genes on the basis of their function, mitochondrial localisation and biological pathway.

- Identification of the specific molecular defect in patients by candidate gene sequence analysis, proof of segregation in the patients' pedigrees and sequencing of ethnically-matched controls. At this stage the presence of the mutation was confirmed in patients and parents and excluded in controls. An amino acid conservation table was also produced for each mutation.
- To further characterize the pathogenic effect of the identified mutations, functional studies were carried out on patients and control fibroblasts. These studies included Western blot to determine the levels of the mutant protein, complementation and silencing studies via lentiviral transduction to restore or reproduce the biochemical phenotype observed in the patient, and sub-mitochondrial localisation to verify the sub-cellular localisation of the protein.

3 MATERIALS and METHODS

3.1 Patient Cohort

In this study a cohort of 12 paediatric patients (from 11 families) with isolated complex I deficiency was investigated.

- Families 1-3: 4 girls from the Middle East area presenting with the same clinical phenotype were recruited for analysis.
 - Patient 1 (family 1): MRI revealed bilateral signal abnormality in the basal ganglia suggestive of Leigh syndrome. Plasma lactate was normal at 1.4mmol/l, but CSF lactate was mildly elevated at 2.8mmol/l, as was the CSF protein at 0.48g/L. Together these results were taken as Leigh syndrome presentation. Biochemical analysis of a muscle biopsy revealed isolated deficiency of respiratory chain complex I. PDHc activity was normal in cultured skin fibroblasts. She died at 5 months of age.
 - Patient 2 (family 1) is the first cousin of Patient 1, this baby girl was born to double first cousin parents who have two healthy older children. She showed metabolic acidosis with increased blood concentrations of lactate (2.6 – 6.8 mmol/l). The CSF lactate was normal at 1.5 mmol/l, subsequently developed recurrent episodes of hypoglycaemia associated with lactic acidosis and vomiting. She developed severe hypoglycaemia. Muscle biopsy was performed at 6 years and revealed a moderate increase in intracytoplasmic lipid deposition, with no ragged red fibres or COX negative fibres. Biochemical analysis demonstrated multiple respiratory chain deficiencies in muscle
 - Patient 3 (family 2) was the fourth child of healthy unrelated parents. She presented with generalised hypotonia, persistent lactic acidosis and Leigh syndrome. Biochemical analysis of a muscle biopsy revealed isolated deficiency of respiratory chain complex I. She developed respiratory failure and died at 3 months of age.
 - Patient 4 (family 3) had cardiomyopathy and a persistent lactic acidosis and biochemistry examination suggested disturbed fatty acid oxidation. Muscle histology revealed excess lipid deposition within the muscle fibres. There were no ragged red fibres or any COX negative fibres. Biochemical analysis of the muscle demonstrated isolated deficiency of complex I.
- Family 4: Patient 5 is the sixth child of healthy Iranian-Jewish first cousin parents. Two sisters and three brothers are unaffected. Pregnancy was uneventful, but soon after birth severe truncal hypotonia was noted. There have

never been any voluntary movements. During the first year, he was extremely irritable with prolonged periods of inconsolable crying. Muscle biopsy was performed at 4 months of age because of persistent elevation of lactate in plasma (6.8 mM, normal 2.1 mM) and CSF (4.3 mM, normal 1.8 mM). Muscle histology was normal, but biochemical analysis revealed isolated deficiency of complex I in muscle mitochondria (7% of the control mean, normalized for citrate synthase activity), with normal activity of other respiratory chain enzyme complexes. He developed progressive microcephaly, and brain MRI at 8 months revealed delayed myelination, ventricular dilatation and abnormal signal in the thalami and basal ganglia. Myoclonic jerks were present from 1 year but at 5 years responded to lamotrigine and clonazepam therapy. Eye movements have always been roving, with no evidence of visual function, and visual evoked potentials demonstrated absent cortical responses at 6 months of age. Bilateral optic atrophy was noted at 2 years. Hearing appears to be normal. Echocardiography revealed mild non-obstructive left ventricular hypertrophy. Poor feeding was present from birth, and from 5 years he has been fed by gastrostomy tube. He has had persistent hepatomegaly with normal liver transaminases and no signs of liver failure or cholestasis. He has had severe scoliosis from 5 years, treated with a corset. He was treated with riboflavin, uridine, creatine, lipoic acid, dichloroacetate and thiamine, without any obvious clinical response. He was 10 years old at the time of enrolment into the study.

- Family 5: Patient 6, the first child of healthy unrelated French parents, was born at 37 weeks of gestation weighing 3.17 kg. The neonatal period was unremarkable, and early developmental milestones were normal. She was first presented to medical attention at 6 months with an episode of respiratory-syncytial-virus-positive bronchiolitis, which was managed conservatively with nasogastric tube feeding. Following discharge, she became more unwell, with pallor, poor feeding, sweating and weight loss of 380 g. At 6.5 months, she presented to the emergency department in cardiogenic shock (O_2 saturation of 90%, heart rate of 180 beats/min and hepatomegaly palpable at 5 cm below the inferior costal margin). Initial blood gas values revealed metabolic acidosis (pH 6.86; base deficit, 22 mM). Before retrieval to the regional cardiac intensive care unit, she was intubated and ventilated; given intraosseous volume replacement, antibiotics and bicarbonate; and started on dopamine infusion. Echocardiogram demonstrated pericardial effusion, biventricular hypertrophy and mild to moderate left ventricular (LV) dysfunction (fractional shortening, 25%). Both atria were enlarged, and there was evidence of diastolic impairment. Apical views showed trabeculation suggestive of noncompaction of the left ventricle (NCLV). Coronary artery anatomy was normal. Despite positive pressure ventilation and inotropic support with dopamine and adrenaline, she remained hypotensive and acidotic (pH 7.2; base deficit, 19 mM), with an elevated blood lactate level (9 mM; reference, <2 mM). The acidosis did not improve, and cardiac function continued to deteriorate. Venous-arterial extracorporeal membrane oxygenation (ECMO) was commenced on day 2 of her critical illness.

The combination of echocardiographic appearances and persistent lactic acidosis on full ECMO support led to the suspicion of an inborn error of metabolism. Urine organic acid analysis demonstrated marked excretion of lactate, pyruvate, ketones and Krebs cycle intermediates (fumarate, malate and 2-oxoglutarate), as well as moderately increased levels of glutarate and 3-hydroxyglutarate. This profile was consistent with, although not diagnostic of, a mitochondrial respiratory chain disorder. Plasma acylcarnitine analysis revealed moderately elevated hydroxybutyrylcarnitine but no other abnormalities. Cranial ultrasound results were normal, and electroencephalographic findings were consistent with a sedated critically unwell infant.

Muscle biopsy showed no ragged-red or cytochrome-c-oxidase negative fibres, but there was increased lipid deposition. Electron microscopy demonstrated accumulation of enlarged and abnormal mitochondria. Spectrophotometric analysis of respiratory chain enzyme activities revealed severe isolated deficiency of complex I in skeletal muscle, with 25% residual activity compared to the lowest control (Patient 6 complex I activity, 0.026; reference range, 0.104-0.268 (ratio to citrate synthase activity)). The activities of complexes II+III and IV were normal. Forty-eight hours after continuous veno-venous haemofiltration was stopped, blood lactate levels rose to 17-18 mM despite maximal medical treatment for low cardiac output, including inotropes, cooling, sedation and muscle relaxation. Cardiac reserve was minimal. On day 24 of her critical illness, she had cardiorespiratory arrest requiring two doses of epinephrine. Output was briefly re-established, but she died later that night.

Postmortem examination revealed an enlarged globular heart (weight, 93 g; weight expected for age, 34 g). Sections from the myocardium showed myocardial hypertrophy without evidence of disarray, but with foci of myofibre loss and replacement fibrosis, focal haemorrhage and haemosiderin deposition within the centres of the LV papillary muscles, and a mild degree of LV endocardial fibrosis. There was no myocarditis. Liver histology revealed marked zonal macrovesicular steatosis. Respiratory chain enzyme activities in the liver were normal (complex I, 0.207; reference range, 0.054-0.221).

- 6 further individual patients (Patients 7-12) from non-consanguineous families were included in the analysis as they all showed isolated complex I deficiency in muscle and clinical features of mitochondrial disease.
- 1 positive control (complex I deficient Patient already genetically diagnosed with *ACAD9* mutations) and 3 negative controls (without mitochondrial disease) were used to compare the results.

All samples were taken after informed patient/parental consent had been obtained, and the study was approved by the local ethics committee.

3.2 Cell culture methods

Fibroblasts from patients' skin biopsies were cultured in DMEM (containing 110 mg/l sodium pyruvate and 4.5 g/l glucose, Gibco), complemented with 10% heat inactivated Fetal Bovine Serum (FBS, Sigma), 100 µg/ml penicillin/streptomycin (10 U/µl penicillin G sodium, 10 µg/µl streptomycin sulphate in 0.85% saline, Gibco), and 1 µg/ml of fungizone (amphotericin B solution sterile-filtered in deionized water, Sigma). Also, as the patients in these study had a respiratory chain defect and it is well known that these defects can inhibit the production of the uridine necessary for nucleic acid synthesis [133], exogenous uridine (Sigma) was added to a final concentration of 50 mg/l. Cells were grown in 175 cm² flasks with 20ml of medium and incubated at 37°C with CO₂ levels set at 5%. At least 1 confluent flask per assay was used, and trypsinization was the standard method used to detach the cells, after 1 wash in 10ml of PBS (Dulbecco's Phosphate Buffered Saline, Sigma). All subsequent steps were carried out on ice wherever possible.

3.3 Biochemical studies

3.3.1 Complex I/Complex IV microplate and dipstick assays

The patients' biochemical defects were confirmed in cultured skin fibroblasts by using either the complex I/complex IV activity dipstick assay or the complex I/IV activity microplate assay (both by MitoSciences). Activities of complexes I and IV were determined in whole cell lysates of patient and control fibroblasts performed according to the manufacturer's instructions (MitoSciences). Cells were lysed by adding the detergent provided in the kit and leaving them on ice for 30 minutes, then the samples were centrifuged at 12,000 g for 20 minutes to collect the membrane debris at the bottom of the tube and separate the supernatant containing proteins. Protein concentration was determined via the Bradford method [134] on the spectrophotometer. The Bradford assay is a colorimetric protein assay based on an absorbance shift of the dye Coomassie Brilliant Blue G-250 in which under acidic conditions the red form of the dye is converted into its blue form to bind to the protein being assayed. The binding of the protein stabilizes the blue form of the Coomassie dye; thus the amount of the complex present in solution is a measure for the protein concentration, and can be estimated by use of an absorbance reading at 595 nm.

The microplate kit is based on the principle of the immunocapture of the complex I or IV at the bottom of the well by a monoclonal antibody pre-bound to the wells; then the appropriate substrate is added and the colorimetric reaction is read by the spectrophotometer as a change in the absorbance.

100 µg of proteins for the complex I assay and 20 µg for the complex IV assay, as suggested by the manufacturer's instructions, and 200 µl of these samples were loaded onto the wells of the microplate. After 3 hours of incubation at room temperature, the microplate was emptied and the wells were rinsed 3 times with

300 μ l of washing buffer. Then 200 μ l of assay solution was added to each well and the absorbance was read every minute for 30 minutes (at room temperature), at 450 nm for complex I, and every minute for 120 minute (at 30°C), at 550 nm for complex IV. During this time the complex I activity is determined by following the oxidation of NADH to NAD⁺ and the simultaneous reduction of a dye which leads to increase absorbance at 450 nm; whereas the complex IV activity is colorimetrically determined by following the oxidation of reduced cytochrome c as an absorbance decrease at 550 nm. A similar principle applies to the dipsticks kit as well. First complex I is immunocaptured (i.e. immuno-precipitated in active form) on the dipstick, then the dipstick is immersed in complex I activity buffer solution containing NADH as a substrate and nitrotetrazolium blue (NBT) as the electron acceptor. Immunocaptured complex I oxidizes NADH and the resulting H⁺ reduces NBT to form a blue-purple precipitate at the complex I antibody line on the dipstick. The signal intensity of this precipitate corresponds to the level of complex I enzyme activity in the sample and may be analysed by a standard imaging system. 30 μ g and 100 μ g of protein extract diluted at 1mg/ml from whole cell lysate for complex I and IV assay respectively, were allowed to be absorbed by the dipstick for 45 minutes, then 30 μ l of washing buffer was added to the dipstick and subsequently 300 μ L of activity buffer solution per dipstick was added, the developing time was 60 minutes. The reads were taken in an optical scanner and the densitometry measurements were carried out using Alpha Ease FC software (Alpha Innotech/Cell Biosciences, Santa Clara, CA, USA). All measurements for both microplate and dipstick assay were done in triplicate and the results expressed as the complex I/complex IV activity ratio for each sample and compared with the fibroblast control range.

3.3.2 Preparation of crude mitochondrial pellets with digitonin (mitoplasts)

At least 1 million of cells were harvested by trypsinization, cells pellets were washed in 5ml PBS supplemented with protease inhibitors (1 mM phenylmethylsulfonyl fluoride (PMSF), 1 μ g/ml of leupeptin and 1 μ g/ml of pepstatin A, all Sigma). From this point onwards all procedures (including centrifugations) were carried out on ice at 4°C. The cells were resuspended in 1ml ice-cold homogenisation buffer (10mM Tris-HCl pH 7.4, 1 mM sodium EDTA (Ethylenediaminetetraacetic acid), 250 mM sucrose, 1 mM PMSF, 1 μ g/ml of pepstatine A, 1 μ g/ml of leupeptine; protease inhibitors were added to the ice-cold buffer shortly before use). Cells were pelleted by centrifugation at 3000 g for 5min and then resuspended in 200 μ l of digitonin per million of cells. After 15 min on ice, cells were centrifuged at 13,000 rpm for 1 min; supernatant was discarded and cells washed once in 500 μ l of PBS with inhibitors, then recollected at the bottom of the tube by centrifugation and resuspended in 200 μ l of PBS with inhibitors. The Bradford method [134] on the spectrophotometer was used to determine protein concentration.

3.3.3 Blue Native studies

Blue native polyacrylamide gel electrophoresis (BN-PAGE) separations were run in non-denaturing conditions by using the Coomassie Brilliant Blue dye to provide the necessary charges to the protein complexes for the electrophoretic separation [135]. Detergents are used only to the extent that they are necessary to lyse lipid membranes in the cell. BN-PAGE is generally used to visualise intact protein complexes, which remain, for the most part, associated and folded as they would be in the cell.

Assembled respiratory chain complexes were detected using BN-PAGE, using a method adapted from Shägger [136]. 12% and 4% separating gel mixes and a 3% stacking gel mix were made up using acrylamide-bis (48% acrylamide, 1.5% bis), 3x gel buffer (1.5 M 6-aminocaproic acid, 150 mM bistris), APS and TEMED. 7 ml of the high and low percentage separating gel mixes were pipetted into the wells of the gradient gel pouring equipment. When the gels had set, the 3% stacking gel was added on top of the high percentage gel and combs placed into position. The gels were sealed with clingfilm and left overnight, or for up to a week at 4°C. All mitochondrial protein preparations (mitoplasts) were diluted to the same concentration (~10 µg in 200 µl final volume) using PBS and protease inhibitors in 10% loading buffer (1M 6aminocaproic acid, 5% Serva blue G), and 15–20 µl of the sample was loaded onto the gels to be used for immunoblotting. Blue native gels were run at 100 V for 20 minutes, then at 4 mA constant current per gel using anode buffer (50 mM bistris, pH 7.0) and cathode buffer A (50 mM tricine, 15 mM bistris, 0.02% Serva blue G, pH 7.0). After the run, the gels were electrotransferred to Hybond-P membrane (GE Healthcare) after this had been wetted in methanol, then equilibrated in Towbin's buffer (TB, 25 mM tris-base, 192 mM glycine, 20% methanol). Electrotransfer was carried out at 100 V for 75 minutes, then the membranes were left overnight to air dry. The next day 2 washes in methanol helped to remove the excess of Serva blue G; the membranes were then equilibrated in PBS until they sank, before being blocked for 1 hour in 10% (w:v) milk powder dissolved in PBS. The blots were placed into 50ml falcon tubes with the protein side facing in and washed 3 times for 3 minutes in 3 ml PBS-T (PBS + 0.3% Tween-20) on roller mixer. Primary antibodies were added (see Table 3 for concentration used) and blots were incubated on the roller mixer for 2 hours. Blots were washed 3 times in PBS-T as before. 3ml of secondary antibody (1/4,000 PBS-T dilution of either goat anti-mouse or goat anti-rabbit conjugated to horseradish peroxidase, Dako) was added. Incubation was for 1 hour. Blots were washed 3 times in PBS-T as before and then developed by using the Western Lighting Chemiluminescence Reagent Plus (Perkin Elmer), with chemiluminescence photographic film for detection of signal. Exposure times of 15s – 15min were used.

During the development, the horseradish peroxidase enzyme (HRP) that is tethered to the antibody of interest catalyses the conversion of the enhanced chemiluminescent substrate into a sensitized reagent in the vicinity of the molecule of interest, which on further oxidation by hydrogen peroxide emits light. 143B206 ρ^0 cells lacking mitochondrially-encoded proteins were obtained as described in King MP&Attardi G [137]. Equal loading was confirmed by reprobing blots with anti-

SDHA, anti-ATP5A1, anti-UQCR2 and anti-MTCO1 antibodies (MitoSciences) (see Table 3 for antibodies dilutions).

3.3.4 Western blot studies

Western blot analysis was performed as described in Williams SL *et al.* [138]. Whole cell lysates were extracted from at ~1 million of cultured fibroblasts and samples were prepared by combining equal amounts of mitochondrial protein preparations with a similar volume of 2x dissociation Buffer (2x DB: 100 mM Tris-HCl pH 6.5, 24% (v/v) glycerol, 8% (w/v) SDS (Sodium Dodecyl Sulfate), 4% (v/v) β -mercaptoethanol, 0.02% (w/v) bromophenol blue). 15-20 μ l was loaded and run into a 12/15% SDS-polyacrylamide gels, 3% stacking gel, and gels were run at 100 V for 15 minutes and then 200 V for 1h. Gels were then electrotransferred to Hybond-P membrane (GE healthcare) as described above, and probed with anti-FOXRED1 antibody (Abnova), anti-VDAC, anti-cytochrome *c* (MitoSciences), and antibodies directed against other complex I subunits and assembly factors listed in Table 3. The secondary antibody was goat anti-mouse or goat anti-rabbit conjugated to horseradish peroxidase (Invitrogen). Developed was carried out by using the Western Lighting Chemiluminescence Reagent Plus (Perkin Elmer), with chemiluminescence photographic film for detection of signal. Exposure times of 15s-15min were used. Densitometry measurements were carried out using Alpha Ease FC software (Alpha Innotech, Cell Biosciences) (see Table 3 for antibodies dilutions).

3.3.5 Submitochondrial fractionation

Mitochondria from 20 confluent 10-cm plates of cultured HeLa S3 cells (a subclone of the HeLa cell line which have been reported to contain human papilloma virus 18 (HPV-18) sequences, as described by Puck and Fisher [139]) were harvested by trypsinisation and isolated by differential centrifugation as reported previously [140]. In particular, cells were washed, pelleted and then resuspended in 5 ml ice-cold homogenisation buffer (10 mM Hepes-NaOH (pH 7.4), 1 mM sodium EDTA, 250 mM sucrose plus protease inhibitors: 1 mM PMSF, 1 μ g/ml of pepstatin A, 1 μ g/ml of leupeptin). Samples were centrifuged at 1,500 g for 10 min to pellet nuclei, and the supernatant was transferred to a clear centrifuge tube; a second centrifugation at 11,500 g for 12 min separated the mitochondria (pellet), which was then resuspended in 100 μ l of homogenisation buffer to be stored. To subfractionate mitochondria, the swell-shrink procedure was used as described [141], except that the inter-membrane space (IMS) was further purified by extraction in 10 mM Hepes-NaOH (pH 7.4), 0.5 mM EDTA, 125 mM sucrose and 0.5% (v/v) Triton X-100 on ice for 30 min, followed by centrifugation at 160,000g, 4°C for 1 h. This procedure uses the action of osmotic and mechanical methods to disrupt mitochondria in order to separate the mitochondrial inner and outer membrane and benefits from the action of substances, such as KH_2PO_4 (pH 7.4) and sucrose plus glycerol, which induce both a pronounced shrinkage of the matrix and a loss of contact between the inner and outer membrane. Mitochondrial pellet

was resuspended in 1 ml of cold 10 mM KH_2PO_4 (pH 7.4) supplemented with protease inhibitors, to which was added cold 32% sucrose (w/v), 30% glycerol (v/v), 10 mM MgCl_2 , 10 mM KH_2PO_4 (pH 7.4) and the samples were left on ice for 30 min. Samples were then centrifuged at 12,000 g, 4°C for 10 min to collect the mitoplasts at the bottom of the tube and the supernatant. Mitoplasts were resuspended in 2 ml of cold 10 mM KH_2PO_4 (pH 7.4) and protease inhibitors, left on ice for 30 min, and subjected to ultracentrifugation at 160,000 g, 4°C for 30 min. After this, the supernatant was stored as mitochondrial matrix fraction and the pellet as inner membrane fraction. The supernatant of the previous step was subjected to ultracentrifugation on a Sorvall Discovery™ 100 SE Centrifuge at 160,000 g, 4°C for 30 min to separate the supernatant (mitochondrial intermembrane space fraction) from the pellet (outer membrane fraction). Fractions were resuspended in a small volume of homogenisation buffer and then stored at -80°C prior to the electrophoretic run. To distinguish soluble and peripheral membrane proteins from integral membrane proteins, mitochondria were extracted with the alkaline carbonate method [142]. The alkaline carbonate method allows the release of soluble proteins that would normally stay associated to the membranes by using other extraction methods. Mitochondrial pellets were resuspended in 2 ml 100 mM Na_2CO_3 (pH 11.5) plus protease inhibitors and incubated on ice for 30 min. After ultracentrifugation at 160,000 g, 4°C for 30 min, the supernatant (soluble and peripheral membrane proteins) and pellet (integral membrane proteins) were collected. Fractions were resuspended in a small volume of homogenisation buffer and the stored at -80°C prior to the electrophoretic run. Purity of the subfractionated mitochondrial compartments was tested by probing with antibodies to detect a specific marker for each submitochondrial fraction: VDAC was used as an outer membrane (OM) marker, cytochrome *c* for the intermembrane space (IMS) and MTCO1 for the inner membrane (IM) (see Table 3 for the dilutions used).

Antigen	Reactivity	MW in kDa	Primary Antibody Dilution	Secondary Antibody Host	Company
MTND1	human	39	1:1,000	mouse	kind gift from Dr A Lombès
MTCO1	human	~56	1:500	mouse	MitoSciences
NDUFA9	human, mouse, rat, bovine	39	1:500	mouse	MitoSciences
NDUFB6	human, mouse, rat, bovine	~17	1:1,500	mouse	MitoSciences
NDUFAF1	human, mouse, rat	~36	1:1,000	rabbit	NovusBiologicals
FOXRED1	human	~53	1:1,000	mouse	Abnova
ATP5A1	human, bovine, mouse, rat, zebrafish	33	1:1,500	mouse	MitoSciences
UQCR2	human, bovine, rat, mouse	~48	1:1,000	mouse	MitoSciences

SDHA	human, bovine, rat, mouse, <i>C. elegans</i>	~70	1:1,000	mouse	MitoSciences
GAPDH	human, mouse	~35	1:1,000	goat	Abcam
VDAC	human, mouse, rat, bovine, horse, rhesus macaque, chimpanzee, pig	~30	1:60,000	rabbit	Calbiochem
Cytochrome-c	human, mouse, rat	~12	1:500	mouse	BD Pharmingen
MTCO2	human	26	1:1,000	mouse	MitoSciences
mtHSP70	human, dog, mouse	~75	1:500	mouse	Enzo (Alexis)
COX5A	human, bovine, mouse, rat, zebrafish	17	1:1,500	mouse	MitoSciences

TABLE 3: list of all the antibodies used for the Western blot and Blue Native studies.

3.4 Genetic studies

3.4.1 DNA and RNA extraction

Total DNA was extracted from one 175cm² flask of fibroblasts from each patient by using the DNeasy blood and tissue kit (Qiagen) by following the manufacturer's instructions. Likewise, total RNA was extracted from cultured skin fibroblasts from the patients using the RNeasy Tissue Kit (Qiagen). The Dneasy/RNeasy membranes combine the binding properties of a silica-based membrane with simple microspin technology. DNA adsorbed to the DNeasy membrane in the presence of high concentrations of chaotropic salt, which removed water from hydrated molecules in solution. Samples were first lysed using proteinase K. Buffering conditions were adjusted to provide optimal DNA binding conditions and the lysate was loaded onto the DNeasy Mini spin column. During centrifugation, DNA was selectively bound to the Dneasy membrane as contaminants passed through. Remaining contaminants and enzyme inhibitors were efficiently removed in two wash steps and DNA was then eluted in TE buffer (Tris-EDTA).

With the RNeasy procedure, all RNA molecules longer than 200 nucleotides were purified. The procedure provided an enrichment for mRNA since most RNAs are shorter than 200 nucleotides (such as 5.8S rRNA, 5S rRNA, and tRNAs, which together comprise 15–20% of total RNA) were selectively excluded. A specialized high-salt buffer system allowed up to 100 µg of RNA longer than 200 bases to bind to the RNeasy silica membrane. Samples were first lysed and homogenized in the presence of a highly denaturing guanidine-thiocyanate-containing buffer, which immediately inactivated RNases to ensure purification of intact RNA. Ethanol was added to provide appropriate binding conditions, and the sample was then applied to an RNeasy Mini spin column, where the total RNA bound to the membrane and

contaminants were efficiently washed away. High-quality RNA was then eluted in 30–100 μ l water.

DNA and RNA quantification was carried out on NanoDrop[®] ND-1000 spectrophotometer (NanoDrop) which measures any purified molecules absorbing at a specific wavelength. A 2 μ l sample was loaded on to the instrument and the absorbance was read in between a 1mm path. Nucleotides, RNA, ssDNA, and dsDNA all absorb at 260 nm and contribute to the total absorbance. That's why the ratio of absorbance at 260 nm and 280 nm is used to assess the purity of DNA and RNA. A ratio of ~1.8 is generally accepted as "pure" for DNA; a ratio of ~2.0 is generally accepted as "pure" for RNA. All the samples were in the acceptable range of purity.

3.4.2 Homozygosity Mapping and Bioinformatics analysis

The technique known as homozygosity mapping assumes that affected offspring co-inherit two copies of a disease-related chromosomal segment from a common ancestor. Autozygosity mapping, first suggest by Lander and Botstein [143], is the method of choice for the discovery of autosomal recessive gene loci by seeking for homozygous regions in consanguineous families.

In order to find the shared genomic region, the DNA of patients was digested with *Xba*I (NEB) and special *Xba*I adaptors were ligated to the ends of the resulting fragments. These *Xba*I adaptors enabled genome amplification using a single universal primer, after the whole genome amplification the DNA fragments were purified and then fragmented by using DNase I to be then hybridised on the array. The array was then scanned using the GCOS software and the GeneChip DNA analysis software (GDAS) from Affymetrix was used to analyse the data. By looking for stretches of homozygous SNPs shared between the affected individuals it was possible to identify a group of candidate genes responsible for the disease.

Whole genome-wide SNP genotyping was done by the UCL Genomics facility at the Institute of Child Health (ICH, London) and performed in the 4 patients of Families 1-3 and in Family 4, using the GeneChip Human Mapping 10K *Xba*I Array (Affymetrix). This SNP-chip detected SNPs spread throughout the genome (with the exception of the Y chromosome) and was analysed following a single hybridization reaction with one individual's genomic DNA. The results were produced as a simple spreadsheet of the SNP allele calls. Whilst each SNP alone is not very informative, it is both their number (10,913 SNPs on the 10K *Xba*I Affymetrix array) and their ability to detect a heterozygous region, and hence exclude linkage, that suggested their potential use in autozygosity mapping.

SNP data was exported into a Microsoft Excel spreadsheet, where it was sorted by chromosome and then by chromosome position. An autosomal recessive model was assumed, and the output data was analysed assuming more than 30 consecutive homozygous SNPs as being significant. The freely downloadable "ExcludeAR" spreadsheets described by Woods *et al.* [144], is a method for seeking autosomal recessive loci by analysing only the affected individuals from a multi-affected pedigree. The primary results from each individual's SNP-chip hybridisation were produced as a simple Excel spreadsheet. For each individual

the results were then sorted by chromosome and genetic distance using a simple “data sort” Excel command. There are four versions of ExcludeAR (AR1–4) for the interpretation of data from one affected individual (AR1), two individuals (AR2), three (AR3), and four (AR4) individuals. The sorted primary SNP allele data was copied and pasted into the ExcludeAR spreadsheet. ExcludeAR first detected runs of consecutive homozygous SNP allele calls identical in all of the affected individuals analysed. It then determined if each run was of statistical significance by calculating the probability that a number of consecutive SNPs would be concordant and homozygous by chance to be of 1 in 1000. This was chosen because it is in common use as the LOD score (logarithm (base 10) of odds) of 3, which is regarded as significant when seeking conventional linkage analysis. ExcludeAR listed the 10 largest homozygous SNP runs by genetic size. For each result the following were given: genetic size, chromosome, genetic location on chromosome, number of homozygous SNPs in run, number of “No Calls” in the run and whether the result reached statistical significance. The autosomal recessive disease gene sought could be located within any of the statistically significant homozygous segments detected.

Dr Alistair Pagnamenta (a previous PhD student in the Mitochondrial Research Group at the UCL Institute of Child Health, London) analysed Family 4 by using ExcludeAR. The genes within the candidate regions were prioritized by bioinformatic analyses, including integration with the Maestro and MitoCarta catalogues [145,4]. Maestro [145] is a tool that integrates data sets that provide complementary clues about mitochondrial localization to assign a specific score for each human gene product, using each of the following eight genome-scale data sets: the **targeting signal score** [whether an N-terminal mitochondrial targeting sequence that directs protein import into the mitochondrion is present, identified by a computational tool called TargetP5]; the **protein domain score** [which records the presence of protein domains found to be exclusively mitochondrial, exclusively non-mitochondrial or shared, based on the SwissProt annotation of all eukaryotic sequences]; the **cis-motif score** [which indicates whether evolutionarily conserved transcriptional regulatory elements (usually enriched upstream of mitochondrial genes) are present]; the **yeast homology score** [which indicates whether an *S. cerevisiae* ortholog is present, with experimental evidence of mitochondrial localization (Saccharomyces Genome Database annotation)]; the **ancestry score** [measures the sequence similarity to proteins from *Rickettsia prowazekii*, the closest living bacterial relative of human mitochondria]; the **coexpression score** [measures transcriptional coexpression with known mitochondrial genes, using genome-scale atlases of RNA expression across diverse tissues]; the **MS/MS score** [indicates the number of tissues in which the protein was detected in a previous proteomic survey of mitochondria isolated from four mouse tissues]; the **induction score** [measures the upregulation of mRNA transcripts in a cellular model of mitochondrial biogenesis].

Each of the 8 scores listed above can be used individually as a weak genome-wide predictor of mitochondrial localization. However, Calvo et al., in order to improve prediction accuracy, integrated the 8 approaches using a naïve Bayes classifier [146] implemented with a computer program called Maestro. Maestro was trained

on the gold standard positive and negative data sets and applied to the Ensembl set of 33,860 human proteins. Then a score threshold was selected (using a conservative threshold of 5.65, corresponding to a false discovery rate of 10% and specificity of 99.4%), dependent on the application, and all the proteins scoring above the threshold were classified as mitochondrial. Although the Maestro integration method does not seem to be biased with respect to protein function, molecular weight, charge or abundance, it seems to have lower sensitivity for proteins localizing to the outer mitochondrial membrane, which may represent evolutionarily recent mitochondrial acquisitions, given the lower number of homologs in fungi and nematodes. Maestro contains an expanded collection of 1,451 human mitochondrial proteins (1,080 genes), which represents the most complete set to date and is useful for identifying genes underlying human diseases characterized by mitochondrial pathology. However, the authors believe that there are still another ~500 genes yet to be identified.

On the other hand, MitoCarta [4] is a protein compendium of the mitochondrion constructed by integrating in-depth protein mass spectrometry, microscopy, and machine learning. Pagliarini *et al.* integrated these mass spectrometry data with six other genome-scale datasets of mitochondrial localization using a Bayesian framework and additionally performed a GFP tagging study focused on mammalian mitochondria. The resulting compendium consists of 1098 genes and their protein expression across 14 mouse tissues. To systematically discover proteins essential for complex I function, Pagliarini *et al.* applied the technique of phylogenetic profiling which uses shared evolutionary history to highlight functionally related proteins [90]. The result was a list of 26 proteins (reported in Table 2) which are possibly involved with complex I biogenesis.

By consulting Maestro and MitoCarta we obtained a list of genes encoding known or predicted mitochondrial proteins that were then selected for sequence analysis.

3.4.3 Sequencing of candidate genes

The exons and intronic boundaries of the selected genes were PCR amplified by using specific primers (listed in Table 4) and performing an initial denaturation at 95°C for 3 min, followed by 35 cycles of 94°C for 30 s, 59°C for 30 s, and 72°C for 40 s, and a final extension at 72°C for 5 min (BioTaq Polymerase plus 10% DMSO and 1M betaine). The addition of 1M betaine (an organic compound also known as trimethylglycine) helped to prevent secondary structures forming in DNA molecules by equalizing the contribution of GC and AT base pairing to the stability of the DNA duplex. Direct sequencing was performed after PCR purification by using the MicroClean PCR clean-up kit (Microzone Ltd). The BigDye[®] Terminator v1.1 Cycle Sequencing Kit (Applied Biosystems) was used and data were analysed using Sequencer[™] version 4.8 (Gene Codes) and the sequences were compared to the reference sequences taken from the Ensembl database (http://www.ensembl.org/Homo_sapiens/Info/Index). Healthy control subjects were screened for the identified mutations via sequence analysis. In order to confirm the expression of the pathogenic mutation complementary DNA was synthesised from

RNA by using the SuperScript® III Reverse Transcriptase (Invitrogen), and the full-length transcript was amplified and sequenced as described above.

Primer Name	Primer Sequence 5'→3'
<i>FOXRED1</i>	
FOXR1 F1	TCGTCTGAATGGCGTTT
FOXR1 R1	GTGTGGGCCATGGTTTC
FOXR1 F2	TAGCTCACCTTTTCTGTGC
FOXR1 R2	TCCCTTGTCGCTAGAGTCC
FOXR1 F3-4	TAGCTCGAAGCTTTCATTGC
FOXR1 R3-4	CAACTCCACTTTCTCGCTTC
FOXR1 F5	ATGACTGAGCTGGACTCCC
FOXR1 R5	GGAGTACCGAGACTCCCAAC
FOXR1 F6	TTACAAGCCCTAGAGAGGGG
FOXR1 R6	CCTTGCTTAGCTTGTGAGTG
FOXR1 F7-8	ATCCTTCCAGCTTTCTTTCC
FOXR1 R7-8	ACACACACACACGCTATCC
FOXR1 F9	GACATCGAAGTTGGATAGCG
FOXR1 R9	ACAGGCATGAGCTACTGTGC
FOXR1 F10	CCTACCTGCACAGGGATTG
FOXR1 R10	ACTACGGCAGTCACGGG
FOXR1 F11	CTCAGCAGCAGGTAGAGGG
FOXR1 R11	GTACTGGGGAAGATGGAAGC
<i>ACAD9</i>	
ACAD9_5'UTRf	CTCTCCATCCCCTGCTGCG
ACAD9_1R	ACATTTCCAGACCAGACCAGC
ACAD9_1Fseq	GCACCAGCCSGCCTGTACG
ACAD9_2F	TTAACTGATATTTCCGTGATGGG
ACAD9_2R	AATAGCCCTTACAATGGAAATCG
ACAD9_3F	TATGATTAATATATAAACACTGTCC
ACAD9_3R	AATACAGAGTGCTTTCTTAAGAGC
ACAD9_4F	GGAGGAATCTAGGGCTGGGC
ACAD9_4R	AGAAGACCTACAGAGAGCACC
ACAD9_5F	CTCTCCTTTCTCCCCACAGC
ACAD9_5R	GAATCTTGGGCAACATCACAGC
ACAD9_6F	CTCAAAGCATTTCATATTTATCCC

ACAD9_6R	TGAAGGTTGTGACTGAGACCC
ACAD9_7F	TAAACACAAAGCCGTAATACCCT
ACAD9_7R	TAGCTGTGTGCCTGTACTION
ACAD9_8F	ACATAGGGGTTTGGTTTTCTCC
ACAD9_8R	CCTTACACACACACACGCGC
ACAD9_9F	GATGGATGGATGAATTGCCTGC
ACAD9_9R	TGCACTCATGACACTACCTGG
ACAD9_10F	GCCTCCTCCCTCTGCCTCC
ACAD9_10R	GGGGCAGCAGGGGGTGGG
ACAD9_11F	ATGTTTGAACCACAGAAATATTCC
ACAD9_11R	GAGACATCAAAGAACACACCG
ACAD9_12F	TTCTGACTTAATTACTTTCTCTCC
ACAD9_12R	CCTCCCTCCAGCGCCAGC
ACAD9_13F	CACCCAGCTCCCTGCAGCG
ACAD9_13R	GCAGGGTGGGGGTGGAGC
ACAD9_14F	CCAGCACACGTGGCACTACC
ACAD9_14R	TTTGGATTACTGTGCCCTAGG
ACAD9_14Fseq	CTTGACCTGGAGTGGGGGC
ACAD9_15F	ACGTTGCTGGACAGTGAGCGC
ACAD9_15R	GCAGGAGGGCATTGAAATAGG
ACAD9_16aF	AGGGCACTGTAGGGATGAGG
ACAD9_16aR	TCTCTTTGAGCTCTAGATTCAGG
ACAD9_16bF	CCTAGAATCGGGAGGGCAGC
ACAD9_16bR	TAAAGTGCAGCAGGACAGATGG
ACAD9_17F	CCAGTTTGGCTGATAGGCTGG
ACAD9_17R	ATCAATAGGGGCCTAGAAGTGG
ACAD9_18F	CCATGTTTGTCTTATCACGGTGC
ACAD9_18R	CAGTTTCCACTATGGTGTCTCC
ACAD9_3'UTRf	CTTTTGTTCCTCCGCTGCACC
ACAD9_3'UTRr	CCTGCTGTCACCCATTAAGG
NDUFAF1	
NDUFAF1_5'UTR_F.a	TCCTTGCTGTCCTTCCTGG
NDUFAF1_5'UTR_R.a	ACGTTCCAAGGCTAATTTACC
NDUFAF1_5'UTR_F.b	GGGAGGTATACGCCAAGGC
NDUFAF1_5'UTR_R.b	ACTATTAAGTGGACAATACCGC
NDUFAF1_ex1_Fa	TGAATTTGAAATTGTGATGCATTC

NDUFAF1_ex1_Ra	TGATCTCCTTGCAAATCCCC
NDUFAF1_ex1_Fb	TTCTCAGAAAATTCTCTAAGCC
NDUFAF1_ex1_Rb	ACTTATCCAAATCTTCTTTCCC
NDUFAF1_ex1_Fc	TGAAGCAATATACCATTTTAGGC
NDUFAF1_ex1_Rc	CAGAGTTCCATATAGCAGTGC
NDUFAF1_ex2_F	TTGCTAATAATGGAGAATGAGG
NDUFAF1_ex2_R	CTCACCCAGCCAAGACCTC
NDUFAF1_ex3_F	CATTTTATCGTTACAATTACATGC
NDUFAF1_ex3_R	GGTATAAGAGCAGTGGCCC
NDUFAF1_ex4_Fa	ATTTTAAACTCCTGGAATAATCTC
NDUFAF1_ex4_Ra	GTAAAACAAAACACTACCATATGATC
NDUFAF1_ex4_Fb	TCCAGAGCTTAACCCAAGGC
NDUFAF1_ex4_Rb	CAGAAGGCGAAGGTTACGG
NDUFAF1_cDNA_5'UTR_F	CTGAAGCTTCTTGGTGGCCC
NDUFAF1_cDNA_1F	GACTGAAGGGGATTTGCAAGG
NDUFAF1_cDNA_1R	GCAGAGGGTGGCCTTCCGG
NDUFAF1_cDNA_2F	TGCACTGCTATATGGAAGTCTG
NDUFAF1_cDNA_2R	TCCAAGGCCGACCATCCCC
NDUFAF1_cDNA_3F	CTGGCAGGAGGTCAAGATTCC
NDUFAF1_cDNA_3'UTR_R	AGTAAAACAAAACACTACCATATGATC
NDUFS4	
NDUFS4_1F	AAATAAAATCCCAAAGAATTTTCGC
NDUFS4_1R	CGAGAAAAGGGTCAACAGAGG
NDUFS4_2F	TAAGACAGATATTGTTAAAGTAGC
NDUFS4_2R	ACAAATATTTCTTCTTAAAATTTAGG
NDUFS4_3F	TGAATAGAGTTGCATGAATATAGG
NDUFS4_3R	CGTCAAAAAGTACTGTCATAAGC
NDUFS4_4F	TACTTATTTGATTTTATAGTAGCTG
NDUFS4_4R	CTCAAATTCTGTATACTTAATTGG
NDUFS4_5F	GAACATTAAGTTAAGTTATAAAAGC
NDUFS4_5R	CTCAAATCTTCTCTCTATATAGG
NDUFS4_5intFseq	CTTATGGTGCAAACCTTTTCTTGG
NDUFS4_cDNA_5'UTR_F	CCATCCATCCTGGCGTTTGC
NDUFS4_cDNA_ex3_F	TAGAAAAGTCAGGATCTTTGTTCC
NDUFS4_cDNA_ex3/4_R	ATAAGGGATCAGCCGTTGATGC
NDUFS4_cDNA_3'UTR_R	AGAGATATAGTCAGTGCCAACC

NDUFAF2	
NDUFAF2_1F	GTCTCCCATTGGTCAGTCGG
NDUFAF2_1R	ATGCGTTAGTTGACTAGGGGC
NDUFAF2_2F	TTAACCTAGAGAAAATTATGATGG
NDUFAF2_2R	ATTCTGTACAAGGTTCAAAGTGC
NDUFAF2_3F	TCAAAGATTAATTGTAGAACTACTG
NDUFAF2_3R	AACTATATATGCTCTTATTGAATTTG
NDUFAF2_4F	TGTTTGTTTCATGCCCTTTCCCC
NDUFAF2_4R	TCTATTCAATAAATGGTGCTGGG
NDUFAF2_5F	CTCCAGTACCTAAAATAATATGG
NDUFAF2_5R	TGAAGCTTCGTATATCCTTGGG
NDUFAF2_6F	TATATAATGTATTTTATTTTATTGGC
NDUFAF2_6R	AATGAACTCAAGATTAATAGAATAGG
NDUFV2	
NDUFV2_5'UTRf	GAAGTCTCCGCCACAGGGCCCC
NDUFV2_5'UTRr	GGCCGCAGTGTCCTTGCCGCCGCC
NDUFV2_1F	ACAGAAAAGAGGGGCTGCTTGG
NDUFV2_1R	TATGAGGAAAAGTAATACCAGCC
NDUFV2_2F	GTTAGAGAGATGAATAGGG
NDUFV2_2R	CTTTCACTGACTCCTGACGGCC
NDUFV2_3F	GGATGGTCTCGATCTCTTGACC
NDUFV2_3R	GTATGTAAATTCTCACGATGACC
NDUFV2_4F	TATATCATGTTGGAATTAATGG
NDUFV2_4R	ACATACAAATGGCTAAAGGGCTCC
NDUFV2_5F	TGAAGAACTTTTCTGTTTTTACC
NDUFV2_5R	ATCCAATAAGATGGCAGAAGTTGG
NDUFV2_6F	GGCGTGAGCCACCGCGCCTGGCC
NDUFV2_6R	TAAAACCTGGATATTTATGGTAACC
NDUFV2_7F	TAGGAGTTACTTAATTGTTGATGCC
NDUFV2_7R	GAGATTCATATAGATAAATACTATCC
NDUFV2_8F	AACTGGGCTCTTGTGAGGTAACC
NDUFV2_8R	ATTATATAATGATGTCTTCACAGCC
NDUFS2	
NDUFS2_5'UTRf	CCAAACCCACAATCAGCCC
NDUFS2_5'UTRr	TACCTCTTTTATTTGTTCTTCCC
NDUFS2_1F	GAGCAGGACTAAAGCATGAGG

NDUFS2_1R	AGCCTTGGAGAAAGTGTGTCG
NDUFS2_2F	TGTTCAGGCCCTTTGTCTAGG
NDUFS2_2R	CCTGTATCTCAGCACTTTCGG
NDUFS2_3F	CCAAGGGAATAACCATGTGGC
NDUFS2_3R	CCCCAGATCCCGCCAAAAG
NDUFS2_4-5-6F	TGAGCCTGTTAGATGTGACCC
NDUFS2_5Fseq	ACCACTTCCCCGTTGAACCC
NDUFS2_5Rseq	TGATATAGTTTCTACAAATATAACCC
NDUFS2_4-5-6R	GGCCTGGGCTGGACATTTGG
NDUFS2_7aF	GGTGCTGAGAGGGCTCTCC
NDUFS2_7aR	CTCCTTCTTCCTTAGCCTCCC
NDUFS2_7bF	GTGAGGAAGAGTATTAACACACC
NDUFS2_7bR	AGGCAGGGGAAACTAGCTGG
NDUFS2_8-9F	CATCCTTCCTAGCCCCATACC
NDUFS2_8-9R	AAAAAATTAGCTGGGCGTAGTGG
NDUFS2_10-11F	GCCTTAGTCTCCCGAGTAGC
NDUFS2_10-11R	CTACTCTACATATGGTCTTTTCC
NDUFS2_12F	GAGAAAAATACTCTTCATGTTAATAC
NDUFS2_12R	ACTTATCTTCCTGTTGTGAGGC
NDUFS2_3'UTRf	CTATTGTGTAGTAGAGGTATCC
NDUFS2_3'UTRr	GAACATTCTTAGGTTTACAGTCC

TABLE 4: Candidate gene primer names and sequences.

3.5 Functional studies

3.5.1 Preparation of lentiviral vectors

Dr Andrew Duncan (a previous post-doctoral research associate in the Mitochondrial Research Group) designed a synthetic codon-optimized *FOXRED1* gene which included a Kozak sequence (to increase translational initiation) and two STOP codons (to ensure efficient termination) and that was generated by assembly of synthetic oligonucleotides (Genart, Regensburg). The gene was then subcloned into a lentiviral vector [147] and expression linked to eGFP through an internal ribosomal entry sequence. This vector utilizes a strong retroviral promoter element derived from the spleen focus-forming virus and a mutated woodchuck posttranslational regulatory element. Vector stocks were pseudotyped with the vesicular stomatitis virus envelope as described previously [148]. About 12 million 293T cells were seeded the day before the transfection and grown in Optimem (Invitrogen). When they reached 70-80% confluence, 10ml of a polyethylenimine

(PEI, Sigma) plus DNA complexes mixture was added to the medium. The cells were incubated at 37°C, 5% CO₂ for 4 hours. The medium was then replaced with complete DMEM. The viral particles were harvested the following day and the day after. The medium from the cells was filtered through a 0.22µm filter and the virus was ultra-centrifuged at 4°C, for 2-3 hours at ~50,000g. The supernatant was carefully decanted off and 150µl of serum free media was added to resuspend the virus, which was then transferred to a cryovial and stored at -80°C. Vector stocks of pGIPZ, a commercially available lentiviral vector system expressing puromycin/eGFP markers and shRNAi against FOXRED1 or scrambled shRNAi controls (Open Biosystems), were prepared in a similar manner for knock-down experiments. Vector stocks were titred by fluorescence-activated cell sorting (FACS) following dilutional transduction of a fixed number of cells, and stored at -80°C until required.

3.5.2 Complementation and RNA interference studies

Patient fibroblasts were transduced with the lentiviral vector expressing eGFP alone or in combination with FOXRED1. Silencing the FOXRED1 gene in control fibroblasts was achieved by transducing the cells with the pGIPZ shRNAi vector. In both cases the transduction was carried out as follows. Patient and control fibroblasts were seeded in a 12 multi well plate (about 100,000 cells per well). The following day 40 µl and 100 µl (in double) of virus were added to the plate, in a minimum amount of complemented media. Two days after infection the media was changed and more serum (20 %) was added. Cells were kept growing for about one week. Transduced cells were enriched for eGFP expression by FACS (Fluorescence-Activated Cell Sorting) and expanded for functional studies. Cells were maintained in culture in presence of 1 mg/ml puromycin (Gibco-Invitrogen) to select the transduced cells; and experiments were carried out between 15 and 20 days after cell transduction to allow for an efficient selection and expansion. FOXRED1-silenced fibroblasts died within 20 days of culture following viral transduction.

4 RESULTS

4.1 Biochemistry

The patient cohort investigated in this study is genetically heterogeneous, originating from several different geographical areas: England, France, the Middle East, Israel, India and Pakistan. The clinical investigations and the biochemical studies on patients' muscles revealed a mitochondrial involvement which has been then further studied by using different biochemical and genetic approaches.

4.1.1 Complex I activity

Prior to this study, complex I deficiency had been demonstrated in skeletal muscle in 11 of the patients, and in fibroblasts in the 12th case (in whom no muscle was available for biochemical analysis). During this study complex I activity was determined in fibroblasts from all 12 patients (see Fig. 6) using an immune-capture method. Activity measurements of mitochondrial complex I normalised to complex IV in patient fibroblasts showed a variable degree of impairment. The 4 patients of Families 1-3 all had a deficiency ranging from ~55% to 70% residual activity compared to the control mean, possibly suggesting a common genetic defect. Three additional patients had residual complex I activities in the range of ~50%-60%, whereas 3 patients showed a mild complex I defect, with residual activity of ~72%-80%. Only Patient 7 and Patient 9 had almost normal complex I activity in fibroblasts (~89% and 98%). All the results are shown in Fig. 6, measurements were done in triplicate and compared to 3 normal controls and 1 positive control.

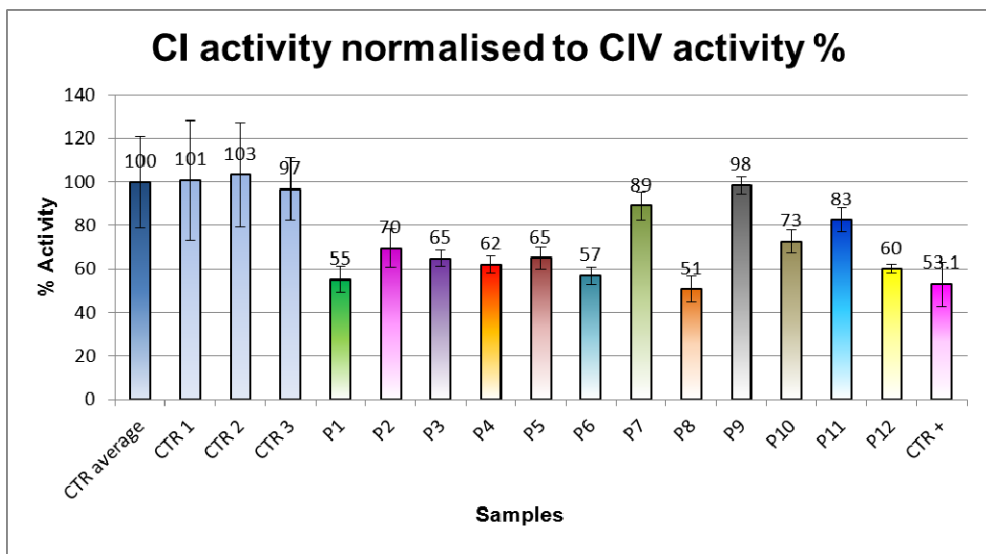


FIGURE 6: *Complex I (CI) activity normalized to complex IV (CIV) activity in all patients (P1-12) compared to 3 healthy controls and 1 positive control (ACAD9 mutated). The assay was carried out with the microplate kit (MitoSciences), all measurements were done in triplicate and results are given as percentages.*

4.1.2 Blue Native studies

BN-PAGE followed by Western blot analysis was used to interrogate complex I assembly in fibroblasts for all the patients in this study. Results were compared to two healthy controls and ρ^0 cells; antibodies against subunits of other OXPHOS complexes [ATP5A1 (complex V), UQCRC2 (complex III) and MTCO1 (complex IV)] were used to determine equal loading of all samples (see Fig. 7).

Complex I holoenzyme mis-assemblies were noted in Patient 1 of Family 1, Patient 6 from Family 5 and Patient 7. Slightly reduced complex I holoenzyme was seen in Patient 3 and 4 of Families 2-3, in the proband from Family 4 and in Patient 8, 10 and 11; Patient 8 disclosed virtually undetectable complex I signal. Patient 9 showed almost normal levels of CI holoenzyme. ρ^0 cells, as expected, showed only a tiny CI subassembly of ~55 kDa, non-containing any mitochondrial encoded subunit.

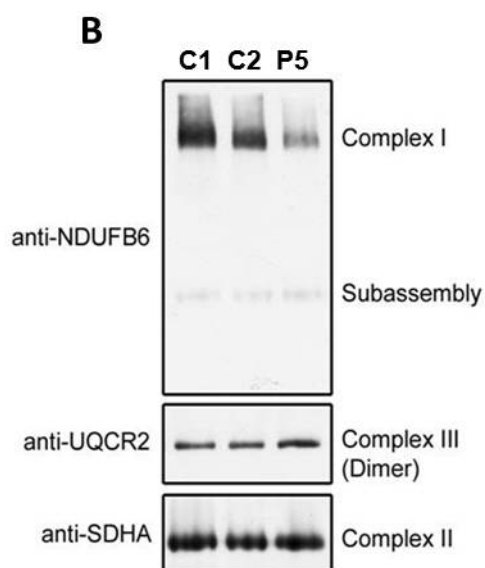
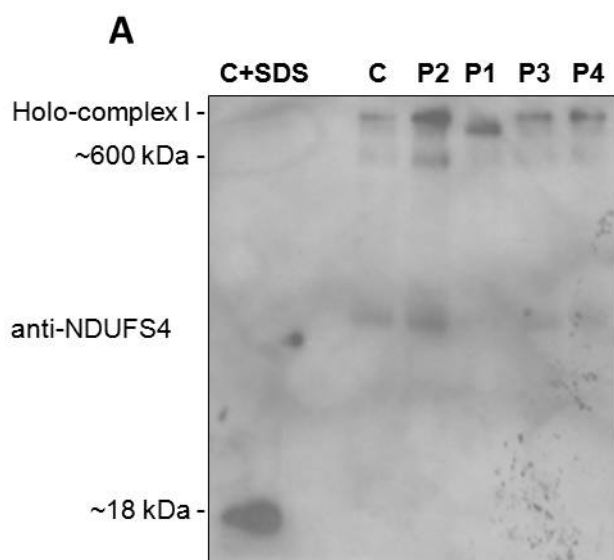
In particular:

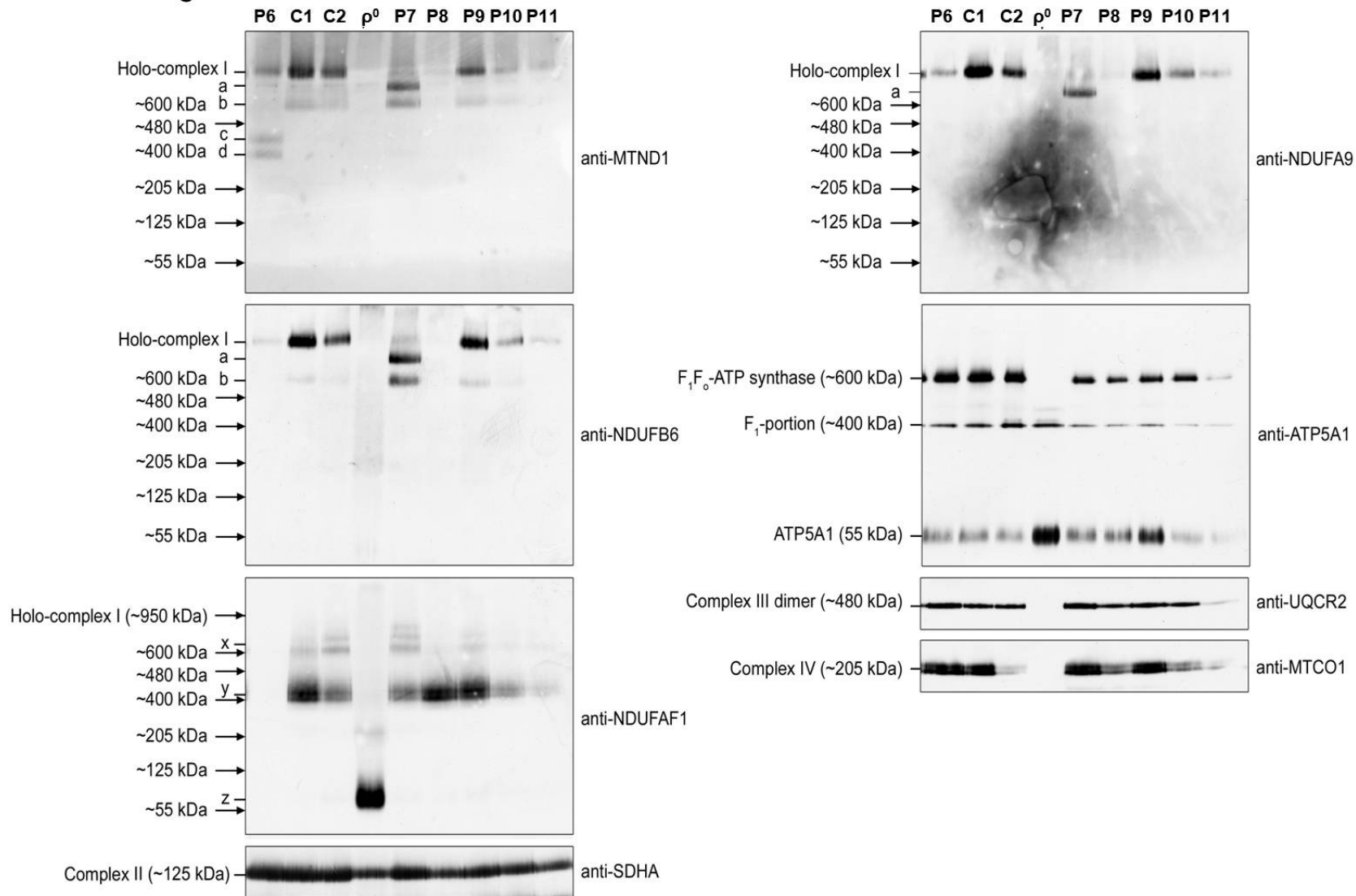
- Patient 1 showed no fully assembled complex I holoenzyme but a subassembly at ~830 kDa when probing with the NDUFS4 antibody, a pattern which has previously been observed in at least 4 patients with NDUFS4 mutations [149,150,49,34] (Fig. 7A Lane P1).
- Patient 2 presented a normal holo-complex I assembly and content when probed with the NDUFS4 antibody, this may exclude defects in those subunits or assembly factors whose mutations result in subassemblies, including: NDUFS1-2-4-6 [151-153,79], NDUFA2 [81], NDUFAF1-2-4 [52,34,48] and NDUFV2 (Fig. 7A Lane P2).
- Patients 3 and 4 had similar appearances on BN-PAGE analysis and they show reduced levels of holo-enzyme complex I but no subassemblies when probed with the NDUFS4 antibody, leading the mutation screening to potentially any complex I subunit, except the ones associated with subassembly intermediates (Fig. 7A Lanes P3 and P4).
- Patient 5 showed a reduced amount of fully assembled complex I compared to two healthy controls when probed with the NDUFB6 antibody. Genetic diagnosis was reached by a homozygosity mapping approach (Fig. 7B Lane P5).
- Patient 6 presented reduced levels of fully assembled complex I and two minor subassemblies at ~400 and ~460 kDa when probing against MTND1.

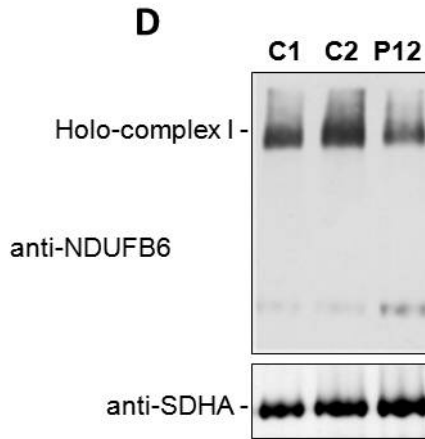
Less holo-complex I was observed when probing against NDUFB6 and NDUF9, and no signal at all was detected when probing against NDUF1. A similar pattern had previously been described by Dunning *et al.* [51] in a patient bearing defects in NDUF1, suggesting this as a potential candidate gene for Patient 6 (Fig. 7C Lane P6).

- Patient 7 had extremely low levels of fully assembled holo-enzyme complex I and two interesting subassemblies at ~600 and ~830 kDa when probing for MTND1, NDUFB6 and NDUF9. A smaller subassembly compared to controls was also noticed when probing against NDUF1. This pattern was compatible with an NDUF4 mutation pattern or NDUF2, NDUF1 or NDUF2 mutations, or other as yet unknown defects (Fig. 7C Lane P7).
- Patient 8 had virtually no or very little complex I with no abnormal subassemblies, when probed with the anti- MTND1, NDUFB6 and NDUF9 antibodies. Only a physiological subassembly at ~400kDa comparable to the one seen in the controls was visible when probed against NDUF1, however the slightly bigger subassemblies above 400kDa which were seen in the controls were absent in Patient 8. This is suggestive of a severe mutation in potentially any subunit of the complex, except for the ones known to be associated with the accumulation of abnormal subassemblies, as already mentioned above (Fig. 7C Lane P8).
- Patient 9 displayed virtually normal levels of holo-complex I and no evidence of subassemblies when probed with the anti- MTND1, NDUFB6, NDUF1 and NDUF9 antibodies. This may suggest a mild defect in any complex I subunit or assembly factor (Fig. 7C Lane P9).
- Patients 10 and 11 showed reduced levels of holo-enzyme complex I but no subassemblies when probed against MTND1, NDUFB6, NDUF1 and NDUF9. This is suggestive of mild/severe mutations in any of the complex I subunits (Fig. 7C Lanes P10 and P11).
- Patient 12 displayed a mild reduction of the holo-complex I, but no indication of subassemblies when probed against MTND1, NDUFB6, NDUF1 and NDUF9. As for Patients 3, 4, 5, 10 and 11, the defect has to be searched in any of the subunits of complex I, since mutations in assembly factors usually result in the stalling of the complex I assembly process and the accumulation of subassembly intermediates (Fig. 7D Lane P12).

FIGURE 7: Blue Native studies on patient fibroblasts. The holo-complex I was detected via different antibodies (listed in Table 3). Patients 1 to 12 have been split in different panels: A to D. For full description of the migration patterns per patient refer to the text above.



C



4.2 Genetics studies

Previous genetic analysis in this patient cohort had excluded mtDNA mutations using a combination of Sanger sequencing of 45 overlapping PCR products and or MitoChip requence analysis (performed by the Neurogenetics diagnostic laboratory at the National Hospital for Neurology, Queen Square, London, or by Dr Andrew Duncan). Homozygosity mapping was performed in suitable pedigrees, either on the hypothesis that the subjects were homozygous by descent, either because of clear consanguinity in the family, or because they originate from a relatively small geographical region.

4.2.1 Homozygosity Mapping and Bioinformatics Analysis

Homozygosity mapping was performed on:

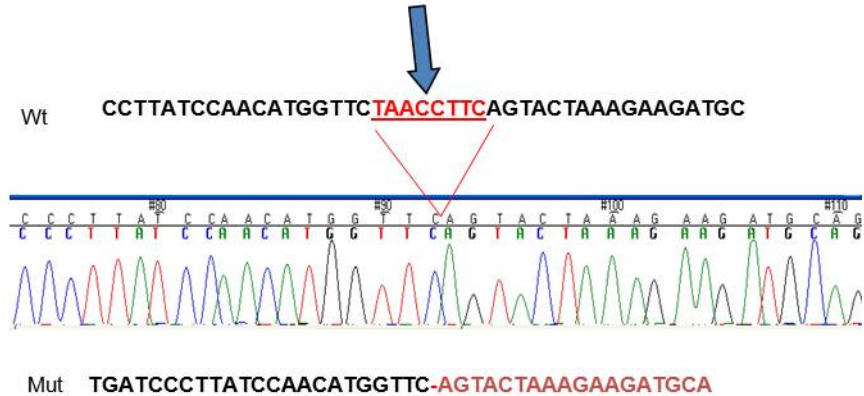
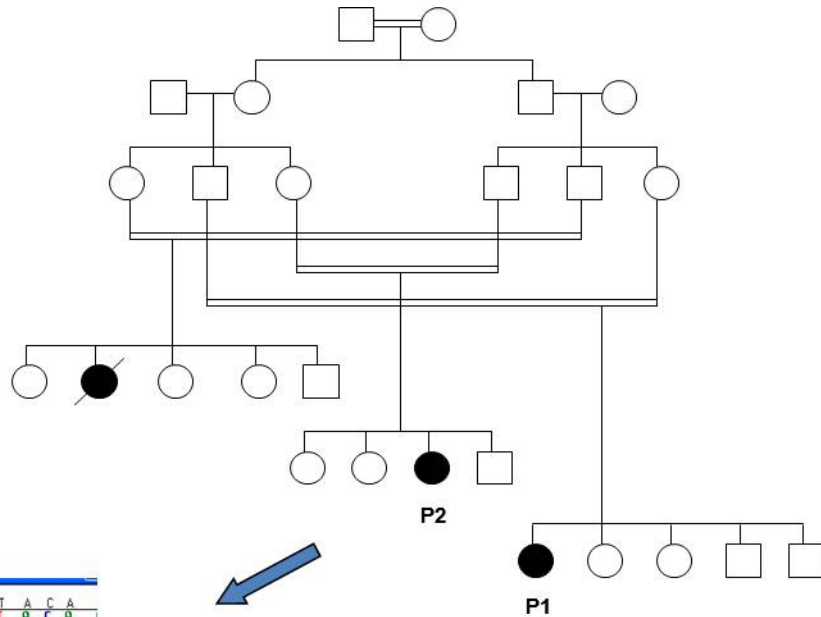
- Families 1-3: the subjects originated from the same geographical region and Patients 1 and 2 were cousins born to first cousin parents, who were born to inbred grandparents themselves. The assumption was that Patients 1-4 would all bear the same defect inherited by descent because of their common origin and the consanguinity. The almost 11,000 SNPs from the whole genome of the 4 probands, obtained by running on a 10K Affymetrix DNA chip, were analysed by using the ExcludeAR program [144], and 10 most significant homozygous regions shared by all 4 patients were selected:

RESULTS

	Chrom	Start	End	Mb	cM	SNPs	Genes in region
Largest	4	182,857,218	183,830,190	~1	3.5	4	4
Second	9	35,099,949	38,288,204	~3.2	2.9	6	78
Third	5	38,436,684	39,448,555	~1	2.2	5	11
Fourth	18	43,988,463	45,928,259	~1.9	2.2	4	20
Fifth	13	104,988,136	105,841,769	~0.8	2.1	4	1
Sixth	1	84,532,511	86,433,862	~1.9	1.8	4	25
Seventh	10	59,938,404	61,209,408	~1.2	1.6	5	11
Eighth	12	86,723,846	89,952,101	~3.2	1.0	4	20
Ninth	4	35,656,022	36,819,542	~1.1	1.0	5	5
Tenth	15	34,347,151	35,200,430	~0.7	0.9	4	24

The regions were submitted to the NCBI Map Viewer website (http://www.ncbi.nlm.nih.gov/mapview/map_search.cgi) and a list of candidate genes was constructed. The genes in the regions were selected by bioinformatics analysis and integration with the Maestro database [145], which assigns a score per each gene according to the probability of its mitochondrial localisation. Given the very small size of the shared homozygous regions and the fact that there was no immediately obvious candidate gene that could explain complex I deficiency in these patients, we assumed that the “identical by descent” hypothesis was no longer plausible to explain their genetic defect. Therefore we started looking at the biggest homozygous regions in the single patients, and found a very large region in Patient 1 on chromosome 5. This region spanned 135 homozygous SNPs and contained the *NDUFS4* gene, previously associated with complex I deficiency and reported to result in a complex I ~830 kDa subassembly on Blue Native gels. Sequencing of the *NDUFS4* gene in Patient 1 revealed a novel 8bp frameshift deletion (c.377_384del), leading to a premature stop codon and thus predicting a truncated protein (Q126fsX2). The same mutation was found in heterozygous state in Patient’s 1 cousin, Patient 2 (Fig. 8). However, this mutation alone cannot account for Patient’s 2 complex I deficiency and the search for this patient’s genetic defect is still on-going. Patients 3 and 4 were screened for *NDUFS4*, *NDUFAF1* and Patient 3 also for *NDUFV2*, according to their homozygosity pattern (i.e. the genes screened were in the patients’ homozygous regions), but no mutations were identified.

FIGURE 8: Family 1 pedigree and electropherograms. The *NDUFS4* c.377_384del; Q126fsX2 mutation was found in homozygous state in Patient 1 (P1) and in heterozygous state in Patient 2 (P2).



- Family 4: the family was studied by Dr Alistair Pagnamenta, who identified a total of 5 candidate regions of homozygosity in the proband (Patient 5) of this Israeli family, which were not shared with his five healthy siblings. These regions spanned a total of 50 Mb and contained 338 genes. The longest region of homozygosity (18.3 Mb) was observed on chromosome 6, but did not contain any candidate genes implicated in complex I function. The third largest region of homozygosity (9.2 Mb on chromosome 18) contained the only known structural subunit of CI located within these homozygous intervals: *NDUFV2*. This gene was sequenced but no pathogenic mutations were identified.

The remaining genes were prioritised by bioinformatics analysis with the integration of the Maestro and MitoCarta databases [145,4]. The top 10 genes encoding known or predicted mitochondrial proteins were selected for sequence analysis out of 337 enclosed in the candidate regions (the sequence analysis was performed by Dr Andrew Duncan, postdoctoral research fellow).

The only potentially pathogenic mutation was found in the *FOXRED1* gene, a homozygous c.1054C>T leading to a missense R352W (Fig. 8A). Restriction Fragment Length Polymorphism (RFLP) analysis was used to confirm the mutation segregation within the pedigree: *MspI* (NewEngland Biolabs) cut the 245 bp wild-type amplicon into two fragments of 121 and 124 bp. The mutation c.1054C>T abolished the restriction site, leaving the 245 bp amplicon uncut (Fig. 8B). Patient 5 was homozygous for the mutation, his parents were heterozygous and unaffected siblings either heterozygous or homozygous for the wild-type sequence. 268 pan-ethnic control alleles were screened and resulted negative for carrying the c.1054C>T mutation in *FOXRED1*.

Amino acid alignment studies showed that the FOXRED1 protein has a well evolutionary-conserved module in its structure. Within a part of this module, the R352 residue is highly conserved across species, suggesting that the amino acid change R352W is likely to have a significant functional impact (Fig. 9).

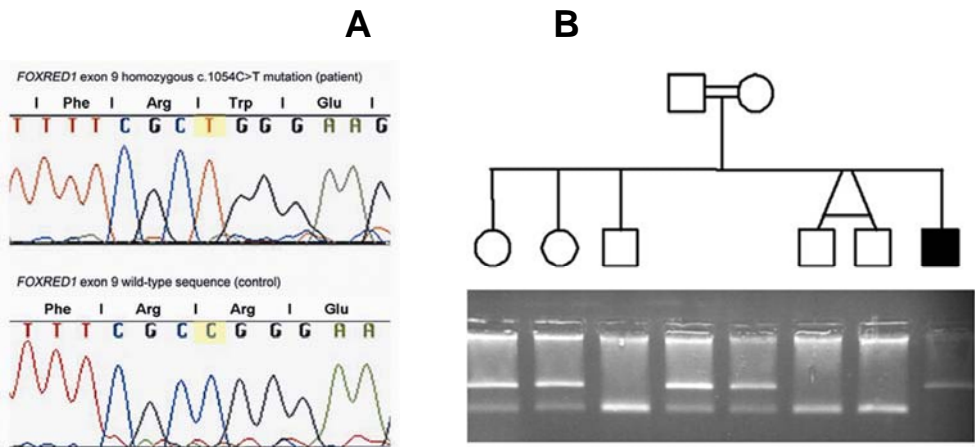


FIGURE 8: *FOXRED1* exon 9 electropherogram showing sequencing results for the *FOXRED1* gene: the c.1054C>T mutation is homozygous in Patient 5 (top panel) while the control sequence is wild-type homozygous (lower panel) (A). *FOXRED1* mutation RFLP analysis showing the segregation of the mutation with disease: none of the family members is homozygous for the c.1054C>T mutation except for the proband (P5). The parents are heterozygous and unaffected siblings either heterozygous or homozygous for the wild-type sequence (B).

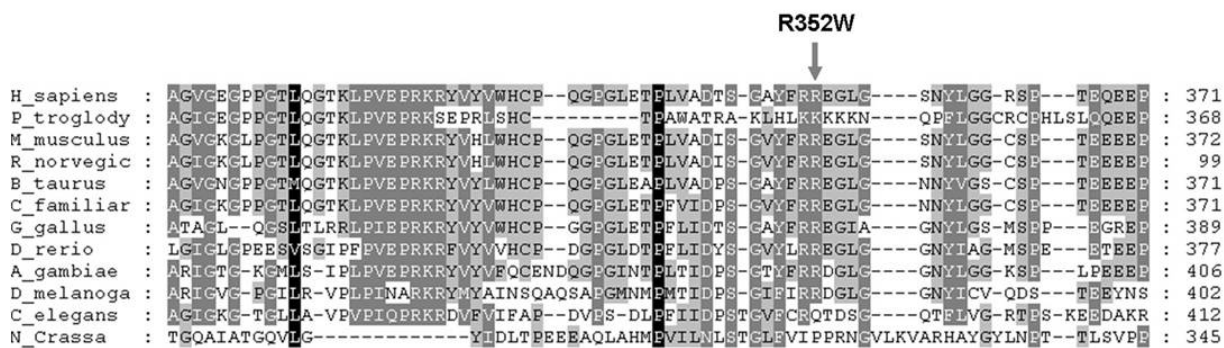


FIGURE 9: *FOXRED1* protein evolutionary conservation. The *FOXRED1* protein has a well-conserved module in its structure across species. Within a part of this module, we found that the R352 residue is highly conserved across species, suggesting that the amino acid change R352W is likely to have a significant functional impact.

4.2.2 Candidate Gene Approach

Patients 6 to 12 were considered single cases and therefore no assumption about the inheritance of the defect was made prior to the study.

Table number 5 summarises the patients' clinical phenotype, biochemical results and genes sequenced. The candidate genes were chosen according to the patient's specific phenotype; however, the selection of suitable candidate genes is always biased by the broad spectrum of presentations of mitochondrial disease, and therefore the gene hunting even in a subset of patients with isolated complex I deficiency may be difficult.

The genes screened were: *NDUFS2*, *NDUFS4*, *NDUFV2*, *NDUFAF1*, *NDUFAF2*, *FOXRED1* and *ACAD9*. Because of the particular Blue native subassemblies

observed in Patient 6 and her phenotype of mitochondrial cardiomyopathy, the genetic screening was directed towards *NDUFAF1*, which has already been described by Dunning *et al.* [51] in a patient with similar BN-PAGE appearances (Patient's 6 pedigree shown in Fig. 10).

The genetic defect identified in Patient 6 was two compound heterozygous mutations in *NDUFAF1*: c.631C>T; R211C and c.733G>A; G245R, which were also confirmed in cDNA. Each parent was heterozygous for one of these mutations (Fig. 11A-B-C), confirming that they were on separate alleles (ie, *in trans*) in the patient. These changes were absent in 240 ethnically matched control alleles and also in 1094 control individuals genotyped in the 1000 Genomes cohort (<http://www.1000genomes.org>). The screening is still on-going for the other patients, in whom no defects were identified in the screened genes.

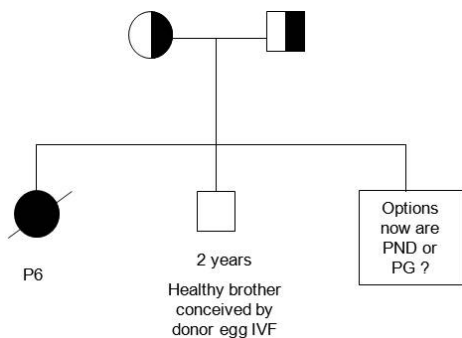


FIGURE 10: Patient 6 (P6) family pedigree. P6 died at 6.5 months of cardiac failure. Her parents subsequently had a healthy boy born after donor egg in vitro fertilization (IVF). Further reproductive options, such as pre-natal diagnosis (PND) or preimplantation genetic diagnosis (PGD) are available now that the genetic defect is known.

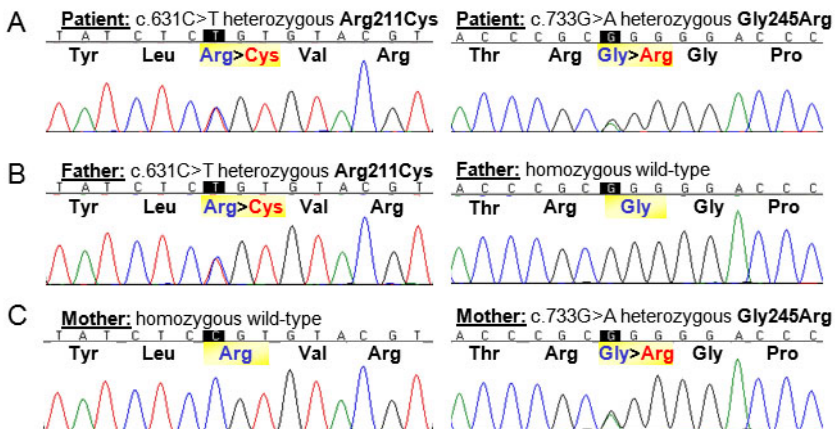


FIGURE 11: Sequencing of exon 2 of the *NDUFAF1* gene revealed two compound heterozygous mutations, c.631C>T; Arg211Cys and c.733G>A; Gly245Arg, in

RESULTS

Patient 6 (A). Her father is heterozygous for the c.631C>T; Arg211Cys mutation and homozygous wild type for the second variant (B), while her mother is heterozygous for the c.733G>A; Gly245Arg mutation and homozygous wild type for the first mutation (C).

Patients	Phenotype	CI activity %*		CI holoenzyme		Genes screened	Defect
		muscle	fibroblasts	quantity	sub- assembly		
P1	LS	27.9	55.2	almost none	yes	<i>NDUFS4</i>	<i>NDUFS4</i> homozygous c.377_384del; Q126fsX2
P2	Congenital LA	44.6	69.5	normal	no	<i>NDUFS4</i> , <i>NDUFAF1</i>	<i>NDUFS4</i> heterozygous c.377_384del; Q126fsX2
P3	LS	41.9	65.0	near normal	no	<i>NDUFS4</i> , <i>NDUFAF1</i>	
P4	HCM+LA	30.6	62.0	near normal	no	<i>NDUFS4</i> , <i>NDUFAF1</i> , <i>NDUFV2</i>	
P5	Infantile encephalopathy	7.0	70.2	less	no	<i>NDUFV2</i> , <i>FOXRED1</i>	<i>FOXRED1</i> homozygous c.1054C>T; R352W
P6	HCM+LA	14.0	56.9	less	yes	<i>NDUFS4</i> , <i>NDUFAF1</i>	<i>NDUFAF1</i> compound heterozygous c.631C>T; R211C + c.733G>A; G245R
P7	LS	36.0	89.1	almost none	yes	<i>NDUFS4</i> , <i>NDUFAF1</i> , <i>NDUFAF2</i> , <i>NDUFV2</i>	
P8	LS	40.9	50.8	almost none	no	<i>NDUFS4</i> , <i>NDUFAF1</i> , <i>NDUFAF2</i> , <i>NDUFS2</i>	

P9	LS	46.2	98.5	near normal	no	<i>NDUFS4</i> , <i>NDUFAF1</i> , <i>NDUFAF2</i> , <i>NDUFS2</i> , <i>ACAD9</i>	
P10	Global DD	41.9	72.6	less	no	<i>NDUFS4</i> , <i>NDUFAF1</i> , <i>NDUFS2</i>	
P11	Alpers	45.1	82.6	less	no	<i>NDUFS4</i> , <i>NDUFS2</i>	
P12	HCM+LA	9.1	60.0	less	no	<i>NDUFS4</i> , <i>NDUFAF1</i>	
CTR+	HCM+LA	26.0	53.1	-	-	<i>ACAD9</i>	<i>ACAD9</i> compound heterozygous c.976G>C; A326P + c.1594C>T R532W

TABLE 5: CI= complex I; HCM = hypertrophic cardiomyopathy; LA = lactic acidosis; LS = Leigh syndrome; DD = developmental delay. * % of the control mean

4.3 Functional studies

4.3.1 Family 1, Patients 1 and 2: *NDUFS4* c.377_384del; Q126fsX2

The genetic defect discovered in *NDUFS4* in Patient 1 and 2 was a novel 8bp frameshift deletion (c.377_384del; Q126fsX2), which is predicted to cause highly deleterious effects. Furthermore mutations in the *NDUFS4* gene have already been linked to complex I deficiency in a number of cases; therefore this particular case was not investigated further, as the case for pathogenicity of this mutation was compelling for Patient 1. The mutation is unlikely to be disease-causing in Patient 2, however, since this patient had only one heterogeneous change in *NDUFS4*. The search for the disease gene in this patient is continuing, by focusing on her regions of homozygosity.

4.3.2 Family 4, Patient 5: *FOXRED1* c.1054C>T; R352W

4.3.2.1 *Lentiviral-mediated complementation and silencing studies*

In order to try and complement the biochemical defect, a synthetic *FOXRED1* gene was expressed in patient fibroblasts, using a lentiviral vector. This transgene rescued the complex I activity to ~90% of control levels (Fig. 12), providing

evidence that the R352W missense mutation in *FOXRED1* was the cause of the observed complex I deficiency in the patient. However, transfection with an empty vector also increased complex I activity in patient fibroblasts slightly (Fig. 12). The mild deficiency of complex I in patient fibroblasts (~70% of control mean) probably explains why only a 10–20% increase in complex I activity was observed after lentiviral transfection with wild-type *FOXRED1* cDNA compared with transfection with an empty vector.

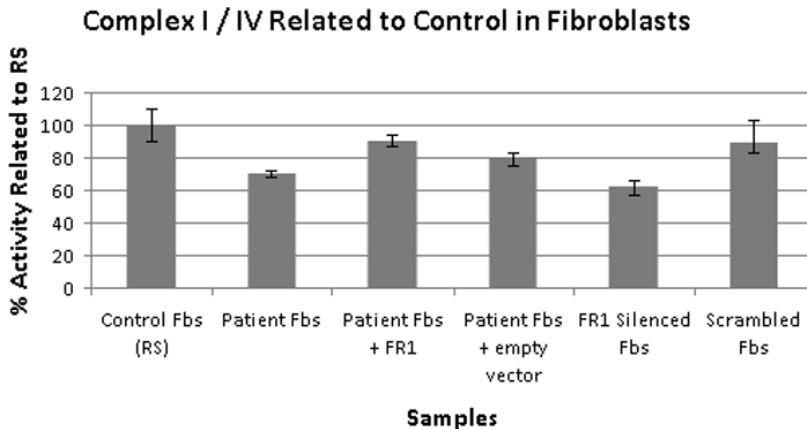


FIGURE 12: Mitochondrial complex I/IV dipstick assay. Dipstick assay shows ~70% residual complex I activity in patient fibroblasts (Fbs) which is recovered to ~90% after complementation with synthetic wild-type *FOXRED1* cDNA. A slight recovery is also seen after transfecting patient Fbs with an empty vector.

FOXRED1-silenced fibroblasts show an ~40% decrease in complex I activity compared with scrambled fibroblasts. Key: Fbs, fibroblasts; RS, reference sample; FR1, *FOXRED1*.

4.3.2.2 *Western blot analysis*

Western blot analysis showed a reduced steady-state level of *FOXRED1* in patient fibroblasts, which increased after lentiviral transduction with wild-type *FOXRED1* cDNA (Fig. 13). Western blot analysis also demonstrated a slight improvement in complex I amount (assessed with anti-NDUFA9 antibody) in patient fibroblasts after transduction with wild-type *FOXRED1* cDNA, compared with human control fibroblasts and patient fibroblasts transduced with an empty vector (Fig. 13). These observations were confirmed by densitometric analysis of the western blots (also shown in Fig. 13).

Stable knockdown of *FOXRED1* expression via lentiviral mediated shRNAi reduced complex I expression, assayed with anti-NDUFA9 antibody in an immunoblot (Fig. 13). Dipstick assay showed ~40% residual complex I activity in *FOXRED1*-silenced fibroblasts compared with human control fibroblasts and fibroblasts transfected

with a scrambled shRNA vector (Fig. 13), confirming that lack of FOXRED1 can cause complex I deficiency.

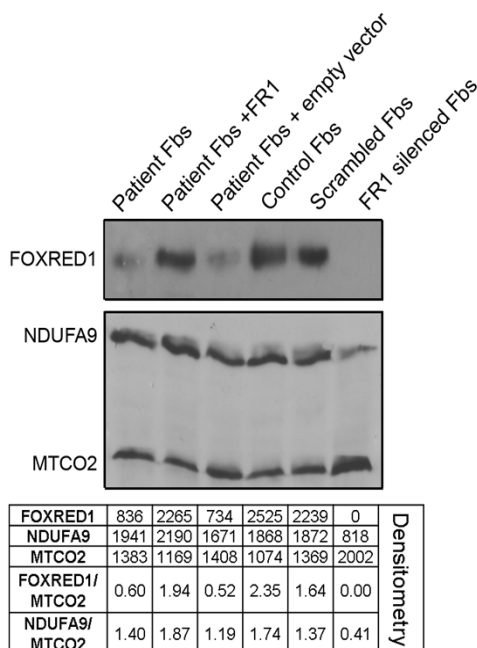


FIGURE 13: Western blot analysis. Western blot analysis shows a gain in FOXRED1 and NDUFA9 protein content in patient fibroblasts when complemented with FOXRED1 wild-type cDNA, compared with patient fibroblasts transduced with an empty vector. FOXRED1-silenced fibroblasts show a reduction in FOXRED1 and NDUFA9 protein content compared with control and scrambled fibroblasts. Probing for MTCO2 (anti-complex IV) demonstrated equal loading. Densitometry measurements were carried out using Alpha Ease FC software (Alpha Innotech/Cell Biosciences, Santa Clara, CA, USA) and confirmed the observations above.

4.3.2.3 Subcellular and submitochondrial localization

In order to identify the subcellular localisation of FOXRED1, HeLa cells were used as controls in Western blot studies. The Western blot results show that the anti-FOXRED1 antibody recognized a protein of the expected size (~53 kDa) in whole mitochondria, confirming mitochondrial localization of FOXRED1 (Fig. 14). A similar band of ~53 kDa is clearly visible in the mitochondrial inner membrane (IM) fraction and in the mitochondrial soluble fraction ("Sol", i.e. mitochondrial inner membrane space (IMS) + matrix (M)). A similar slightly bigger polypeptide is

detected in the IMS as well as in the matrix, indicating that FOXRED1 may enter the mitochondrial matrix as a precursor containing its mitochondrial import sequence, which is then cleaved to release the mature functional protein. Probing the same western blot with control antibodies anti-voltage-dependent anion channel (VDAC), anti-cytochrome c and anti-MTCO2 (cytochrome c oxidase subunit II) revealed the expected submitochondrial localizations for these proteins (outer membrane (OM), IMS and IM, respectively).

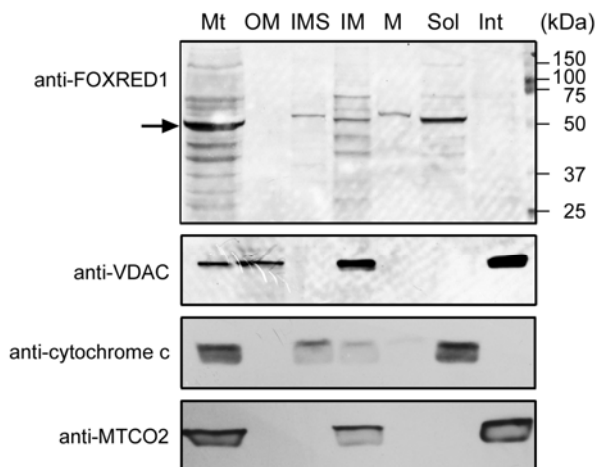


FIGURE 14: Submitochondrial fractionation. The ~53 kDa FOXRED1 protein (indicated by the arrow) shows a clear mitochondrial localization; more specifically, it is contained within the soluble fraction and associated with the IM. The slightly larger band detected in the IMS and the M may represent an immature polypeptide containing a mitochondrial targeting sequence, which is then cleaved to release the mature protein. The smaller mature protein then associates with the IM to achieve its fully functional state. Antibodies against mitochondrial proteins were used to test the purity of the fractions: anti-VDAC for the OM (and IM), anti-cytochrome c for the IMS (also visible as associated with the IM) and anti-MTCO2 for the IM. Key: MT, whole mitochondria; OM, outer membrane; IMS, intermembrane space; M, matrix; SOL, soluble fraction; INT, integral proteins fraction.

4.3.3 Patient 6: *NDUFAF1* c.631C>T; R211C and c.733G>A; G245R

The compound heterozygous mutations detected in patient 6 had never been described before, however the *NDUFAF1* gene had been previously associated with one case of isolated complex I deficiency and a multisystem disease presentation including hypertrophic cardiomyopathy [51]. Dunning *et al.*

demonstrated the role of NDUFAF1 in complex I assembly, after Janssen *et al.* [154] observed that the deletion of the *Neurospora crassa* CIA30 gene (homologue of human *NDUFAF1*) resulted in severe disruption of the assembly process, Human CIA30 could therefore be considered as a candidate gene for complex I deficiency in humans. The functional studies we have carried out aimed to determine the pathogenicity of these two new mutations, considering the role of the NDUFAF1 protein already consolidated for the human complex I biogenesis process. Phylogenetic analysis demonstrated that Arg211 and Gly245 are highly conserved amino acids (Fig. 15).

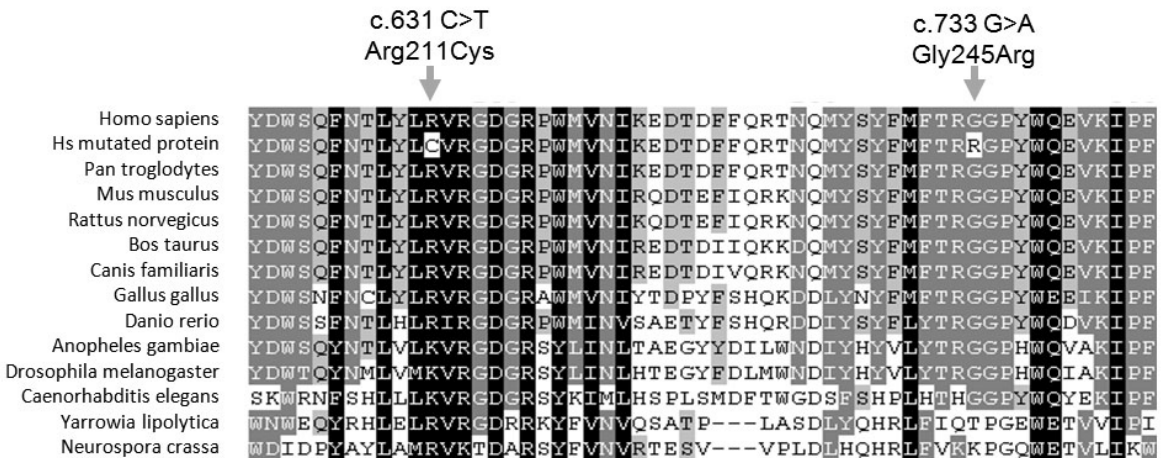


FIGURE 15: The amino acid residues affected by the missense mutations in exon 2 are 33 amino acids apart within the NDUFAF1 protein and are highly conserved from humans to the nematode *Caenorhabditis elegans* and fungi.

4.3.3.1 Western blot

Western blot analysis demonstrated a severe reduction in NDUFAF1 protein levels in patient's mitoplasts compared to three control mitoplasts isolated from fibroblasts; normal staining of SDHA confirmed equal loading of all samples. Levels of ND1 (a core subunit assembled early into the nascent complex I enzyme) were normal, whereas levels of NDUFA9 (a membrane arm subunit that was incorporated later) were reduced in patients. As expected, ρ^0 cells lacked mitochondrially encoded ND1 but had normal levels of all nuclear-encoded proteins analysed (Fig. 16).

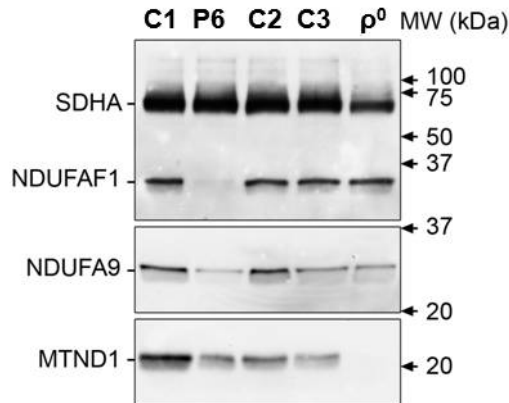


FIGURE 16: Western blot analysis demonstrated a severe reduction in NDUFAF1 protein levels in Patient 6 (P6) mitoplasts compared to 3 control (C1-3) mitoplasts isolated from fibroblasts; normal staining of SDHA confirmed equal loading of all samples. Levels of ND1 (a core subunit assembled early into the nascent complex I enzyme) were normal, whereas levels of NDUFA9 (a membrane arm subunit that is incorporated later) were reduced in Patient 6. As expected, ρ^0 cells lacked mitochondrially encoded ND1 but had normal levels of all nuclear-encoded proteins analysed.

5 DISCUSSION

The clinical presentation of the patients was heterogeneous, classic mitochondrial disease features overlapping with minor signs: Leigh syndrome, congenital lactic acidosis, hypertrophic cardiomyopathy, encephalopathy, developmental delay, Alpers' disease.

Mitochondrial complex I activity was reduced in all patients' fibroblasts. This assay confirmed the presence of the defect in another tissue other than muscle, which is usually assayed in diagnostic biochemical investigations. A discrepancy between the defect seen in muscle and in fibroblasts is often noticed, this is probably due to the different mitochondrial content and energy requirement of the two tissues of the same patient, not to mention the tissue specific gene expression, therefore the complex I activity impairment is usually more pronounced in muscle.

5.1 *NDUFS4*

Families 1 to 3: Patients 1, 2, 3 and 4 had a complex I activity reduction in the range of 50% to 70% residual activity of the control mean. Patient number 1 had the most severe defect (55%) compared to patients 2, 3 and 4. Whereas for Patients 3 and 4 the Blue native pattern showed less fully assembled complex I and normal levels in Patient 2, a ~830 kDa subassembly of complex I in Patient 1 was displayed when probed with the *NDUFS4* antibody. The presence of that particular subassembly in Patient 1 suggested a defect in the *NDUFS4* gene; however a homozygosity mapping approach was undertaken on the assumption that all the 4 patients shared the same defect inherited as an ancestral allele.

Since only 10 very small sized homozygous regions were found to be shared between the patients, and there was no obvious candidate gene, the "identical by descent" hypothesis was no longer suitable to explain their genetic defect. The biggest homozygous region in Patient 1 was on chromosome 5 and included *NDUFS4*; sequencing of this gene revealed a novel homozygous 8 bp frameshift deletion (g.98539_98546del) located in exon 4 leading to a premature stop codon and thus predicting a truncated protein (c.377_384del; Q126fsX2).

The *NDUFS4* gene encodes the 18 kDa subunit of complex I and consists of five exons interspersed by long introns. The protein is located in the iron-sulphur protein fraction of complex I, and all the *NDUFS4* gene homologues (including birds, *Drosophila* and *Anopheles*) have a highly conserved C-terminus containing a canonical RVSTK phosphorylation site (positions 129–131) in the last residues, with the highest phosphorylation score for the cAMP-dependent protein kinase A (PKA). Investigation of murine [155-157] and human cell cultures [158] showed that activation of the cAMP cascade or direct addition of dibutyryl cAMP promotes *in vivo* serine phosphorylation of an 18 kDa subunit of complex I, this being associated with stimulation of the NADH-ubiquinone oxidoreductase activity of the complex. More recently it has been found that cAMP-dependent phosphorylation of

the RVSTK site of the *NDUFS4* protein promotes import/maturation in mitochondria of this nuclear encoded protein [159]. In human and mammalian complex I the *NDUFS4* subunit is present in both the C-terminal serine phosphorylated and non-phosphorylated form, and the *NDUFS4* protein is phosphorylated by PKA at the serine of the C-terminal RVSTK consensus site.

In vivo the activity of the complex can depend on the exchange of pre-existing, possibly functionally impaired, *NDUFS4* subunits in the complex with the newly synthesized protein [29].

Most of the reported *NDUFS4* mutations, including this novel mutation (see Table 1), result in the loss of the conserved phosphorylation site, so that the *NDUFS4* subunit is unable to activate the complex. Furthermore, in line with the data shown by other groups, the mutation found in Patient 1 prevents normal assembly of a functional complex in the inner mitochondrial membrane, thus leading to an impaired function of respiratory chain complex I.

Because Patient 2 has a different clinical phenotype and is heterozygous for the Q126fsX2 mutation without a second pathogenic mutation, we suspect that her mitochondrial disorder has a different genetic basis than Patient 1. The occurrence of two separate recessive disorders is not unusual in highly inbred pedigrees. The *NDUFS4* sequence was wild type in Patients 3 and 4, who both had isolated complex I deficiency, suggesting there are at least 2 causes of isolated complex I deficiency in this relatively small community. In conclusion, a homozygosity mapping approach may not be able to unravel the genetic defect even in highly inbred families. Secondly, the *NDUFS4* gene should be considered a hotspot of mutations for complex I deficient Leigh syndrome, which is one of the most common presentations of mitochondrial disease in childhood. The presence of the ~830 kDa subassembly of complex I is highly suspicious of an underlying *NDUFS4* mutation.

5.2 *FOXRED1*

Family 4, Patient 5 is the sixth child of a consanguineous Iranian-Jewish family affected by early-onset complex I deficient encephalomyopathy; he presented with 7% residual complex I activity in muscle and 70% in fibroblasts. BN-PAGE analysis provided evidence of reduced amounts of complex I holoenzyme but no subassemblies were identified. An integrative genomics approach, combining homozygosity mapping and bioinformatic analyses, was used to investigate the defect.

Five candidate regions of homozygosity, unique to the proband and not shared with unaffected siblings, were identified by whole genome-wide SNP analysis. No mutations were identified in *NDUFV2*, the only known structural subunit of complex I located within the homozygous intervals. 337 other genes located within the candidate regions were prioritized by bioinformatics analysis, and 11 genes encoding known or predicted mitochondrial proteins were sequenced. The only pathogenic mutation identified in these 11 genes was a homozygous missense

mutation c.1054C>T in *FOXRED1*. This mutation segregated with disease in the family; both parents and two siblings were heterozygous for the mutation, while the other three siblings were homozygous for the wild-type sequence. The mutation was not found in 268 pan-ethnic healthy control alleles. Western blot analysis showed a reduced steady-state level of FOXRED1 in patient fibroblasts.

Restoration of complex I activity after lentiviral transduction of patient fibroblasts with wild-type *FOXRED1* cDNA confirmed that the *FOXRED1* mutation is the cause of Patient's 5 complex I deficiency. FOXRED1 is a 486 amino acid protein, with an approximate mass of 53 kDa. It contains an FAD-dependent oxidoreductase domain, which may be involved in electron transfer. The mutation is predicted to cause the substitution of a highly conserved arginine residue by tryptophan (Arg352Trp). An *in silico* analysis using MitoProt II-v1.101 [160] confirmed the presence of a putative N-terminal mitochondrial localization sequence, spanning amino acids 1–23 (MIRRVLPHGMRGRLLTRPGTRR). This sequence has a positive net charge of +1 and a predicted cleavage site at position 24; the probability of import into mitochondria was also very high at 0.9546. Western blot data confirmed mitochondrial localization of FOXRED1, with an expected band of ~53 kDa in the whole mitochondrial fraction. In addition, a band slightly larger than ~53 kDa was observed in the IMS and the matrix. Based on this observation, we postulate that a FOXRED1 precursor containing its mitochondrial import sequence may be imported into mitochondria via a classical importation mechanism (such as the TOM/TIM machinery), and that the import sequence is subsequently cleaved within the matrix to release the mature protein [161]. We also speculate that this mature protein then associates with the mitochondrial IM, near the respiratory chain supercomplexes and probably adjacent to the complex I holoenzyme, in order to exert its chaperone function. FOXRED1 is not one of the known 45 subunits of complex I, as established by proteomics studies [162]. However, the association of a homozygous *FOXRED1* mutation with isolated complex I deficiency in our patient suggests that FOXRED1 must be a chaperone or other factor necessary for assembly, stability and/or correct functioning of complex I.

The tissue specificity of complex I residual activity (7% in muscle and 70% in fibroblasts) observed in this patient, is probably due to a difference in tissue specific expression of *FOXRED1*. Only one other case has been reported with *FOXRED1* mutations [39] (compound heterozygous c.694C>T; Q232X and c.1289A>G; N430S); a boy who presented with Leigh syndrome, he is alive at 22. His complex I defect (9% in fibroblasts, no value for muscle but reported isolated complex I deficiency) was more pronounced than in Patient 5; that's also in line with the type of mutations found: the Patient described by Calvo *et al.* [39] bore a nonsense mutation, causing a loss of expression of the allele, and a missense mutation with mild effects; whereas Patient 5 carried a homozygous missense mutation causing a rather severe amino acid change (arginine to tryptophan) but both alleles were still expressed.

A role for FOXRED1 in complex I activity is also supported by the absence of *FOXRED1* orthologues in the yeast *Saccharomyces cerevisiae*, which has a

functional respiratory chain but lacks the entire complex I holoenzyme, but the presence of *FOXRED1* orthologues in higher order fungi such as *Neurospora crassa*, which do contain complex I. Further evidence indicating that FOXRED1 is needed for complex I function comes from a large-scale bioinformatic survey, which identified FOXRED1 as one of 19 putative complex I assembly factors [4]. Finally, steady-state mRNA transcripts for *FOXRED1* have been detected in 12 human tissues, implying that the protein is widely expressed, in common with all previously identified complex I assembly factors.

The localization of FOXRED1 within mitochondria, decrease in complex I activity upon silencing of its expression in wild-type fibroblasts and the complex I deficiency in patient muscle and fibroblasts, corrected by expression of wild-type *FOXRED1* in patient fibroblasts, together with reduction of complex I holoenzyme assembly arising from a mutation in the coding sequence of *FOXRED1*, strongly support a bona fide role in complex I function, assembly and/or stability.

Taken together, these results demonstrate that the Arg352Trp mutation in *FOXRED1* causes an isolated complex I defect associated with infantile-onset encephalomyopathy, and that the FOXRED1 product is needed for fully efficient complex I activity in human cells.

5.3 *NDUFAF1*

Family 5, Patient 6 had 57% residual complex I activity in fibroblasts and 14% in muscle. She presented with respiratory-syncytial-virus-positive bronchiolitis and later developed hypertrophic cardiomyopathy. A combined biochemical and genetic approach was employed, using BN-PAGE to identify abnormal complex I assembly intermediates in the patient's cultured skin fibroblasts, followed by candidate gene sequencing of known complex I assembly factors previously associated with cardiomyopathy, was used to search for the underlying genetic defect in this patient. This approach revealed two compound heterozygous missense mutations in *NDUFAF1* (c.631C>T; R211C and c.733G>A; G245R) as a novel cause of fatal infantile HCM.

The pathogenicity of the *NDUFAF1* mutations is supported by several lines of evidence. The healthy parents were each heterozygous for one of the missense mutations observed in their daughter, and these mutations were not present in 120 control subjects and 1094 individuals genotyped for the 1000 Genomes Project. The affected amino acid residues are highly phylogenetically conserved, from fungi (*Neurospora crassa* and *Yarrowia lipolytica*) to humans in the case of Arg211Cys, and from nematodes to humans in the case of Gly245Arg. Finally, functional studies demonstrated a severe reduction in the steady-state levels of NDUFAF1 protein in Western blots of patient fibroblasts, with accumulation of abnormal complex I assembly intermediates on BN-PAGE analysis similar to those seen in the only other patient previously reported to have complex I deficiency caused by NDUFAF1 mutations [51]. A relatively high expression of *NDUFAF1* in cardiac tissues supports a specific role for this assembly factor in heart mitochondria [154]. In addition, mitochondria play critical roles in intracellular calcium homeostasis,

generation of reactive oxygen species (especially at complex I) and control of apoptosis; disruption of these functions is likely to contribute to HCM pathogenesis. It is interesting to note that both our case and the previously reported case with *NDUFAF1* mutations had cardiomyopathy apparently triggered by viral illnesses, at 6 months in our case and at 15 months in the previous case [51]. *NDUFAF1* has recently been implicated in immune pathways, including T cell activation [163,164], and we speculate that this may explain why viral infection triggered decompensation and development of HCM in both patients with *NDUFAF1* mutations.

These results confirm *NDUFAF1* as a bona fide assembly factor of complex I, mutations of which cause isolated complex I deficiency.

5.4 Other Patients in the cohort

Patients 7 to 12 displayed a variable degree of impairment of the complex I activity, ranging from 51% to 89% of the control mean in fibroblasts, furthermore combining this information with the Blue native pattern for complex I was not sufficient to narrow the subset of candidate genes that could be responsible for the defect in these patients. Only Patient 7 showed subassemblies at ~600 and ~830 kDa, compatible with an *NDUFS4* mutation pattern or *NDUFA2*, *NDUFS1* or *NDUFAF2* mutations, however no defects in these genes were detected. Patient 8 displayed a severe defect in complex I holoenzyme levels, but no subassemblies were detected; this is suggestive of a severe mutation in potentially any subunit of the complex or assembly factor. The genes screened were *NDUFS2*, *NDUFS4*, *NDUFAF1*, and *NDUFAF2* but no mutations were identified. Patients 9 to 12 showed a variable degree of complex I assembly impairment but no subassemblies and the search for the genetic defect in the selected genes did not identify the responsible mutation (see Table 5). For these patients future studies will consider a next generation sequencing approach followed by bioinformatics analysis to select the subset of candidate genes which may be responsible for the disease.

5.5 Complex I assembly

Only little is understood about the assembly process of complex I. Recent x-ray crystallographic studies have demonstrated the complex I holoenzyme to be an L-shaped macromolecule composed of four functional modules: the dehydrogenase N module is responsible for NADH oxidation, the hydrogenase Q module is responsible for ubiquinone reduction, and the proton translocase proximal PP and distal PD modules are responsible for proton translocation across the IMM [19,18]. The matrix arm contains the N and Q modules, while the P module is located in the membrane arm. Assembly of complex I has been extensively studied in the fungus *N. crassa* and in human cells [30,34,33,37]; these studies, together with the phylogenetic profiling work of Pagliarini *et al.* [4], have led to the identification of 26 known and putative complex I assembly factors (see Table 2). Sixteen of these

have already been associated with human disease, including nine complex I deficiency syndromes and one mitochondrial disorder with multiple respiratory chain deficiencies [38-40,65]. Interestingly, mutations in seven of these putative complex I assembly factors have been linked to non-mitochondrial diseases such as peroxisomal disorders, organic acidemias and a ketone body utilisation defect (see Table 2). It is not clear whether reduced complex I activity may be involved in the pathogenesis of any of these disorders. While the precise mechanism of complex I assembly is still debated, a consensus view of a dynamic multidirectional process that includes the possibility of direct subunit exchange into pre-existing mature complex I has recently been proposed [30].

Various models have been suggested for complex I assembly, but the current consensus model proposes that the ND1 core subunit anchors an early Q subassembly to the IMM, then further subunits and/or subassemblies are added to both the Q and P modules and finally the N module is added to form the complex I holoenzyme [3]. However, the precise order of subunit incorporation into the nascent enzyme is not known, nor the nature and number of additional factors required for integrity of the assembly process.

Studies of assembly intermediates in fibroblasts from patients carrying mutations in the complex I assembly factor genes have suggested that NDUFAF1 and C20ORF7 are involved early in complex I assembly, while NDUFAF2 appears to function at a later stage [4-6]. C20ORF7 appears to be necessary to form an early assembly intermediate of ~400 kDa, which contains the ND1 subunit, while NDUFAF2 associates with a larger subassembly of ~830 kDa. FOXRED1 is an additional putative assembly factor exerting its role in a later stage during complex I assembly and it's recently been linked to human disease [38,39].

The function of FOXRED1 is not clear, it contains an FAD-dependent oxidoreductase domain, which may be involved in electron transfer; furthermore, its four human homologs (DMGDH, SARDH, PIPOX and PDPR) perform redox reactions in amino acid catabolism, suggesting a potential link between amino acid metabolism and electron transfer to complex I.

NDUFAF1 was initially identified as the human homologue of CIA30, one of the first two complex I assembly factors identified in *N. crassa* [33], and was demonstrated to be a ubiquitously expressed, mitochondrially targeted protein [154,165]. NDUFAF1 is a protein of 327 amino acids and ~37.7 kDa and contains no predicted transmembrane domains. Ryan *et al.* [166] described its N-terminally processed mitochondrial targeting signal, and Dunning *et al.* [51] showed that NDUFAF1 peripherally associates with the matrix face of the mitochondrial inner membrane. A role for NDUFAF1 in complex I assembly is also supported by RNA interference experiments, which showed disrupted complex I assembly in HeLa cells [165], and by recent studies of the testicular nuclear receptor (TR4)/ knockout mouse model [53]. TR4 is a member of the nuclear receptor superfamily of transcription factors and appears to regulate complex I activity by binding to hormone response elements in the NDUFAF1 promoter sequence. TR4^{-/-} mice had a ragged-red fibre myopathy associated with complex I deficiency and reduced NDUFAF1 gene expression. Furthermore, lentiviral overexpression of NDUFAF1

was able to restore complex I activity and ATP generation to control levels in primary fibroblasts from TR4^{-/-} mice. The precise function of NDUFAF1 remains obscure; this is also true for all currently known complex I assembly factors. NDUFAF1 appears to be involved at an intermediate stage of complex I assembly, in contrast to C20orf7, NDUFAF3 and NDUFAF4, which are needed early in the assembly process, and to NDUFAF2, which has a role in the late stages [30]. Tandem affinity purification experiments demonstrated that NDUFAF1 copurifies with two other putative complex I assembly factors, ECSIT and ACAD9 [37,40]. Interestingly, ACAD9 mutations have recently been reported to cause complex-I-deficient HCM, including a fatal infantile phenotype similar to that of our patient with NDUFAF1 mutations [59,40].

There are also a number of putative assembly factors that have not yet been shown to cause human disease, including ECSIT, PHB, PTC1 and 17 further factors identified by Pagliarini *et al.* [2]. It is likely that many more assembly factors of complex I will be identified, bearing in mind that the much smaller complex IV, which has only 13 subunits, requires more than 15 assembly factors for its assembly [7]. Possible functions of the various putative complex I assembly factors/chaperones include iron-sulphur cluster synthesis (eg, NUBPL), translational coactivation of complex I subunits (as has been suggested for C20orf7 for ND1) and direction of nuclear-encoded complex I subunits to the correct intramitochondrial compartment (ie, to the matrix side of the enzyme or to the intermembrane space) [30].

The NDUF54 subunit is a small protein of 18 kDa [21], which is thought to be important in complex I assembly and function. Mutational analyses of complex I deficient patients have revealed several loss-of-function mutations in the *NDUF54* gene [109,150,167,149]. Complex I assembly studies of patient fibroblasts showed that the NDUF54 subunit is inserted in the complex at late stage of assembly process [29,27,49] and that the absence of NDUF54 leads to the formation of a partially assembled ~830 kDa subcomplex and lack of fully assembled complex I [150,49,34]. Despite this absence of fully assembled complex I in Blue native gels in NDUF54 patient samples, some complex I activity could still be measured by spectrophotometric analysis [168]. So far, no explanation could be given for this discrepancy between the BN-PAGE findings and the spectrophotometric assay. Studies on NDUF54 patient fibroblasts revealed that this ~830 kDa subassembly was unable to incorporate radioactive labelled subunits: NDUF56, NDUF54 and NDUFV1-V3 [29]. Moreover, this ~830 kDa subassembly is also observed in patient fibroblasts with mutations in subunits NDUF56 and NDUFV1 [34,79]. These data suggest that the ~830 kDa complex I subassembly lacks the tip of complex I representing the NADH dehydrogenase module. The spectrophotometric assay is based on measuring the rotenone-sensitive 2,6-dichloroindophenol reduction by electrons accepted from decylubiquinone. Because the electrons for the oxidation of decylubiquinone come from NADH in this assay, this would not be possible for the ~830 kDa subassembly which lacks the NADH dehydrogenase module. In addition, a separate NADH dehydrogenase module would not be able to donate its electrons to decylubiquinone, since it lacks the ubiquinone-binding site. This

suggests that binding of the NADH dehydrogenase module to the ~830 kDa subassembly is necessary for spectrophotometric activity. Evidence of loose binding of the NADH dehydrogenase module to the ~830 kDa subassembly comes from the investigation of supercomplexes in muscle tissue. Complex I forms, together with complexes III and IV, supramolecular structures called supercomplexes. The supercomplexes might serve to reduce the diffusion distance of the substrates, to improve electron transfer, to decrease the reactive oxygen species formation and to stabilize the individual complexes [169,170]. In a *NDUFS4* KO mouse model, mild extraction conditions allowed detection of active fully assembled complex I from muscle [171], but only in association with complex III. This finding provides evidence that complex III helps to stabilise complex I. It is noteworthy that the ~830 kDa-complex III₂ supercomplex was also observed in wild type and heterozygous muscle samples. This suggests that the association of the NADH dehydrogenase module to the ~830kDa subassembly might occur after the formation of an ~830kDa-CIII₂ supercomplex or that the NADH dehydrogenase module was lost after supercomplex formation. The presence of the assembly factor *NDUFAF2* in the ~830kDa-CIII₂ supercomplex indicates that this supercomplex is likely a physiological entity and not an artefact of the procedure. Interestingly, the presence of a tiny amount of *NDUFAF2* in complex I + complex III₂ supercomplexes might indicate that this assembly factor is released after the addition of the NADH dehydrogenase module. The disconnection of the electron input module from the NADH dehydrogenase module might represent a general mechanism of unplugging a possibly crippled complex from its electron influx.

Establishing a genetic diagnosis in mitochondrial disease is challenging and achieved in only a minority of cases because of complex genetics, including bigenomic inheritance. Diagnosis is guided by biochemical findings in biopsied tissue, which may show an isolated deficiency of one respiratory chain enzyme complex (most commonly complex I or complex IV) or a combined defect affecting multiple enzymes. Complex I deficiency is genetically heterogeneous and may arise from mutations in the 45 structural subunits of the enzyme (including 7 mtDNA-encoded subunits and 38 nuclear-encoded subunits) or in any of the known and putative assembly factors [4,38,39,59]. As a first level of investigation, the entire mtDNA was screened in the patients by the diagnostic lab and subsequently, as for research purposes, a systematic analysis of candidate nuclear genes was performed.

There does not appear to be any particular genotype–phenotype correlation for the complex I assembly disorders, in common with many mitochondrial disorders (see Table).

Most patients presented with a progressive encephalopathy, frequently fulfilling the criteria for Leigh syndrome [8].

Hypertrophic cardiomyopathy was observed in the patient with *NDUFAF1* mutations, as well as our patient with *FOXRED1* mutations. All patients had lactic acidemia, except for those with *NDUFAF2* mutations, in whom only CSF lactate levels were elevated. Severe isolated complex I deficiency was observed in skeletal muscle of all cases (residual activity 0–40% of controls), with normal

activities of other respiratory chain enzyme complexes. There was a suggestion that *NDUFAF2*-related disease has a characteristic neuroradiological appearance, with a predilection for the mamillothalamic tracts, substantia nigra/medial lemniscus, medial longitudinal fasciculus and spinothalamic tracts, but this has not been found in all cases reported to date [176].

In the absence of clear genotype–phenotype correlations, the approach to a genetic diagnosis for patients with complex I deficiency remains empirical. The first-line genetic investigation (after screening for mtDNA rearrangements and common point mutations m.3243A>G and m.8344A>G) should be complete mitochondrial genome sequence analysis. Subsequent investigations will be directed at nuclear-encoded structural subunits and known assembly factors of complex I and/or homozygosity mapping in suitable families. However, this approach may not be successful in all cases, since an unknown number of complex I assembly factors remain to be identified, and since complex I deficiency may occasionally be secondary to another disease process, such as 3-hydroxyisobutyryl-CoA hydrolase deficiency [172].

Taking into account the costs of sequencing the mitochondrial genome, 38 nuclear-encoded structural subunits and at least nine assembly factors, and the possibility of an underlying defect in a hitherto unrecognized gene, whole-exome sequence analysis using next-generation sequencing technologies may be a faster and cheaper route to find the genetic defect in many patients with isolated complex I deficiency in the future [173].

However, further studies are needed to incorporate known and unidentified complex I assembly factors into a more complete complex I assembly model. Identification of additional assembly factors remains a challenge, but should increase our understanding not only of complex I biogenesis but also of mitochondrial involvement in other common pathways or diseases, including neurodegeneration and cancer.

6 CONCLUSIONS

The denomination of “mitochondrial disease” can be applied to the clinical syndromes associated to anomalies in the final oxidative metabolism pathway [174]. Mitochondria are the organelles in charge for the accomplishment of this pathway; their biogenesis is the result of a complex interaction between the nuclear and the mitochondrial genome. Mitochondrial diseases may be caused by mutations in either genome; their molecular aetiology is often unresolved in a broad group of patients, in particular those in the neonatal, infantile and childhood age [175]. The direct consequence of this is that many patients never receive a genetic diagnosis.

In this study we have unravelled the genetic defect in 3 patients of the 12 studied in the present cohort of complex I deficient patients. Our combined biochemical and genetic approach allowed us the identification of a novel defect in a gene already associated with complex I deficiency: *NDUFS4*. This gene encodes for a subunit of the complex I which is involved in the activation of the complex via the phosphorylation of the C-terminal part of the protein mediated by PKA. Most of the mutations reported so far in the *NDUFS4* gene (including the one described in this study) prevent the phosphorylation of the subunit by altering the C-terminal part of it, either by frameshift or nonsense mutations.

Furthermore, we have discovered a new complex I assembly factor: FOXRED1, which had never previously been identified to be involved in the process or associated with human disease. The function of FOXRED1 is not clear, it contains an FAD-dependent oxidoreductase domain, which may be involved in electron transfer. Its four human homologs (DMGDH, SARDH, PIPOX and PDPR) perform redox reactions in amino acid catabolism, suggesting a potential link between amino acid metabolism and electron transfer to complex I. Also, given the fact that the complex I Blue Native pattern in patient fibroblasts reflects only a reduction in the content of the fully assembled holoenzyme but no complex I subassemblies were detected, it is conceivable to postulate that FOXRED1 takes part in the final stages of the complex I assembly process, when the holoenzyme is nearly mature. Future studies will focus on the attribution of a role in the complex I assembly/function of FOXRED1.

Two novel compound heterozygous mutations in *NDUFAF1* were also identified in this study. *NDUFAF1* appears to be involved at an intermediate stage of complex I assembly, in contrast to *C20orf7*, *NDUFAF3* and *NDUFAF4*, which are needed early in the assembly process, and to *NDUFAF2*, which has a role in the late stages [30]. Tandem affinity purification experiments demonstrated that *NDUFAF1* copurifies with two other putative complex I assembly factors, *ECSIT* and *ACAD9* [37,40]. Interestingly, *ACAD9* mutations have recently been reported to cause complex-I-deficient HCM, including a fatal infantile phenotype similar to that of our patient with *NDUFAF1* mutations [59,40]. Also, *NDUFAF1* has recently been

implicated in immune pathways, including T cell activation [141,142], and we speculate that this may explain why viral infection triggered decompensation and development of HCM in both patients with *NDUFAF1* mutations.

Even though it is not possible to delineate a clear phenotypic:genotypic correlation, especially in the field of mitochondrial disease, there are some common characteristics shared between patients carrying mutations in the same gene. For example hypertrophic cardiomyopathy is usually observed in mutations in *NDUFAF1*, as well as in *FOXRED1* and *ACAD9*. A very common characteristic in mitochondrial patients is lactic acidaemia, except for those with *NDUFAF2* mutations, in whom only CSF lactate levels are generally elevated.

Unravelling the genetic cause of mitochondrial disease is very important in order to give better prognostics and to provide parents with prenatal diagnosis and further reproductive options. Understanding the molecular mechanisms of the disease will also allow the experimentation of old and new therapeutic compounds that may be able to improve the clinical phenotype. New genetic techniques such as the Next Generation Sequencing Approach will help in the high throughput sequencing of the whole genome in search for the defect underlying mitochondrial disease.

REFERENCES

1. Taylor R.W. and Turnbull D.M., "Mitochondrial DNA mutations in human disease", *Nat Rev Genet*, Vol. 6, no. 5, 2005, pp. 389-402.
2. Wai T., Teoli D., Shoubridge E.A., "The mitochondrial DNA genetic bottleneck results from replication of a subpopulation of genomes", *Nat Genet*, Vol. 40, no. 12, 2008, pp. 1484-1488.
3. Chinnery P.F. and Samuels D.C., "Relaxed replication of mtDNA: A model with implications for the expression of disease", *Am J Hum Genet*, Vol. 64, no. 4, 1999, pp. 1158-1165.
4. Pagliarini D.J., Calvo S.E., Chang B., Sheth S.A., Vafai S.B., Ong S.E., Walford G.A., Sugiana C., Boneh A., Chen W.K., Hill D.E., Vidal M., Evans J.G., Thorburn D.R., Carr S.A., Mootha V.K., "A mitochondrial protein compendium elucidates complex I disease biology", *Cell*, Vol. 134, no. 1, 2008, pp. 112-123.
5. Taylor S.W., Fahy E., Zhang B., Glenn G.M., Warnock D.E., Wiley S., Murphy A.N., Gaucher S.P., Capaldi R.A., Gibson B.W., Ghosh S.S., "Characterization of the human heart mitochondrial proteome", *Nat Biotechnol*, Vol. 21, no. 3, 2003, pp. 281-286.
6. MITCHELL P., "Coupling of phosphorylation to electron and hydrogen transfer by a chemi-osmotic type of mechanism", *Nature*, Vol. 191, no. 1961, pp. 144-148.
7. Schagger H., "Respiratory chain supercomplexes of mitochondria and bacteria", *Biochim Biophys Acta*, Vol. 1555, no. 1-3, 2002, pp. 154-159.
8. Schafer E., Seelert H., Reifschneider N.H., Krause F., Dencher N.A., Vonck J., "Architecture of active mammalian respiratory chain supercomplexes", *J Biol Chem*, Vol. 281, no. 22, 2006, pp. 15370-15375.
9. Bianchi C., Genova M.L., Parenti C.G., Lenaz G., "The mitochondrial respiratory chain is partially organized in a supercomplex assembly: kinetic evidence using flux control analysis", *J Biol Chem*, Vol. 279, no. 35, 2004, pp. 36562-36569.
10. Dimroth P., Kaim G., Matthey U., "Crucial role of the membrane potential for ATP synthesis by F(1)F(o) ATP synthases", *J Exp Biol*, Vol. 203, no. Pt 1, 2000, pp. 51-59.

REFERENCES

11. Schultz B.E. and Chan S.I., "Structures and proton-pumping strategies of mitochondrial respiratory enzymes", *Annu Rev Biophys Biomol Struct*, Vol. 30, no. 2001, pp. 23-65.
12. Porter R.K. and Brand M.D., "Mitochondrial proton conductance and H⁺/O ratio are independent of electron transport rate in isolated hepatocytes", *Biochem J*, Vol. 310 (Pt 2), no. 1995, pp. 379-382.
13. Skladal D., Halliday J., Thorburn D.R., "Minimum birth prevalence of mitochondrial respiratory chain disorders in children", *Brain*, Vol. 126, no. Pt 8, 2003, pp. 1905-1912.
14. Munnich A. and Rustin P., "Clinical spectrum and diagnosis of mitochondrial disorders", *Am J Med Genet*, Vol. 106, no. 1, 2001, pp. 4-17.
15. Kirby D.M., Crawford M., Cleary M.A., Dahl H.H., Dennett X., Thorburn D.R., "Respiratory chain complex I deficiency: an underdiagnosed energy generation disorder", *Neurology*, Vol. 52, no. 6, 1999, pp. 1255-1264.
16. Bernier F.P., Boneh A., Dennett X., Chow C.W., Cleary M.A., Thorburn D.R., "Diagnostic criteria for respiratory chain disorders in adults and children", *Neurology*, Vol. 59, no. 9, 2002, pp. 1406-1411.
17. Clason T., Ruiz T., Schagger H., Peng G., Zickermann V., Brandt U., Michel H., Radermacher M., "The structure of eukaryotic and prokaryotic complex I", *J Struct Biol*, Vol. 169, no. 1, 2010, pp. 81-88.
18. Efremov R.G., Baradaran R., Sazanov L.A., "The architecture of respiratory complex I", *Nature*, Vol. 465, no. 7297, 2010, pp. 441-445.
19. Hunte C., Zickermann V., Brandt U., "Functional modules and structural basis of conformational coupling in mitochondrial complex I", *Science*, Vol. 329, no. 5990, 2010, pp. 448-451.
20. Sazanov L.A., Peak-Chew S.Y., Fearnley I.M., Walker J.E., "Resolution of the membrane domain of bovine complex I into subcomplexes: implications for the structural organization of the enzyme", *Biochemistry*, Vol. 39, no. 24, 2000, pp. 7229-7235.
21. Carroll J., Fearnley I.M., Shannon R.J., Hirst J., Walker J.E., "Analysis of the subunit composition of complex I from bovine heart mitochondria", *Mol Cell Proteomics*, Vol. 2, no. 2, 2003, pp. 117-126.
22. Finel M., Skehel J.M., Albracht S.P., Fearnley I.M., Walker J.E., "Resolution of NADH:ubiquinone oxidoreductase from bovine heart mitochondria into two subcomplexes, one of which contains the redox

- centers of the enzyme", *Biochemistry*, Vol. 31, no. 46, 1992, pp. 11425-11434.
23. Sazanov L.A. and Hinchliffe P., "Structure of the hydrophilic domain of respiratory complex I from *Thermus thermophilus*", *Science*, Vol. 311, no. 5766, 2006, pp. 1430-1436.
 24. Lazarou M., Thorburn D.R., Ryan M.T., McKenzie M., "Assembly of mitochondrial complex I and defects in disease", *Biochim Biophys Acta*, Vol. 1793, no. 1, 2009, pp. 78-88.
 25. Vogel R.O., Smeitink J.A., Nijtmans L.G., "Human mitochondrial complex I assembly: a dynamic and versatile process", *Biochim Biophys Acta*, Vol. 1767, no. 10, 2007, pp. 1215-1227.
 26. Smeitink J., Sengers R., Trijbels F., van den Heuvel L., "Human NADH:ubiquinone oxidoreductase", *J Bioenerg Biomembr*, Vol. 33, no. 3, 2001, pp. 259-266.
 27. Antonicka H., Ogilvie I., Taivassalo T., Anitori R.P., Haller R.G., Vissing J., Kennaway N.G., Shoubridge E.A., "Identification and characterization of a common set of complex I assembly intermediates in mitochondria from patients with complex I deficiency", *J Biol Chem*, Vol. 278, no. 44, 2003, pp. 43081-43088.
 28. Tuschen G., Sackmann U., Nehls U., Haiker H., Buse G., Weiss H., "Assembly of NADH: ubiquinone reductase (complex I) in *Neurospora* mitochondria. Independent pathways of nuclear-encoded and mitochondrially encoded subunits", *J Mol Biol*, Vol. 213, no. 4, 1990, pp. 845-857.
 29. Lazarou M., McKenzie M., Ohtake A., Thorburn D.R., Ryan M.T., "Analysis of the assembly profiles for mitochondrial- and nuclear-DNA-encoded subunits into complex I", *Mol Cell Biol*, Vol. 27, no. 12, 2007, pp. 4228-4237.
 30. McKenzie M. and Ryan M.T., "Assembly factors of human mitochondrial complex I and their defects in disease", *IUBMB Life*, Vol. 62, no. 7, 2010, pp. 497-502.
 31. Devenish R.J., Prescott M., Roucou X., Nagley P., "Insights into ATP synthase assembly and function through the molecular genetic manipulation of subunits of the yeast mitochondrial enzyme complex", *Biochim Biophys Acta*, Vol. 1458, no. 2-3, 2000, pp. 428-442.

32. Fontanesi F., Soto I.C., Horn D., Barrientos A., "Assembly of mitochondrial cytochrome c-oxidase, a complicated and highly regulated cellular process", *Am J Physiol Cell Physiol*, Vol. 291, no. 6, 2006, pp. C1129-C1147.
33. Kuffner R., Rohr A., Schmiede A., Krull C., Schulte U., "Involvement of two novel chaperones in the assembly of mitochondrial NADH:Ubiquinone oxidoreductase (complex I)", *J Mol Biol*, Vol. 283, no. 2, 1998, pp. 409-417.
34. Ogilvie I., Kennaway N.G., Shoubridge E.A., "A molecular chaperone for mitochondrial complex I assembly is mutated in a progressive encephalopathy", *J Clin Invest*, Vol. 115, no. 10, 2005, pp. 2784-2792.
35. Bych K., Kerscher S., Netz D.J., Pierik A.J., Zwicker K., Huynen M.A., Lill R., Brandt U., Balk J., "The iron-sulphur protein Ind1 is required for effective complex I assembly", *EMBO J*, Vol. 27, no. 12, 2008, pp. 1736-1746.
36. Saada A., Vogel R.O., Hoefs S.J., van den Brand M.A., Wessels H.J., Willems P.H., Venselaar H., Shaag A., Barghuti F., Reish O., Shohat M., Huynen M.A., Smeitink J.A., van den Heuvel L.P., Nijtmans L.G., "Mutations in NDUFAF3 (C3ORF60), encoding an NDUFAF4 (C6ORF66)-interacting complex I assembly protein, cause fatal neonatal mitochondrial disease", *Am J Hum Genet*, Vol. 84, no. 6, 2009, pp. 718-727.
37. Vogel R.O., Janssen R.J., van den Brand M.A., Dieteren C.E., Verkaart S., Koopman W.J., Willems P.H., Pluk W., van den Heuvel L.P., Smeitink J.A., Nijtmans L.G., "Cytosolic signaling protein Ecsit also localizes to mitochondria where it interacts with chaperone NDUFAF1 and functions in complex I assembly", *Genes Dev*, Vol. 21, no. 5, 2007, pp. 615-624.
38. Fassone E., Duncan A.J., Taanman J.W., Pagnamenta A.T., Sadowski M.I., Holand T., Qasim W., Rutland P., Calvo S.E., Mootha V.K., Bitner-Glindzicz M., Rahman S., "FOXRED1, encoding an FAD-dependent oxidoreductase complex-I-specific molecular chaperone, is mutated in infantile-onset mitochondrial encephalopathy", *Hum Mol Genet*, Vol. 19, no. 24, 2010, pp. 4837-4847.
39. Calvo S.E., Tucker E.J., Compton A.G., Kirby D.M., Crawford G., Burt N.P., Rivas M., Guiducci C., Bruno D.L., Goldberger O.A., Redman M.C., Wiltshire E., Wilson C.J., Altshuler D., Gabriel S.B., Daly M.J., Thorburn D.R., Mootha V.K., "High-throughput, pooled sequencing identifies mutations in NUBPL and FOXRED1 in human complex I deficiency", *Nat Genet*, Vol. 42, no. 10, 2010, pp. 851-858.

REFERENCES

40. Nouws J., Nijtmans L., Houten S.M., van den Brand M., Huynen M., Venselaar H., Hoefs S., Gloerich J., Kronick J., Hutchin T., Willems P., Rodenburg R., Wanders R., van den Heuvel L., Smeitink J., Vogel R.O., "Acyl-CoA dehydrogenase 9 is required for the biogenesis of oxidative phosphorylation complex I", *Cell Metab*, Vol. 12, no. 3, 2010, pp. 283-294.
41. Sheftel A.D., Stehling O., Pierik A.J., Netz D.J., Kerscher S., Elsasser H.P., Wittig I., Balk J., Brandt U., Lill R., "Human ind1, an iron-sulfur cluster assembly factor for respiratory complex I", *Mol Cell Biol*, Vol. 29, no. 22, 2009, pp. 6059-6073.
42. Helm M., Brule H., Degoul F., Capanec C., Leroux J.P., Giege R., Florentz C., "The presence of modified nucleotides is required for cloverleaf folding of a human mitochondrial tRNA", *Nucleic Acids Res*, Vol. 26, no. 7, 1998, pp. 1636-1643.
43. Pintard L., Bujnicki J.M., Lapeyre B., Bonnerot C., "MRM2 encodes a novel yeast mitochondrial 21S rRNA methyltransferase", *EMBO J*, Vol. 21, no. 5, 2002, pp. 1139-1147.
44. Carilla-Latorre S., Gallardo M.E., Annesley S.J., Calvo-Garrido J., Grana O., Accari S.L., Smith P.K., Valencia A., Garesse R., Fisher P.R., Escalante R., "MidA is a putative methyltransferase that is required for mitochondrial complex I function", *J Cell Sci*, Vol. 123, no. Pt 10, 2010, pp. 1674-1683.
45. Carroll J., Fearnley I.M., Skehel J.M., Runswick M.J., Shannon R.J., Hirst J., Walker J.E., "The post-translational modifications of the nuclear encoded subunits of complex I from bovine heart mitochondria", *Mol Cell Proteomics*, Vol. 4, no. 5, 2005, pp. 693-699.
46. Sugiana C., Pagliarini D.J., McKenzie M., Kirby D.M., Salemi R., bu-Amereo K.K., Dahl H.H., Hutchison W.M., Vascotto K.A., Smith S.M., Newbold R.F., Christodoulou J., Calvo S., Mootha V.K., Ryan M.T., Thorburn D.R., "Mutation of C20orf7 disrupts complex I assembly and causes lethal neonatal mitochondrial disease", *Am J Hum Genet*, Vol. 83, no. 4, 2008, pp. 468-478.
47. Saada A., Edvardson S., Shaag A., Chung W.K., Segel R., Miller C., J alas C., Elpeleg O., "Combined OXPHOS complex I and IV defect, due to mutated complex I assembly factor C20ORF7", *J Inherit Metab Dis*, Vol. 2011, pp.
48. Saada A., Edvardson S., Rapoport M., Shaag A., Amry K., Miller C., Lorberboum-Galski H., Elpeleg O., "C6ORF66 is an assembly factor of

- mitochondrial complex I", *Am J Hum Genet*, Vol. 82, no. 1, 2008, pp. 32-38.
49. Ugalde C., Janssen R.J., van den Heuvel L.P., Smeitink J.A., Nijtmans L.G., "Differences in assembly or stability of complex I and other mitochondrial OXPHOS complexes in inherited complex I deficiency", *Hum Mol Genet*, Vol. 13, no. 6, 2004, pp. 659-667.
50. Vogel R.O., Dieteren C.E., van den Heuvel L.P., Willems P.H., Smeitink J.A., Koopman W.J., Nijtmans L.G., "Identification of mitochondrial complex I assembly intermediates by tracing tagged NDUFS3 demonstrates the entry point of mitochondrial subunits", *J Biol Chem*, Vol. 282, no. 10, 2007, pp. 7582-7590.
51. Dunning C.J., McKenzie M., Sugiana C., Lazarou M., Silke J., Connelly A., Fletcher J.M., Kirby D.M., Thorburn D.R., Ryan M.T., "Human CIA30 is involved in the early assembly of mitochondrial complex I and mutations in its gene cause disease", *EMBO J*, Vol. 26, no. 13, 2007, pp. 3227-3237.
52. Fassone E., Taanman J.W., Hargreaves I.P., Sebire N.J., Cleary M.A., Burch M., Rahman S., "Mutations in the mitochondrial complex I assembly factor NDUFAF1 cause fatal infantile hypertrophic cardiomyopathy", *J Med Genet*, Vol. 48, no. 10, 2011, pp. 691-697.
53. Liu S., Lee Y.F., Chou S., Uno H., Li G., Brookes P., Massett M.P., Wu Q., Chen L.M., Chang C., "Mice Lacking TR4 Nuclear Receptor Develop Mitochondrial Myopathy with Deficiency in Complex I", *Mol Endocrinol*, Vol. 2011, pp.
54. Xiao C., Shim J.H., Kluppel M., Zhang S.S., Dong C., Flavell R.A., Fu X.Y., Wrana J.L., Hogan B.L., Ghosh S., "Ecsit is required for Bmp signaling and mesoderm formation during mouse embryogenesis", *Genes Dev*, Vol. 17, no. 23, 2003, pp. 2933-2949.
55. Kopp E., Medzhitov R., Carothers J., Xiao C., Douglas I., Janeway C.A., Ghosh S., "ECSIT is an evolutionarily conserved intermediate in the Toll/IL-1 signal transduction pathway", *Genes Dev*, Vol. 13, no. 16, 1999, pp. 2059-2071.
56. Vogel R.O., van den Brand M.A., Rodenburg R.J., van den Heuvel L.P., Tsuneoka M., Smeitink J.A., Nijtmans L.G., "Investigation of the complex I assembly chaperones B17.2L and NDUFAF1 in a cohort of CI deficient patients", *Mol Genet Metab*, Vol. 91, no. 2, 2007, pp. 176-182.
57. Zhang J., Zhang W., Zou D., Chen G., Wan T., Zhang M., Cao X., "Cloning and functional characterization of ACAD-9, a novel member of human acyl-

- CoA dehydrogenase family", *Biochem Biophys Res Commun*, Vol. 297, no. 4, 2002, pp. 1033-1042.
58. Gerards M., van den Bosch B.J., Danhauser K., Serre V., van W.M., Wanders R.J., Nicolaes G.A., Sluiter W., Schoonderwoerd K., Scholte H.R., Prokisch H., Rotig A., de Coo I.F., Smeets H.J., "Riboflavin-responsive oxidative phosphorylation complex I deficiency caused by defective ACAD9: new function for an old gene", *Brain*, Vol. 134, no. Pt 1, 2011, pp. 210-219.
59. Haack T.B., Danhauser K., Haberberger B., Hoser J., Strecker V., Boehm D., Uziel G., Lamantea E., Invernizzi F., Poulton J., Rolinski B., Iuso A., Biskup S., Schmidt T., Mewes H.W., Wittig I., Meitinger T., Zeviani M., Prokisch H., "Exome sequencing identifies ACAD9 mutations as a cause of complex I deficiency", *Nat Genet*, Vol. 42, no. 12, 2010, pp. 1131-1134.
60. Hoefs S.J., Dieteren C.E., Rodenburg R.J., Naess K., Bruhn H., Wibom R., Wagena E., Willems P.H., Smeitink J.A., Nijtmans L.G., van den Heuvel L.P., "Baculovirus complementation restores a novel NDUFAF2 mutation causing complex I deficiency", *Hum Mutat*, Vol. 30, no. 7, 2009, pp. E728-E736.
61. Brandt U., "Energy converting NADH:quinone oxidoreductase (complex I)", *Annu Rev Biochem*, Vol. 75, no. 2006, pp. 69-92.
62. Vahsen N., Cande C., Briere J.J., Benit P., Joza N., Larochette N., Mastroberardino P.G., Pequignot M.O., Casares N., Lazar V., Feraud O., Debili N., Wissing S., Engelhardt S., Madeo F., Piacentini M., Penninger J.M., Schagger H., Rustin P., Kroemer G., "AIF deficiency compromises oxidative phosphorylation", *EMBO J*, Vol. 23, no. 23, 2004, pp. 4679-4689.
63. Chinta S.J., Rane A., Yadava N., Andersen J.K., Nicholls D.G., Polster B.M., "Reactive oxygen species regulation by AIF- and complex I-depleted brain mitochondria", *Free Radic Biol Med*, Vol. 46, no. 7, 2009, pp. 939-947.
64. El G., V, Csaba Z., Olivier P., Lelouvier B., Schwendimann L., Dournaud P., Verney C., Rustin P., Gressens P., "Apoptosis-inducing factor deficiency induces early mitochondrial degeneration in brain followed by progressive multifocal neuropathology", *J Neuropathol Exp Neurol*, Vol. 66, no. 9, 2007, pp. 838-847.
65. Ghezzi D., Sevrioukova I., Invernizzi F., Lamperti C., Mora M., D'Adamo P., Novara F., Zuffardi O., Uziel G., Zeviani M., "Severe X-linked mitochondrial encephalomyopathy associated with a mutation in apoptosis-inducing factor", *Am J Hum Genet*, Vol. 86, no. 4, 2010, pp. 639-649.

REFERENCES

66. Miramar M.D., Costantini P., Ravagnan L., Saraiva L.M., Haouzi D., Brothers G., Penninger J.M., Peleato M.L., Kroemer G., Susin S.A., "NADH oxidase activity of mitochondrial apoptosis-inducing factor", *J Biol Chem*, Vol. 276, no. 19, 2001, pp. 16391-16398.
67. Churbanova I.Y. and Sevrioukova I.F., "Redox-dependent changes in molecular properties of mitochondrial apoptosis-inducing factor", *J Biol Chem*, Vol. 283, no. 9, 2008, pp. 5622-5631.
68. Distelmaier F., Koopman W.J., van den Heuvel L.P., Rodenburg R.J., Mayatepek E., Willems P.H., Smeitink J.A., "Mitochondrial complex I deficiency: from organelle dysfunction to clinical disease", *Brain*, Vol. 132, no. Pt 4, 2009, pp. 833-842.
69. Valsecchi F., Koopman W.J., Manjeri G.R., Rodenburg R.J., Smeitink J.A., Willems P.H., "Complex I disorders: causes, mechanisms, and development of treatment strategies at the cellular level", *Dev Disabil Res Rev*, Vol. 16, no. 2, 2010, pp. 175-182.
70. Janssen R.J., Nijtmans L.G., van den Heuvel L.P., Smeitink J.A., "Mitochondrial complex I: structure, function and pathology", *J Inherit Metab Dis*, Vol. 29, no. 4, 2006, pp. 499-515.
71. Schuelke M., Smeitink J., Mariman E., Loeffen J., Plecko B., Trijbels F., Stockler-Ipsiroglu S., van den Heuvel L., "Mutant NDUFV1 subunit of mitochondrial complex I causes leukodystrophy and myoclonic epilepsy", *Nat Genet*, Vol. 21, no. 3, 1999, pp. 260-261.
72. Benit P., Beugnot R., Chretien D., Giurgea I., De Lonlay-Debeney P., Issartel J.P., Corral-Debrinski M., Kerscher S., Rustin P., Rotig A., Munnich A., "Mutant NDUFV2 subunit of mitochondrial complex I causes early onset hypertrophic cardiomyopathy and encephalopathy", *Hum Mutat*, Vol. 21, no. 6, 2003, pp. 582-586.
73. Benit P., Chretien D., Kadhon N., De Lonlay-Debeney P., Cormier-Daire V., Cabral A., Peudenier S., Rustin P., Munnich A., Rotig A., "Large-scale deletion and point mutations of the nuclear NDUFV1 and NDUFS1 genes in mitochondrial complex I deficiency", *Am J Hum Genet*, Vol. 68, no. 6, 2001, pp. 1344-1352.
74. Loeffen J., Elpeleg O., Smeitink J., Smeets R., Stockler-Ipsiroglu S., Mandel H., Sengers R., Trijbels F., van den Heuvel L., "Mutations in the complex I NDUFS2 gene of patients with cardiomyopathy and encephalomyopathy", *Ann Neurol*, Vol. 49, no. 2, 2001, pp. 195-201.

75. Benit P., Slama A., Cartault F., Giurgea I., Chretien D., Lebon S., Marsac C., Munnich A., Rotig A., Rustin P., "Mutant NDUFS3 subunit of mitochondrial complex I causes Leigh syndrome", *J Med Genet*, Vol. 41, no. 1, 2004, pp. 14-17.
76. Triepels R.H., van den Heuvel L.P., Loeffen J.L., Buskens C.A., Smeets R.J., Rubio Gozalbo M.E., Budde S.M., Mariman E.C., Wijburg F.A., Barth P.G., Trijbels J.M., Smeitink J.A., "Leigh syndrome associated with a mutation in the NDUFS7 (PSST) nuclear encoded subunit of complex I", *Ann Neurol*, Vol. 45, no. 6, 1999, pp. 787-790.
77. Loeffen J., Smeitink J., Triepels R., Smeets R., Schuelke M., Sengers R., Trijbels F., Hamel B., Mullaart R., van den Heuvel L., "The first nuclear-encoded complex I mutation in a patient with Leigh syndrome", *Am J Hum Genet*, Vol. 63, no. 6, 1998, pp. 1598-1608.
78. van den Heuvel L., Ruitenbeek W., Smeets R., Gelman-Kohan Z., Elpeleg O., Loeffen J., Trijbels F., Mariman E., de B.D., Smeitink J., "Demonstration of a new pathogenic mutation in human complex I deficiency: a 5-bp duplication in the nuclear gene encoding the 18-kD (AQDQ) subunit", *Am J Hum Genet*, Vol. 62, no. 2, 1998, pp. 262-268.
79. Kirby D.M., Salemi R., Sugiana C., Ohtake A., Parry L., Bell K.M., Kirk E.P., Boneh A., Taylor R.W., Dahl H.H., Ryan M.T., Thorburn D.R., "NDUFS6 mutations are a novel cause of lethal neonatal mitochondrial complex I deficiency", *J Clin Invest*, Vol. 114, no. 6, 2004, pp. 837-845.
80. Fernandez-Moreira D., Ugalde C., Smeets R., Rodenburg R.J., Lopez-Laso E., Ruiz-Falco M.L., Briones P., Martin M.A., Smeitink J.A., Arenas J., "X-linked NDUFA1 gene mutations associated with mitochondrial encephalomyopathy", *Ann Neurol*, Vol. 61, no. 1, 2007, pp. 73-83.
81. Hoefs S.J., Dieteren C.E., Distelmaier F., Janssen R.J., Epplen A., Swarts H.G., Forkink M., Rodenburg R.J., Nijtmans L.G., Willems P.H., Smeitink J.A., van den Heuvel L.P., "NDUFA2 complex I mutation leads to Leigh disease", *Am J Hum Genet*, Vol. 82, no. 6, 2008, pp. 1306-1315.
82. Berger I., Hershkovitz E., Shaag A., Edvardson S., Saada A., Elpeleg O., "Mitochondrial complex I deficiency caused by a deleterious NDUFA11 mutation", *Ann Neurol*, Vol. 63, no. 3, 2008, pp. 405-408.
83. Loeffen J., Smeets R., Smeitink J., Triepels R., Sengers R., Trijbels F., van den Heuvel L., "The human NADH: ubiquinone oxidoreductase NDUFS5 (15 kDa) subunit: cDNA cloning, chromosomal localization, tissue distribution and the absence of mutations in isolated complex I-deficient patients", *J Inherit Metab Dis*, Vol. 22, no. 1, 1999, pp. 19-28.

84. Gerards M., Sluiter W., van den Bosch B.J., de W.E., Calis C.M., Frentzen M., Akbari H., Schoonderwoerd K., Scholte H.R., Jongbloed R.J., Hendrickx A.T., de C., I, Smeets H.J., "Defective complex I assembly due to C20orf7 mutations as a new cause of Leigh syndrome", *J Med Genet*, Vol. 2009, pp.
85. Herzer M., Koch J., Prokisch H., Rodenburg R., Rauscher C., Radauer W., Forstner R., Pilz P., Rolinski B., Freisinger P., Mayr J.A., Sperl W., "Leigh disease with brainstem involvement in complex I deficiency due to assembly factor NDUFAF2 defect", *Neuropediatrics*, Vol. 41, no. 1, 2010, pp. 30-34.
86. Bitner-Glindzicz M., Pembrey M., Duncan A., Heron J., Ring S.M., Hall A., Rahman S., "Prevalence of mitochondrial 1555A->G mutation in European children", *N Engl J Med*, Vol. 360, no. 6, 2009, pp. 640-642.
87. Thorburn D.R., "Mitochondrial disorders: prevalence, myths and advances", *J Inherit Metab Dis*, Vol. 27, no. 3, 2004, pp. 349-362.
88. Swalwell H., Kirby D.M., Blakely E.L., Mitchell A., Salemi R., Sugiana C., Compton A.G., Tucker E.J., Ke B.X., Lamont P.J., Turnbull D.M., McFarland R., Taylor R.W., Thorburn D.R., "Respiratory chain complex I deficiency caused by mitochondrial DNA mutations", *Eur J Hum Genet*, Vol. 19, no. 7, 2011, pp. 769-775.
89. Lebon S., Chol M., Benit P., Mugnier C., Chretien D., Giurgea I., Kern I., Girardin E., Hertz-Pannier L., de L.P., Rotig A., Rustin P., Munnich A., "Recurrent de novo mitochondrial DNA mutations in respiratory chain deficiency", *J Med Genet*, Vol. 40, no. 12, 2003, pp. 896-899.
90. Pellegrini M., Marcotte E.M., Thompson M.J., Eisenberg D., Yeates T.O., "Assigning protein functions by comparative genome analysis: protein phylogenetic profiles", *Proc Natl Acad Sci U S A*, Vol. 96, no. 8, 1999, pp. 4285-4288.
91. He M., Rutledge S.L., Kelly D.R., Palmer C.A., Murdoch G., Majumder N., Nicholls R.D., Pei Z., Watkins P.A., Vockley J., "A new genetic disorder in mitochondrial fatty acid beta-oxidation: ACAD9 deficiency", *Am J Hum Genet*, Vol. 81, no. 1, 2007, pp. 87-103.
92. Belostotsky R., Seboun E., Idelson G.H., Milliner D.S., Becker-Cohen R., Rinat C., Monico C.G., Feinstein S., Ben-Shalom E., Magen D., Weissman I., Charon C., Frishberg Y., "Mutations in DHAPSL are responsible for primary hyperoxaluria type III", *Am J Hum Genet*, Vol. 87, no. 3, 2010, pp. 392-399.

REFERENCES

93. Kassovska-Bratinova S., Fukao T., Song X.Q., Duncan A.M., Chen H.S., Robert M.F., Perez-Cerda C., Ugarte M., Chartrand C., Vobecky S., Kondo N., Mitchell G.A., "Succinyl CoA: 3-oxoacid CoA transferase (SCOT): human cDNA cloning, human chromosomal mapping to 5p13, and mutation detection in a SCOT-deficient patient", *Am J Hum Genet*, Vol. 59, no. 3, 1996, pp. 519-528.
94. Vockley J., Parimoo B., Tanaka K., "Molecular characterization of four different classes of mutations in the isovaleryl-CoA dehydrogenase gene responsible for isovaleric acidemia", *Am J Hum Genet*, Vol. 49, no. 1, 1991, pp. 147-157.
95. Gallardo M.E., Desviat L.R., Rodriguez J.M., Esparza-Gordillo J., Perez-Cerda C., Perez B., Rodriguez-Pombo P., Criado O., Sanz R., Morton D.H., Gibson K.M., Le T.P., Ribes A., de Cordoba S.R., Ugarte M., Penalva M.A., "The molecular basis of 3-methylcrotonylglycinuria, a disorder of leucine catabolism", *Am J Hum Genet*, Vol. 68, no. 2, 2001, pp. 334-346.
96. Sherman E.A., Strauss K.A., Tortorelli S., Bennett M.J., Knerr I., Morton D.H., Puffenberger E.G., "Genetic mapping of glutaric aciduria, type 3, to chromosome 7 and identification of mutations in c7orf10", *Am J Hum Genet*, Vol. 83, no. 5, 2008, pp. 604-609.
97. Ferdinandusse S., Denis S., Clayton P.T., Graham A., Rees J.E., Allen J.T., McLean B.N., Brown A.Y., Vreken P., Waterham H.R., Wanders R.J., "Mutations in the gene encoding peroxisomal alpha-methylacyl-CoA racemase cause adult-onset sensory motor neuropathy", *Nat Genet*, Vol. 24, no. 2, 2000, pp. 188-191.
98. Mihalik S.J., Morrell J.C., Kim D., Sacksteder K.A., Watkins P.A., Gould S.J., "Identification of PAHX, a Refsum disease gene", *Nat Genet*, Vol. 17, no. 2, 1997, pp. 185-189.
99. Joza N., Oudit G.Y., Brown D., Benit P., Kassiri Z., Vahsen N., Benoit L., Patel M.M., Nowikovsky K., Vassault A., Backx P.H., Wada T., Kroemer G., Rustin P., Penninger J.M., "Muscle-specific loss of apoptosis-inducing factor leads to mitochondrial dysfunction, skeletal muscle atrophy, and dilated cardiomyopathy", *Mol Cell Biol*, Vol. 25, no. 23, 2005, pp. 10261-10272.
100. Hangen E., Blomgren K., Benit P., Kroemer G., Modjtahedi N., "Life with or without AIF", *Trends Biochem Sci*, Vol. 35, no. 5, 2010, pp. 278-287.
101. Klein J.A., Longo-Guess C.M., Rossmann M.P., Seburn K.L., Hurd R.E., Frankel W.N., Bronson R.T., Ackerman S.L., "The harlequin mouse

- mutation downregulates apoptosis-inducing factor", *Nature*, Vol. 419, no. 6905, 2002, pp. 367-374.
102. Susin S.A., Lorenzo H.K., Zamzami N., Marzo I., Snow B.E., Brothers G.M., Mangion J., Jacotot E., Costantini P., Loeffler M., Larochette N., Goodlett D.R., Aebbersold R., Siderovski D.P., Penninger J.M., Kroemer G., "Molecular characterization of mitochondrial apoptosis-inducing factor", *Nature*, Vol. 397, no. 6718, 1999, pp. 441-446.
103. Cheung E.C., Joza N., Steenaart N.A., McClellan K.A., Neuspiel M., McNamara S., MacLaurin J.G., Rippstein P., Park D.S., Shore G.C., McBride H.M., Penninger J.M., Slack R.S., "Dissociating the dual roles of apoptosis-inducing factor in maintaining mitochondrial structure and apoptosis", *EMBO J*, Vol. 25, no. 17, 2006, pp. 4061-4073.
104. Benit P., Goncalves S., Dassa E.P., Briere J.J., Rustin P., "The variability of the harlequin mouse phenotype resembles that of human mitochondrial-complex I-deficiency syndromes", *PLoS One*, Vol. 3, no. 9, 2008, pp. e3208-
105. van Empel V.P., Bertrand A.T., van der Nagel R., Kostin S., Doevendans P.A., Crijns H.J., de W.E., Sluiter W., Ackerman S.L., De Windt L.J., "Downregulation of apoptosis-inducing factor in harlequin mutant mice sensitizes the myocardium to oxidative stress-related cell death and pressure overload-induced decompensation", *Circ Res*, Vol. 96, no. 12, 2005, pp. e92-e101.
106. Pospisilik J.A., Knauf C., Joza N., Benit P., Orthofer M., Cani P.D., Ebersberger I., Nakashima T., Sarao R., Neely G., Esterbauer H., Kozlov A., Kahn C.R., Kroemer G., Rustin P., Burcelin R., Penninger J.M., "Targeted deletion of AIF decreases mitochondrial oxidative phosphorylation and protects from obesity and diabetes", *Cell*, Vol. 131, no. 3, 2007, pp. 476-491.
107. Kruse S.E., Watt W.C., Marcinek D.J., Kapur R.P., Schenkman K.A., Palmiter R.D., "Mice with mitochondrial complex I deficiency develop a fatal encephalomyopathy", *Cell Metab*, Vol. 7, no. 4, 2008, pp. 312-320.
108. Loeffen J.L., Smeitink J.A., Trijbels J.M., Janssen A.J., Triepels R.H., Sengers R.C., van den Heuvel L.P., "Isolated complex I deficiency in children: clinical, biochemical and genetic aspects", *Hum Mutat*, Vol. 15, no. 2, 2000, pp. 123-134.
109. Budde S.M., van den Heuvel L.P., Smeets R.J., Skladal D., Mayr J.A., Boelen C., Petruzzella V., Papa S., Smeitink J.A., "Clinical heterogeneity in

- patients with mutations in the NDUFS4 gene of mitochondrial complex I", *J Inherit Metab Dis*, Vol. 26, no. 8, 2003, pp. 813-815.
110. Rahman S., Blok R.B., Dahl H.H., Danks D.M., Kirby D.M., Chow C.W., Christodoulou J., Thorburn D.R., "Leigh syndrome: clinical features and biochemical and DNA abnormalities", *Ann Neurol*, Vol. 39, no. 3, 1996, pp. 343-351.
111. Qi X., Lewin A.S., Hauswirth W.W., Guy J., "Optic neuropathy induced by reductions in mitochondrial superoxide dismutase", *Invest Ophthalmol Vis Sci*, Vol. 44, no. 3, 2003, pp. 1088-1096.
112. Melov S., Doctrow S.R., Schneider J.A., Haberson J., Patel M., Coskun P.E., Huffman K., Wallace D.C., Malfroy B., "Lifespan extension and rescue of spongiform encephalopathy in superoxide dismutase 2 nullizygous mice treated with superoxide dismutase-catalase mimetics", *J Neurosci*, Vol. 21, no. 21, 2001, pp. 8348-8353.
113. Wispe J.R., Warner B.B., Clark J.C., Dey C.R., Neuman J., Glasser S.W., Crapo J.D., Chang L.Y., Whitsett J.A., "Human Mn-superoxide dismutase in pulmonary epithelial cells of transgenic mice confers protection from oxygen injury", *J Biol Chem*, Vol. 267, no. 33, 1992, pp. 23937-23941.
114. Mortiboys H., Thomas K.J., Koopman W.J., Klaffke S., Abou-Sleiman P., Olpin S., Wood N.W., Willems P.H., Smeitink J.A., Cookson M.R., Bandmann O., "Mitochondrial function and morphology are impaired in parkin-mutant fibroblasts", *Ann Neurol*, Vol. 64, no. 5, 2008, pp. 555-565.
115. Lash L.H., "Mitochondrial glutathione transport: physiological, pathological and toxicological implications", *Chem Biol Interact*, Vol. 163, no. 1-2, 2006, pp. 54-67.
116. Kelso G.F., Porteous C.M., Coulter C.V., Hughes G., Porteous W.K., Ledgerwood E.C., Smith R.A., Murphy M.P., "Selective targeting of a redox-active ubiquinone to mitochondria within cells: antioxidant and antiapoptotic properties", *J Biol Chem*, Vol. 276, no. 7, 2001, pp. 4588-4596.
117. Skulachev V.P., Antonenko Y.N., Cherepanov D.A., Chernyak B.V., Izyumov D.S., Khailova L.S., Klishin S.S., Korshunova G.A., Lyamzaev K.G., Pletjushkina O.Y., Roginsky V.A., Rokitskaya T.I., Severin F.F., Severina I.I., Simonyan R.A., Skulachev M.V., Sumbatyan N.V., Sukhanova E.I., Tashlitsky V.N., Trendeleva T.A., Vysokikh M.Y., Zvyagilskaya R.A., "Prevention of cardiolipin oxidation and fatty acid cycling as two antioxidant mechanisms of cationic derivatives of

- plastoquinone (SkQs)", *Biochim Biophys Acta*, Vol. 1797, no. 6-7, 2010, pp. 878-889.
118. Xi J., Wang H., Mueller R.A., Norfleet E.A., Xu Z., "Mechanism for resveratrol-induced cardioprotection against reperfusion injury involves glycogen synthase kinase 3 β and mitochondrial permeability transition pore", *Eur J Pharmacol*, Vol. 604, no. 1-3, 2009, pp. 111-116.
119. Marriage B., Clandinin M.T., Glerum D.M., "Nutritional cofactor treatment in mitochondrial disorders", *J Am Diet Assoc*, Vol. 103, no. 8, 2003, pp. 1029-1038.
120. Panetta J., Smith L.J., Boneh A., "Effect of high-dose vitamins, coenzyme Q and high-fat diet in paediatric patients with mitochondrial diseases", *J Inherit Metab Dis*, Vol. 27, no. 4, 2004, pp. 487-498.
121. Penn A.M., Lee J.W., Thuillier P., Wagner M., Maclure K.M., Menard M.R., Hall L.D., Kennaway N.G., "MELAS syndrome with mitochondrial tRNA(Leu)(UUR) mutation: correlation of clinical state, nerve conduction, and muscle 31P magnetic resonance spectroscopy during treatment with nicotinamide and riboflavin", *Neurology*, Vol. 42, no. 11, 1992, pp. 2147-2152.
122. Bernsen P.L., Gabreels F.J., Ruitenbeek W., Hamburger H.L., "Treatment of complex I deficiency with riboflavin", *J Neurol Sci*, Vol. 118, no. 2, 1993, pp. 181-187.
123. Mathews P.M., Andermann F., Silver K., Karpati G., Arnold D.L., "Proton MR spectroscopic characterization of differences in regional brain metabolic abnormalities in mitochondrial encephalomyopathies", *Neurology*, Vol. 43, no. 12, 1993, pp. 2484-2490.
124. Nagao M. and Tanaka K., "FAD-dependent regulation of transcription, translation, post-translational processing, and post-processing stability of various mitochondrial acyl-CoA dehydrogenases and of electron transfer flavoprotein and the site of holoenzyme formation", *J Biol Chem*, Vol. 267, no. 25, 1992, pp. 17925-17932.
125. Saijo T. and Tanaka K., "Isoalloxazine ring of FAD is required for the formation of the core in the Hsp60-assisted folding of medium chain acyl-CoA dehydrogenase subunit into the assembly competent conformation in mitochondria", *J Biol Chem*, Vol. 270, no. 4, 1995, pp. 1899-1907.
126. Olsen R.K., Olpin S.E., Andresen B.S., Miedzybrodzka Z.H., Pourfarzam M., Merinero B., Frerman F.E., Beresford M.W., Dean J.C., Cornelius N., Andersen O., Oldfors A., Holme E., Gregersen N., Turnbull D.M., Morris

- A.A., "ETFDH mutations as a major cause of riboflavin-responsive multiple acyl-CoA dehydrogenation deficiency", *Brain*, Vol. 130, no. Pt 8, 2007, pp. 2045-2054.
127. Grad L.I. and Lemire B.D., "Riboflavin enhances the assembly of mitochondrial cytochrome c oxidase in *C. elegans* NADH-ubiquinone oxidoreductase mutants", *Biochim Biophys Acta*, Vol. 1757, no. 2, 2006, pp. 115-122.
128. Brini M., Pinton P., King M.P., Davidson M., Schon E.A., Rizzuto R., "A calcium signaling defect in the pathogenesis of a mitochondrial DNA inherited oxidative phosphorylation deficiency", *Nat Med*, Vol. 5, no. 8, 1999, pp. 951-954.
129. Visch H.J., Rutter G.A., Koopman W.J., Koenderink J.B., Verkaart S., de G.T., Varadi A., Mitchell K.J., van den Heuvel L.P., Smeitink J.A., Willems P.H., "Inhibition of mitochondrial Na⁺-Ca²⁺ exchange restores agonist-induced ATP production and Ca²⁺ handling in human complex I deficiency", *J Biol Chem*, Vol. 279, no. 39, 2004, pp. 40328-40336.
130. Visch H.J., Koopman W.J., Leusink A., van Emst-de Vries SE, van den Heuvel L.W., Willems P.H., Smeitink J.A., "Decreased agonist-stimulated mitochondrial ATP production caused by a pathological reduction in endoplasmic reticulum calcium content in human complex I deficiency", *Biochim Biophys Acta*, Vol. 1762, no. 1, 2006, pp. 115-123.
131. Visch H.J., Koopman W.J., Zeegers D., van Emst-de Vries SE, van Kuppeveld F.J., van den Heuvel L.W., Smeitink J.A., Willems P.H., "Ca²⁺-mobilizing agonists increase mitochondrial ATP production to accelerate cytosolic Ca²⁺ removal: aberrations in human complex I deficiency", *Am J Physiol Cell Physiol*, Vol. 291, no. 2, 2006, pp. C308-C316.
132. Rahman S. and Hanna M.G., "Diagnosis and therapy in neuromuscular disorders: diagnosis and new treatments in mitochondrial diseases", *J Neurol Neurosurg Psychiatry*, Vol. 80, no. 9, 2009, pp. 943-953.
133. Chretien D. and Rustin P., "Mitochondrial oxidative phosphorylation: pitfalls and tips in measuring and interpreting enzyme activities", *J Inherit Metab Dis*, Vol. 26, no. 2-3, 2003, pp. 189-198.
134. Bradford M.M., "A rapid and sensitive method for the quantitation of microgram quantities of protein utilizing the principle of protein-dye binding", *Anal Biochem*, Vol. 72, no. 1976, pp. 248-254.

REFERENCES

135. Schagger H. and von J.G., "Blue native electrophoresis for isolation of membrane protein complexes in enzymatically active form", *Anal Biochem*, Vol. 199, no. 2, 1991, pp. 223-231.
136. Schagger H., "Quantification of oxidative phosphorylation enzymes after blue native electrophoresis and two-dimensional resolution: normal complex I protein amounts in Parkinson's disease conflict with reduced catalytic activities", *Electrophoresis*, Vol. 16, no. 5, 1995, pp. 763-770.
137. King M.P. and Attardi G., "Human cells lacking mtDNA: repopulation with exogenous mitochondria by complementation", *Science*, Vol. 246, no. 4929, 1989, pp. 500-503.
138. Williams S.L., Valnot I., Rustin P., Taanman J.W., "Cytochrome c oxidase subassemblies in fibroblast cultures from patients carrying mutations in COX10, SCO1, or SURF1", *J Biol Chem*, Vol. 279, no. 9, 2004, pp. 7462-7469.
139. Puck T.T. and Fisher H.W., "GENETICS OF SOMATIC MAMMALIAN CELLS : I. DEMONSTRATION OF THE EXISTENCE OF MUTANTS WITH DIFFERENT GROWTH REQUIREMENTS IN A HUMAN CANCER CELL STRAIN (HELA)", *J Exp Med*, Vol. 104, no. 3, 1956, pp. 427-434.
140. Rickwood D., Wilson M.T., Darley-Usmar V.M., "Mitochondria: a practical approach", 1987, pp. 6-
141. Zhang L., Shimoji M., Thomas B., Moore D.J., Yu S.W., Marupudi N.I., Torp R., Torgner I.A., Ottersen O.P., Dawson T.M., Dawson V.L., "Mitochondrial localization of the Parkinson's disease related protein DJ-1: implications for pathogenesis", *Hum Mol Genet*, Vol. 14, no. 14, 2005, pp. 2063-2073.
142. Fujiki Y., Hubbard A.L., Fowler S., Lazarow P.B., "Isolation of intracellular membranes by means of sodium carbonate treatment: application to endoplasmic reticulum", *J Cell Biol*, Vol. 93, no. 1, 1982, pp. 97-102.
143. Lander E.S. and Botstein D., "Homozygosity mapping: a way to map human recessive traits with the DNA of inbred children", *Science*, Vol. 236, no. 4808, 1987, pp. 1567-1570.
144. Woods C.G., Valente E.M., Bond J., Roberts E., "A new method for autozygosity mapping using single nucleotide polymorphisms (SNPs) and EXCLUDEAR", *J Med Genet*, Vol. 41, no. 8, 2004, pp. e101-
145. Calvo S., Jain M., Xie X., Sheth S.A., Chang B., Goldberger O.A., Spinazzola A., Zeviani M., Carr S.A., Mootha V.K., "Systematic

- identification of human mitochondrial disease genes through integrative genomics", *Nat Genet*, Vol. 38, no. 5, 2006, pp. 576-582.
146. Jansen R., Yu H., Greenbaum D., Kluger Y., Krogan N.J., Chung S., Emili A., Snyder M., Greenblatt J.F., Gerstein M., "A Bayesian networks approach for predicting protein-protein interactions from genomic data", *Science*, Vol. 302, no. 5644, 2003, pp. 449-453.
147. Qasim W., Mackey T., Sinclair J., Chatziandreu I., Kinnon C., Thrasher A.J., Gaspar H.B., "Lentiviral vectors for T-cell suicide gene therapy: preservation of T-cell effector function after cytokine-mediated transduction", *Mol Ther*, Vol. 15, no. 2, 2007, pp. 355-360.
148. Demaison C., Parsley K., Brouns G., Scherr M., Battmer K., Kinnon C., Grez M., Thrasher A.J., "High-level transduction and gene expression in hematopoietic repopulating cells using a human immunodeficiency [correction of imunodeficiency] virus type 1-based lentiviral vector containing an internal spleen focus forming virus promoter", *Hum Gene Ther*, Vol. 13, no. 7, 2002, pp. 803-813.
149. Scacco S., Petruzzella V., Budde S., Vergari R., Tamborra R., Panelli D., van den Heuvel L.P., Smeitink J.A., Papa S., "Pathological mutations of the human NDUFS4 gene of the 18-kDa (AQDQ) subunit of complex I affect the expression of the protein and the assembly and function of the complex", *J Biol Chem*, Vol. 278, no. 45, 2003, pp. 44161-44167.
150. Leshinsky-Silver E., Lebre A.S., Minai L., Saada A., Steffann J., Cohen S., Rotig A., Munnich A., Lev D., Lerman-Sagie T., "NDUFS4 mutations cause Leigh syndrome with predominant brainstem involvement", *Mol Genet Metab*, Vol. 97, no. 3, 2009, pp. 185-189.
151. Hoefs S.J., Skjeldal O.H., Rodenburg R.J., Nedregard B., van Kaauwen E.P., Spiekerkotter U., von Kleist-Retzow J.C., Smeitink J.A., Nijtmans L.G., van den Heuvel L.P., "Novel mutations in the NDUFS1 gene cause low residual activities in human complex I deficiencies", *Mol Genet Metab*, Vol. 100, no. 3, 2010, pp. 251-256.
152. Ferreira M., Torraco A., Rizza T., Fattori F., Meschini M.C., Castana C., Go N.E., Nargang F.E., Duarte M., Piemonte F., Dionisi-Vici C., Videira A., Vilarinho L., Santorelli F.M., Carrozzo R., Bertini E., "Progressive cavitating leukoencephalopathy associated with respiratory chain complex I deficiency and a novel mutation in NDUFS1", *Neurogenetics*, Vol. 12, no. 1, 2011, pp. 9-17.
153. Iuso A., Scacco S., Piccoli C., Bellomo F., Petruzzella V., Trentadue R., Minuto M., Ripoli M., Capitanio N., Zeviani M., Papa S., "Dysfunctions of

- cellular oxidative metabolism in patients with mutations in the NDUFS1 and NDUFS4 genes of complex I", *J Biol Chem*, Vol. 281, no. 15, 2006, pp. 10374-10380.
154. Janssen R., Smeitink J., Smeets R., van Den H.L., "CIA30 complex I assembly factor: a candidate for human complex I deficiency?", *Hum Genet*, Vol. 110, no. 3, 2002, pp. 264-270.
155. Scacco S., Vergari R., Scarpulla R.C., Technikova-Dobrova Z., Sardanelli A., Lambo R., Lorusso V., Papa S., "cAMP-dependent phosphorylation of the nuclear encoded 18-kDa (IP) subunit of respiratory complex I and activation of the complex in serum-starved mouse fibroblast cultures", *J Biol Chem*, Vol. 275, no. 23, 2000, pp. 17578-17582.
156. Technikova-Dobrova Z., Sardanelli A.M., Speranza F., Scacco S., Signorile A., Lorusso V., Papa S., "Cyclic adenosine monophosphate-dependent phosphorylation of mammalian mitochondrial proteins: enzyme and substrate characterization and functional role", *Biochemistry*, Vol. 40, no. 46, 2001, pp. 13941-13947.
157. Pasdois P., Deveaud C., Voisin P., Bouchaud V., Rigoulet M., Beauvoit B., "Contribution of the phosphorylable complex I in the growth phase-dependent respiration of C6 glioma cells in vitro", *J Bioenerg Biomembr*, Vol. 35, no. 5, 2003, pp. 439-450.
158. Papa S., Scacco S., Sardanelli A.M., Vergari R., Papa F., Budde S., van den Heuvel L., Smeitink J., "Mutation in the NDUFS4 gene of complex I abolishes cAMP-dependent activation of the complex in a child with fatal neurological syndrome", *FEBS Lett*, Vol. 489, no. 2-3, 2001, pp. 259-262.
159. De R.D., Panelli D., Sardanelli A.M., Papa S., "cAMP-dependent protein kinase regulates the mitochondrial import of the nuclear encoded NDUFS4 subunit of complex I", *Cell Signal*, Vol. 20, no. 5, 2008, pp. 989-997.
160. Claros M.G. and Vincens P., "Computational method to predict mitochondrially imported proteins and their targeting sequences", *Eur J Biochem*, Vol. 241, no. 3, 1996, pp. 779-786.
161. Schmidt O., Pfanner N., Meisinger C., "Mitochondrial protein import: from proteomics to functional mechanisms", *Nat Rev Mol Cell Biol*, Vol. 11, no. 9, 2010, pp. 655-667.
162. Carroll J., Fearnley I.M., Skehel J.M., Shannon R.J., Hirst J., Walker J.E., "Bovine complex I is a complex of 45 different subunits", *J Biol Chem*, Vol. 281, no. 43, 2006, pp. 32724-32727.

163. Kaminski M.M., Sauer S.W., Klemke C.D., Suss D., Okun J.G., Krammer P.H., Gulow K., "Mitochondrial reactive oxygen species control T cell activation by regulating IL-2 and IL-4 expression: mechanism of ciprofloxacin-mediated immunosuppression", *J Immunol*, Vol. 184, no. 9, 2010, pp. 4827-4841.
164. West A.P., Brodsky I.E., Rahner C., Woo D.K., Erdjument-Bromage H., Tempst P., Walsh M.C., Choi Y., Shadel G.S., Ghosh S., "TLR signalling augments macrophage bactericidal activity through mitochondrial ROS", *Nature*, Vol. 472, no. 7344, 2011, pp. 476-480.
165. Vogel R.O., Janssen R.J., Ugalde C., Grovenstein M., Huijbens R.J., Visch H.J., van den Heuvel L.P., Willems P.H., Zeviani M., Smeitink J.A., Nijtmans L.G., "Human mitochondrial complex I assembly is mediated by NDUFAF1", *FEBS J*, Vol. 272, no. 20, 2005, pp. 5317-5326.
166. Ryan M.T., Voos W., Pfanner N., "Assaying protein import into mitochondria", *Methods Cell Biol*, Vol. 65, no. 2001, pp. 189-215.
167. Petruzzella V., Vergari R., Puzziferri I., Boffoli D., Lamantea E., Zeviani M., Papa S., "A nonsense mutation in the NDUFS4 gene encoding the 18 kDa (AQDQ) subunit of complex I abolishes assembly and activity of the complex in a patient with Leigh-like syndrome", *Hum Mol Genet*, Vol. 10, no. 5, 2001, pp. 529-535.
168. Benit P., Steffann J., Lebon S., Chretien D., Kadhom N., de L.P., Goldenberg A., Dumez Y., Dommergues M., Rustin P., Munnich A., Rotig A., "Genotyping microsatellite DNA markers at putative disease loci in inbred/multiplex families with respiratory chain complex I deficiency allows rapid identification of a novel nonsense mutation (IVS1nt -1) in the NDUFS4 gene in Leigh syndrome", *Hum Genet*, Vol. 112, no. 5-6, 2003, pp. 563-566.
169. Acin-Perez R., Fernandez-Silva P., Peleato M.L., Perez-Martos A., Enriquez J.A., "Respiratory active mitochondrial supercomplexes", *Mol Cell*, Vol. 32, no. 4, 2008, pp. 529-539.
170. Schagger H. and Pfeiffer K., "Supercomplexes in the respiratory chains of yeast and mammalian mitochondria", *EMBO J*, Vol. 19, no. 8, 2000, pp. 1777-1783.
171. Quintana A., Kruse S.E., Kapur R.P., Sanz E., Palmiter R.D., "Complex I deficiency due to loss of Ndufs4 in the brain results in progressive encephalopathy resembling Leigh syndrome", *Proc Natl Acad Sci U S A*, Vol. 107, no. 24, 2010, pp. 10996-11001.

REFERENCES

172. Loupatty F.J., Clayton P.T., Ruiten J.P., Ofman R., Ijlst L., Brown G.K., Thorburn D.R., Harris R.A., Duran M., Desousa C., Krywawych S., Heales S.J., Wanders R.J., "Mutations in the gene encoding 3-hydroxyisobutyryl-CoA hydrolase results in progressive infantile neurodegeneration", *Am J Hum Genet*, Vol. 80, no. 1, 2007, pp. 195-199.
173. Ng S.B., Buckingham K.J., Lee C., Bigham A.W., Tabor H.K., Dent K.M., Huff C.D., Shannon P.T., Jabs E.W., Nickerson D.A., Shendure J., Bamshad M.J., "Exome sequencing identifies the cause of a mendelian disorder", *Nat Genet*, Vol. 42, no. 1, 2010, pp. 30-35.
174. DiMauro S. and Schon E.A., "Mitochondrial disorders in the nervous system", *Annu Rev Neurosci*, Vol. 31, no. 2008, pp. 91-123.
175. Tucker E.J., Compton A.G., Thorburn D.R., "Recent advances in the genetics of mitochondrial encephalopathies", *Curr Neurol Neurosci Rep*, Vol. 10, no. 4, 2010, pp. 277-285.
176. Barghuti F., Elian K., Gomori J.M., Shaag A., Edvardson S., Saada A., Elpeleg O., "The unique neuroradiology of complex I deficiency due to NDUFA12L defect", *Mol Genet Metab*, Vol. 94, no. 1, 2008, pp. 78-82

APPENDIX

Scientific articles published during the PhD.

The articles relevant to this study are indicated by the asterisks and attached as full paper.

1. * Fassone E, Taanman JW, Hargreaves IP, Sebire NJ, Cleary MA, Burch M, Rahman S.
Mutations in the mitochondrial complex I assembly factor NDUFAF1 cause fatal infantile hypertrophic cardiomyopathy.
J Med Genet. 2011 Oct;48(10):691-7.
2. Ronchi D, Fassone E, Bordoni A, Sciacco M, Lucchini V, Di Fonzo A, Rizzuti M, Colombo I, Napoli L, Ciscato P, Moggio M, Cosi A, Collotta M, Corti S, Bresolin N, Comi GP.
Two novel mutations in PEO1 (Twinkle) gene associated with chronic external ophthalmoplegia.
J Neurol Sci. 2011 Sep 15;308(1-2):173-6.
3. Pitceathly RD, Fassone E, Taanman JW, Sadowski M, Fratter C, Mudanohwo EE, Woodward CE, Sweeney MG, Holton JL, Hanna MG, Rahman S.
Kearns--Sayre syndrome caused by defective R1/p53R2 assembly.
J Med Genet. 2011 Sep;48(9):610-7. Epub 2011 Mar 4.
4. Ronchi D, Bordoni A, Cosi A, Rizzuti M, Fassone E, Di Fonzo A, Servida M, Sciacco M, Collotta M, Ronzoni M, Lucchini V, Mattioli M, Moggio M, Bresolin N, Corti S, Comi GP.
Unusual adult-onset Leigh syndrome presentation due to the mitochondrial m.9176T>C mutation.
Biochem Biophys Res Commun. 2011 Aug 26;412(2):245-8. Epub 2011 Jul 27.
5. * Fassone E, Duncan AJ, Taanman JW, Pagnamenta AT, Sadowski MI, Holand T, Qasim W, Rutland P, Calvo SE, Mootha VK, Bitner-Glindzicz M, Rahman S.
FOXRED1, encoding an FAD-dependent oxidoreductase complex-I-specific molecular chaperone, is mutated in infantile-onset mitochondrial encephalopathy.
Hum Mol Genet. 2010 Dec 15;19(24):4837-47. Epub 2010 Sep 21.

6. Crugnola V, Lamperti C, Lucchini V, Ronchi D, Peverelli L, Prella A, Sciacco M, Bordoni A, Fassone E, Fortunato F, Corti S, Silani V, Bresolin N, Di Mauro S, Comi GP, Moggio M.
Mitochondrial respiratory chain dysfunction in muscle from patients with amyotrophic lateral sclerosis.
Arch Neurol. 2010 Jul;67(7):849-54.
7. Ronchi D, Virgilio R, Bordoni A, Fassone E, Sciacco M, Ciscato P, Moggio M, Govoni A, Corti S, Bresolin N, Comi GP.
The m.12316G>A mutation in the mitochondrial tRNA Leu(CUN) gene is associated with mitochondrial myopathy and respiratory impairment.
J Neurol Sci. 2010 May 15;292(1-2):107-10. Epub 2010 Feb 18.
8. Virgilio R, Ronchi D, Bordoni A, Fassone E, Bonato S, Donadoni C, Torgano G, Moggio M, Corti S, Bresolin N, Comi GP.
Mitochondrial DNA G8363A mutation in the tRNA Lys gene: clinical, biochemical and pathological study.
J Neurol Sci. 2009 Jun 15;281(1-2):85-92. Epub 2009 Mar 10. Review.
9. Di Fonzo A, Ronchi D, Lodi T, Fassone E, Tigano M, Lamperti C, Corti S, Bordoni A, Fortunato F, Nizzardo M, Napoli L, Donadoni C, Salani S, Saladino F, Moggio M, Bresolin N, Ferrero I, Comi GP.
The mitochondrial disulfide relay system protein GFER is mutated in autosomal-recessive myopathy with cataract and combined respiratory-chain deficiency.
Am J Hum Genet. 2009 May;84(5):594-604. Epub 2009 Apr 30.

FOXRED1, encoding an FAD-dependent oxidoreductase complex-I-specific molecular chaperone, is mutated in infantile-onset mitochondrial encephalopathy

Elisa Fassone^{1,2}, Andrew J. Duncan¹, Jan-Willem Taanman³, Alistair T. Pagnamenta⁴, Michael I. Sadowski⁵, Tatjana Holand⁶, Waseem Qasim⁶, Paul Rutland¹, Sarah E. Calvo⁷, Vamsi K. Mootha⁷, Maria Bitner-Glindzicz¹ and Shamima Rahman^{1,8,9,*}

¹Clinical and Molecular Genetics Unit, UCL Institute of Child Health, London WC1N 1EH, UK, ²Dino Ferrari Centre, Department of Neurological Sciences, University of Milan, I.R.C.C.S. Foundation Ca' Granda, Ospedale Maggiore Policlinico, 20122 Milan, Italy, ³Department of Clinical Neurosciences, Institute of Neurology, University College London, London NW3 2PF, UK, ⁴Monaco Group, Wellcome Trust Centre for Human Genetics, Oxford OX3 7BN, UK, ⁵Division of Mathematical Biology, National Institute for Medical Research, London NW7 1AA, UK, ⁶Molecular Immunology Unit, Institute of Child Health, University College London, London WC1N 1EH, UK, ⁷Broad Institute of MIT and Harvard, Cambridge, MA 02142, USA, ⁸MRC Centre for Neuromuscular Diseases, National Hospital for Neurology, Queen Square, London WC1N 3BG, UK and ⁹Metabolic Unit, Great Ormond Street Hospital, London WC1N 3JH, UK

Received July 19, 2010; Revised August 27, 2010; Accepted September 16, 2010

Complex I is the first and largest enzyme in the respiratory chain and is located in the inner mitochondrial membrane. Complex I deficiency is the most commonly reported mitochondrial disorder presenting in childhood, but the molecular basis of most cases remains elusive. We describe a patient with complex I deficiency caused by mutation of the molecular chaperone FOXRED1. A combined homozygosity mapping and bioinformatics approach in a consanguineous Iranian-Jewish pedigree led to the identification of a homozygous mutation in FOXRED1 in a child who presented with infantile-onset encephalomyopathy. Silencing of FOXRED1 in human fibroblasts resulted in reduced complex I steady-state levels and activity, while lentiviral-mediated FOXRED1 transgene expression rescued complex I deficiency in the patient fibroblasts. This FAD-dependent oxidoreductase, which has never previously been associated with human disease, is now shown to be a complex I-specific molecular chaperone. The discovery of the c.1054C>T; p.R352W mutation in the FOXRED1 gene is a further contribution towards resolving the complex puzzle of the genetic basis of human mitochondrial disease.

INTRODUCTION

Complex I (NADH: ubiquinone oxidoreductase, EC 1.6.5.3) is the largest enzyme in the inner mitochondrial membrane (IMM) and provides the entry point into the respiratory chain for electrons derived from fuel oxidation. However, despite its fundamental role in mitochondrial energy generation, complex I remains the least well understood of the

respiratory chain complexes. Although the crystal structure has been elucidated (1), little is known about the function of many of the 45 subunits, and the factors necessary for and mechanisms of assembly of this macromolecular complex remain largely unknown.

Mitochondrial diseases are characterized by extreme clinical, biochemical and genetic heterogeneity (2). Isolated deficiency of complex I is the most commonly identified

*To whom correspondence should be addressed at: Clinical and Molecular Genetics Unit, UCL Institute of Child Health, 30 Guilford Street, London WC1N 1EH, UK. Tel: +44 2079052608; Fax: +44 2074046191; Email: s.rahman@ich.ucl.ac.uk

biochemical defect in childhood-onset mitochondrial disease (3). Only seven of the 45 different subunits of complex I are encoded by mitochondrial DNA (mtDNA), and mutations in these mitochondrial subunits account for ~25% of complex I deficiency (4). Mutations in 12 of the 38 nuclear-encoded subunits (NDUFS1, MIM 157655; NDUFS2, MIM 602985; NDUFS3, MIM 603846; NDUFS4, MIM 602694; NDUFS6, MIM 603848; NDUFS7, MIM 601825; NDUFS8, MIM 602141; NDUFV1, MIM 161015; NDUFV2, MIM 600532; NDUF1A, MIM 300078; NDUF1A2, MIM 602137; and NDUF1A11, MIM 612638) have been implicated in a further 20% of complex I deficiency, most commonly presenting in childhood as fatal infantile lactic acidosis, Leigh syndrome, leukodystrophy or hypertrophic cardiomyopathy (5,6).

More than half of complex I deficiency is believed to be caused by mutations in ancillary factors necessary for proper complex I assembly and functioning, but to date relatively few patients have been reported to have mitochondrial disease secondary to a mutation in a complex I assembly factor [NDUFAF1 (7), MIM 606934; NDUFAF2 (8), MIM 609653; NDUFAF3 (9), MIM 612911; NDUFAF4 (10), MIM 611776; C8ORF38 (11), MIM 612392; and C20ORF7 (12), MIM 612360]. Both mutations in structural complex I subunits and assembly factors reduce the amount of the fully assembled functional complex by affecting the rate of complex I assembly and/or its stability (5). Currently, treatment strategies for isolated complex I deficiency are lacking because of limited insights into its pathophysiology.

We now report a novel disorder affecting complex I activity and stability, caused by a homozygous mutation in the putative molecular chaperone FOXRED1, which we identified by a combined homozygosity mapping and bioinformatics approach.

RESULTS

Biochemistry

Spectrophotometric analysis of respiratory chain enzyme activities revealed severe isolated deficiency of complex I in skeletal muscle from the proband (7% residual activity compared with the mean control, normalized for citrate synthase), with normal activities of other respiratory chain complexes (data not shown). There was a milder deficiency of complex I in patient fibroblasts, with 70% residual activity (data not shown). Immunoblot analysis of one-dimensional Blue-Native polyacrylamide gel electrophoresis (BN-PAGE) gels showed marked reduction of complex I holoenzyme in patient fibroblast mitochondria (Fig. 1).

Homozygosity mapping and bioinformatics analysis

Previous genetic analysis in this patient had excluded mtDNA mutations and mutations in seven structural subunits of complex I (NDUFS2, NDUFS3, NDUFS4, NDUFS6, NDUFS7, NDUFS8 and NDUFV1) as the cause of his complex I deficiency. We then used a homozygosity mapping approach to identify the responsible gene. Whole genome-wide SNP analysis revealed five candidate regions of homozygosity in the proband which were not shared with his five healthy siblings. These regions were further confirmed

by microsatellite analysis, which allowed refinement of these five candidate intervals to a total of 50 Mb (Supplementary Material, Table S1). These regions contained 338 genes. The longest region of homozygosity (18.3 Mb) was observed on chromosome 6, but did not contain any candidate genes implicated in complex I function. The third largest region of homozygosity (9.2 Mb on chromosome 18) contained the only known structural subunit of complex I located within these homozygous intervals: *NDUFV2* (MIM 600532; NM_021074).

The remaining 337 genes within the candidate regions were prioritized by bioinformatic analyses, including integration with the MitoCarta catalogue (11) and 11 genes encoding known or predicted mitochondrial proteins were selected for sequence analysis (Supplementary Material, Table S2).

DNA sequence analysis

No mutations were identified in *NDUFV2*. Only one possibly pathogenic mutation was identified in the other 11 genes sequenced: a homozygous c.1054C>T (p.R352W) mutation present in both predicted transcripts of *FOXRED1* (NM_017547) on chromosome 11q24.2 (Fig. 2). Both parents of the proband were heterozygous for the mutation, as were two of his siblings. Three siblings were homozygous for the wild-type sequence (Fig. 3). The mutation was not found in 268 pan-ethnic healthy control alleles. Sequence analysis of 24 further patients with isolated complex I deficiency without a genetic diagnosis did not reveal any mutations in *FOXRED1*. The arginine at position 352 of the FOXRED1 protein is highly conserved through evolution (Fig. 4).

Lentiviral-mediated complementation and silencing studies

Mitochondrial complex I activity in patient fibroblasts was shown to be ~70% of controls, relative to residual complex IV activity, using the mitochondrial dipstick assay kits (Fig. 5A), which was in agreement with the spectrophotometric assays. Expression of a synthetic *FOXRED1* gene in patient fibroblasts, using a lentiviral vector, rescued the complex I activity to ~90% of control levels (Fig. 5A), providing evidence that the R352W missense mutation in FOXRED1 was the cause of the observed complex I deficiency in the patient. However, transfection with an empty vector also increased complex I activity in patient fibroblasts slightly (Fig. 5A). The mild deficiency of complex I in patient fibroblasts probably explains why only a 10–20% increase in complex I activity was observed after lentiviral transfection with wild-type *FOXRED1* cDNA compared with transfection with an empty vector.

Western blot analysis showed a reduced steady-state level of FOXRED1 in patient fibroblasts, which increased after lentiviral transduction with wild-type *FOXRED1* cDNA (Fig. 5B). Western blot analysis also demonstrated a slight improvement in complex I amount (assessed with anti-NDUFA9 antibody) in patient fibroblasts after transduction with wild-type *FOXRED1* cDNA, compared with human control fibroblasts and patient fibroblasts transduced with an empty vector (Fig. 5B). These observations were confirmed by densitometric analysis of the western blots (Fig. 5B).

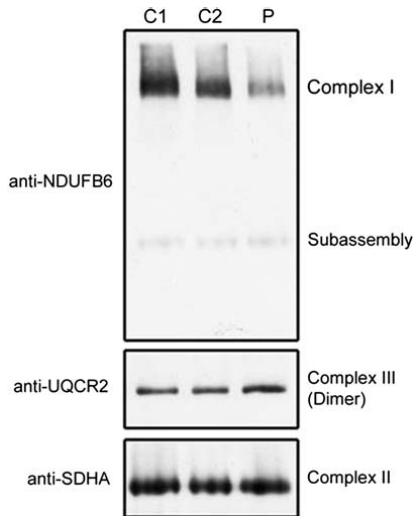


Figure 1. BN-PAGE of complex I holoenzyme. BN-PAGE shows that the complex I holoenzyme steady-state level is reduced in patient (P) fibroblasts compared with two healthy controls (C1 and C2), probed with the anti-NDUFB6 antibody. Probing for UQCR2 (anti-complex III) and SDHA (anti-complex II) demonstrated equal loading.

Stable knockdown of *FOXRED1* expression via lentiviral-mediated shRNAi-reduced complex I expression, assayed with anti-NDUFA9 antibody (Fig. 5B). Dipstick assay showed ~40% residual complex I activity in *FOXRED1*-silenced fibroblasts compared with human control fibroblasts and scrambled fibroblasts (Fig. 5A), confirming that lack of FOXRED1 can cause complex I deficiency.

Subcellular and submitochondrial localization

Transfection of mammalian cells with a C-terminally labelled *FOXRED1*-YFP fusion plasmid demonstrated typical punctuate mitochondrial fluorescent staining, supporting mitochondrial localization of the protein (Fig. 6B). The western blot in Figure 7 shows that the anti-FOXRED1 antibody recognized a protein of the expected size (~53 kDa) in whole mitochondria, confirming mitochondrial localization of FOXRED1. A similar band of ~53 kDa is clearly visible in the mitochondrial inner membrane (IM) fraction and in the mitochondrial soluble fraction (i.e. mitochondrial inner membrane space (IMS) + matrix (M), indicated in Fig. 7 as 'Sol'). A similar slightly bigger polypeptide is detected in the IMS as well as in the matrix, indicating that FOXRED1 may enter the mitochondrial matrix as a precursor containing its mitochondrial import sequence, which is then cleaved to release the mature functional protein. Probing the same western blot with control antibodies anti-voltage-dependent anion channel (VDAC), anti-cytochrome *c* and anti-MTCO2 (cytochrome *c* oxidase subunit II) revealed the expected submitochondrial localizations for these proteins (outer membrane (OM), IMS and IM, respectively).

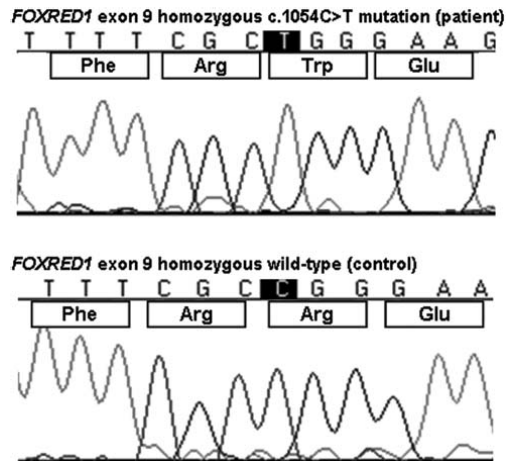


Figure 2. *FOXRED1* exon 9 electropherogram. Electropherogram showing sequencing results for the *FOXRED1* gene: the c.1054C>T mutation is homozygous in the patient (top panel) while the control sequence is wild-type homozygous (lower panel).

FOXRED1 protein modelling

The FOXRED1 (Uniprot AC: Q96CU9; ID: FXRD1_HUMAN) sequence was used to search the PDB using a profile generated versus the Swiss-Prot database (13) with four iterations of PSI-BLAST (14). PSI-BLAST was run with a profile inclusion score of 0.001 and default parameters otherwise. Several potential templates were identified; these were consistently related to the sarcosine oxidases. The top hit reported by the PSIBLAST run was 2gb0, a monomeric sarcosine oxidase from *Bacillus* spp. (15). The alignment was edited manually to ensure that the secondary structure of the observed template agreed with the prediction made by PSIPRED (16). The residue of interest, R352 in FOXRED1, aligns to F256 in the template, which is at the end of a short strand in the central sheet of the second domain in 2gb0 (Supplementary Material, Fig. S1). Protein modelling using the *Bacillus* monomeric sarcosine oxidase structure as a template suggested that mutation of arginine to tryptophan at position 352 could impinge on the FAD-binding site (Fig. 8).

mRNA coexpression analysis

Bioinformatics analysis using the mouse GNF1M tissue atlas showed a strong positive correlation between expression of *FOXRED1* and expression of known complex I subunits (Supplementary Material, Fig. S2), implying a functional association. This correlation was stronger than for all previously identified assembly factors for complex I.

DISCUSSION

We used an integrative genomics approach, combining homozygosity mapping and bioinformatic analyses, to investigate a consanguineous Iranian-Jewish family in which the sixth child

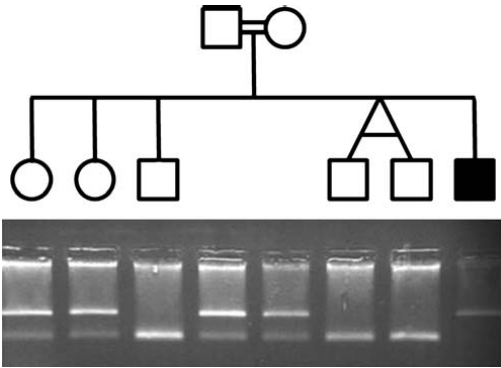


Figure 3. *FOXRED1* mutation RFLP analysis. RFLP analysis shows segregation of the mutation with disease: none of the family members is homozygous for the c.1054C>T mutation except for the proband. The parents are heterozygous and unaffected siblings either heterozygous or homozygous for the wild-type sequence.

was affected by early-onset complex I deficient encephalomyopathy. Five candidate regions of homozygosity, unique to the proband and not shared with unaffected siblings, were identified by whole genome-wide SNP analysis. No mutations were identified in *NDUFV2*, the only known structural subunit of complex I located within the homozygous intervals. Three hundred and thirty seven other genes located within the candidate regions were prioritized by bioinformatic analyses, and 11 genes encoding known or predicted mitochondrial proteins were sequenced.

The only pathogenic mutation identified in these 11 genes was a homozygous missense mutation c.1054C>T in *FOXRED1*. This mutation segregated with disease in the family; both parents and two siblings were heterozygous for the mutation, while the other three siblings were homozygous for the wild-type sequence. The mutation was not found in 268 pan-ethnic healthy control alleles. Western blot analysis showed a reduced steady-state level of FOXRED1 in patient fibroblasts and BN-PAGE analysis provided evidence of reduced amounts of complex I holoenzyme. Restoration of complex I activity after lentiviral transduction of patient fibroblasts with wild-type *FOXRED1* cDNA confirmed that the *FOXRED1* mutation is the cause of this patient's complex I deficiency.

FOXRED1 is a 486 amino acid protein, with an approximate mass of 53 kDa. It contains an FAD-dependent oxidoreductase domain, which may be involved in electron transfer. The mutation is predicted to cause the substitution of a highly conserved arginine residue by tryptophan (R352W). Our *in silico* modelling studies suggested that the mutation is likely to affect FOXRED1 protein structure. Mutation from arginine to the much larger tryptophan is likely to result in close proximity of the tryptophan sidechain to the FAD-binding site, thus interfering with FAD binding.

Mehrle *et al.* (17) have previously investigated subcellular localization of a large number of human proteins. Transfection of mammalian cells with a C-terminally labelled *FOXRED1*-

YFP fusion plasmid demonstrated typical punctuate mitochondrial fluorescent staining, supporting mitochondrial localization of the protein (Fig. 6B). Furthermore, an N-terminal CFP-*FOXRED1* fusion protein failed to localize with mitochondria (Fig. 6A), suggesting that FOXRED1 has an N-terminal mitochondrial targeting sequence which was masked by the N-terminal fusion sequence (17). We performed *in silico* analysis using MitoProt II-v1.101 (18), which confirmed the presence of a putative N-terminal mitochondrial localization sequence, spanning amino acids 1–23 (MIRRVLPHGMGRGLLRRPGTRR). This sequence has a positive net charge of +1 and a predicted cleavage site at position 24; the probability of import into mitochondria was also very high at 0.9546.

Our western blot data confirm mitochondrial localization of FOXRED1, with an expected band of ~53 kDa in the whole mitochondrial fraction (Fig. 7). In addition, a band slightly larger than ~53 kDa was observed in the IMS and the matrix. Based on this observation, we postulate that a FOXRED1 precursor containing its mitochondrial import sequence may be imported into mitochondria via a classical importation mechanism (such as the TOM/TIM machinery), and that the import sequence is subsequently cleaved within the matrix to release the mature protein (19). We also speculate that this mature protein then associates with the mitochondrial IM, near the respiratory chain supercomplexes and probably adjacent to the complex I holoenzyme, in order to exert its chaperone function.

FOXRED1 is not one of the known 45 subunits of complex I, as established by proteomics studies (20). However, the association of a homozygous *FOXRED1* mutation with isolated complex I deficiency in our patient suggests that FOXRED1 must be a chaperone or other factor necessary for assembly, stability and/or correct functioning of complex I. Bioinformatics analysis using the mouse GNFM tissue atlas showed coexpression of *FOXRED1* with other complex I subunits, implying a functional association. A role for FOXRED1 in complex I activity is also supported by the absence of *FOXRED1* orthologues in the yeast *Saccharomyces cerevisiae*, which has a functional respiratory chain but lacks the entire complex I holoenzyme, but the presence of *FOXRED1* orthologues in higher order fungi such as *Neurospora crassa*, which do contain complex I. Further evidence indicating that FOXRED1 is needed for complex I function comes from a large-scale bioinformatic survey, which identified FOXRED1 as one of 19 putative complex I assembly factors (11). Finally, steady-state mRNA transcripts for FOXRED1 have been detected in 12 human tissues, implying that the protein is widely expressed, in common with all previously identified complex I assembly factors (Supplementary Material, Fig. S3).

Comparatively little is understood about the assembly process of complex I. The enzyme is L-shaped, containing membrane and matrix arms, and has three functional modules: the dehydrogenase N module (responsible for accepting electrons from NADH), the hydrogenase Q module (transfers electrons to coenzyme Q10) and the proton translocase P module (transfers protons across the IMM). The matrix arm contains the N and Q modules, while the P module is located in the membrane arm. Various

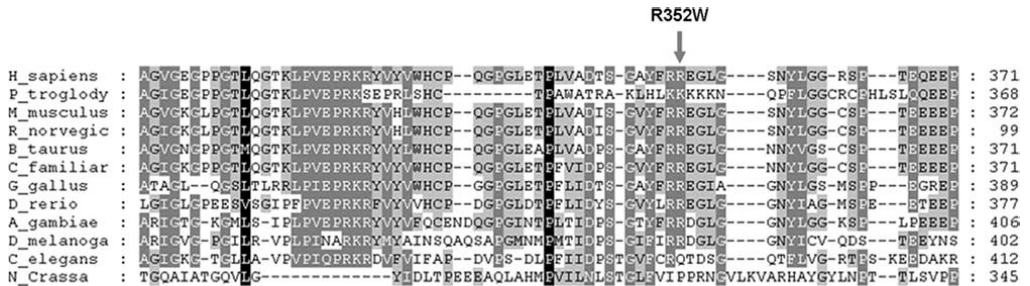


Figure 4. *FOXRED1* protein evolutionary conservation. The *FOXRED1* protein has a well-conserved module in its structure across species. Within a part of this module, we found that the R352 residue is highly conserved across species, suggesting that the amino acid change R352W is likely to have a significant functional impact.

models have been suggested for complex I assembly, but the current consensus model proposes that the ND1 core subunit anchors an early Q subassembly to the IMM, then further subunits and/or subassemblies are added to both the Q and P modules and finally the N module is added to form the complex I holoenzyme (5). However, the precise order of subunit incorporation into the nascent enzyme is not known, nor the nature and number of additional factors required for integrity of the assembly process.

Human complex I deficiency has previously been linked to mutations in six complex I assembly factor genes (see above). Studies of assembly intermediates in fibroblasts from patients carrying mutations in these six genes have suggested that NDUFAF1 and C20ORF7 are involved early in complex I assembly, while NDUFAF2 appears to function at a later stage (7,8,12). C20ORF7 appears to be necessary to form an early assembly intermediate of ~400 kDa, which contains the ND1 subunit, while NDUFAF2 associates with a larger subassembly of ~830 kDa. *FOXRED1* constitutes a seventh putative assembly factor linked to human disease. There are also a number of putative assembly factors that have not yet been shown to cause human disease, including ECSIT (MIM 608388), PHB (MIM 176705), PTC1 (NM_015545) and 17 further factors identified by Pagliarini *et al.* (11). It is likely that many more assembly factors of complex I will be identified, bearing in mind that the much smaller complex IV, which has only 13 subunits, requires more than 15 assembly factors for its assembly (21).

There does not appear to be any particular genotype–phenotype correlation for the complex I assembly disorders, in common with many mitochondrial disorders (Table 1). Most patients presented with a progressive encephalopathy, frequently fulfilling the criteria for Leigh syndrome (22). Hypertrophic cardiomyopathy was observed in the patient with *NDUFAF1* mutations, as well as our patient with *FOXRED1* mutations. All patients had lactic acidemia, except for those with *NDUFAF2* mutations, in whom only CSF lactate levels were elevated. Severe isolated complex I deficiency was observed in skeletal muscle of all cases (residual activity 0–40% of controls), with normal activities of other respiratory chain enzyme complexes. There was a suggestion that *NDUFAF2*-related disease has a characteristic

neuroradiological appearance, with a predilection for the mamillothalamic tracts, substantia nigra/medial lemniscus, medial longitudinal fasciculus and spinothalamic tracts, but this has not been found in all cases reported to date.

In the absence of clear genotype–phenotype correlations, the approach to a genetic diagnosis for patients with complex I deficiency remains empirical. The first-line genetic investigation (after screening for mtDNA rearrangements and common point mutations m.3243A>G and m.8344A>G) should be complete mitochondrial genome sequence analysis. Subsequent investigations will be directed at nuclear-encoded structural subunits and known assembly factors of complex I and/or homozygosity mapping in suitable families. However, this approach may not be successful in all cases, since an unknown number of complex I assembly factors remain to be identified, and since complex I deficiency may occasionally be secondary to another disease process, such as 3-hydroxyisobutyryl-CoA hydrolase deficiency (23). Taking into account the costs of sequencing the mitochondrial genome, 38 nuclear-encoded structural subunits and at least seven assembly factors, and the possibility of an underlying defect in a hitherto unrecognized gene, whole-exome sequence analysis using next-generation sequencing technologies may be a faster and cheaper route to diagnosis for many patients with isolated complex I deficiency in the future (24).

The localization of *FOXRED1* within mitochondria, decrease in complex I activity upon silencing of its expression in wild-type fibroblasts and the complex I deficiency in patient muscle and fibroblasts, corrected by expression of wild-type *FOXRED1* in patient fibroblasts, together with reduction of complex I holoenzyme assembly arising from a mutation in the coding sequence of *FOXRED1*, strongly support a bona fide role in complex I function, assembly and/or stability. Taken together, our results demonstrate that the R352W mutation in *FOXRED1* causes an isolated complex I defect associated with infantile-onset encephalomyopathy, and that the *FOXRED1* product is needed for fully efficient complex I activity in human cells.

Further studies are needed to incorporate known and unidentified complex I assembly factors into a more complete complex I assembly model. Identification of additional assembly factors remains a challenge, but should increase

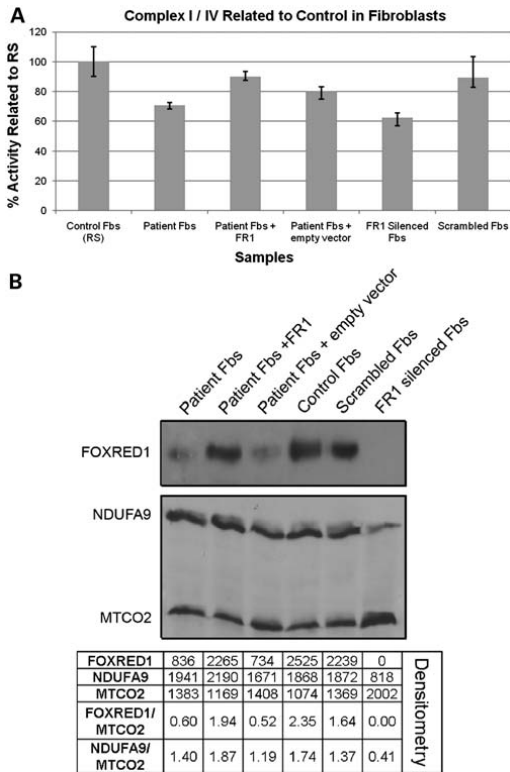


Figure 5. (A) Mitochondrial complex I/IV dipstick assay. Dipstick assay shows ~70% residual complex I activity in patient fibroblasts (Fbs) which is recovered to ~90% after complementation with synthetic wild-type *FOXRED1* cDNA. A slight recovery is also seen after transfecting patient Fbs with an empty vector. *FOXRED1*-silenced fibroblasts show an ~40% decrease in complex I activity compared with scrambled fibroblasts. Key: Fbs, fibroblasts; RS, reference sample; FR1, *FOXRED1*. (B) Western blot analysis. Western blot analysis shows a gain in *FOXRED1* and *NDUFA9* protein content in patient fibroblasts when complemented with *FOXRED1* wild-type cDNA, compared with patient fibroblasts transduced with an empty vector. *FOXRED1*-silenced fibroblasts show a reduction in *FOXRED1* and *NDUFA9* protein content compared with control and scrambled fibroblasts. Probing for *MTCO2* (anti-complex IV) demonstrated equal loading. Densitometry measurements were carried out using Alpha Ease FC software (Alpha Innotech/Cell Biosciences, Santa Clara, CA, USA) and confirmed the observations above.

our understanding not only of complex I biogenesis but also of mitochondrial involvement in other common pathways or diseases, including neurodegeneration and cancer.

MATERIALS AND METHODS

Patient

The patient is the sixth child of healthy Iranian-Jewish first cousin parents. Two sisters and three brothers are unaffected. Pregnancy was uneventful, but soon after birth severe truncal

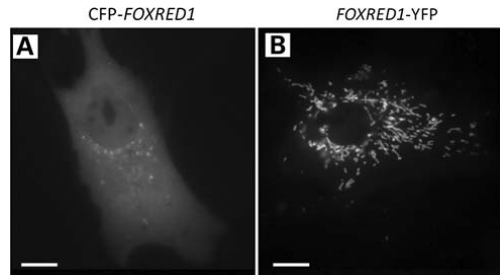


Figure 6. *FOXRED1* mitochondrial localization. Figures taken from the LIFEdB database, clone ID: DKFZp586B1920. (A) Low-intensity non-specific cytoplasmic and nuclear staining of the N-terminally tagged *FOXRED1* protein. (B) High-intensity fluorescent staining of the C-terminally tagged *FOXRED1* protein, with a characteristic punctate signal typical of a mitochondrially targeted protein. These images suggest that N-terminal tagging of the *FOXRED1* protein interferes with the recognition of the mitochondrial targeting sequence. Bar, 10 μ m.

hypotonia was noted. There have never been any voluntary movements. During the first year, he was extremely irritable with prolonged periods of inconsolable crying. Muscle biopsy was performed at 4 months of age because of persistent elevation of lactate in plasma (6.8 mM, normal <2.1) and CSF (4.3 mM, normal <1.8). Muscle histology was normal, but biochemical analysis revealed isolated deficiency of complex I in muscle mitochondria (7% of the control mean, normalized for citrate synthase activity), with normal activity of other respiratory chain enzyme complexes.

He developed progressive microcephaly, and brain MRI at 8 months revealed delayed myelination, ventricular dilatation and abnormal signal in the thalami and basal ganglia. Myoclonic jerks were present from 1 year but at 5 years responded to lamotrigine and clonazepam therapy. Eye movements have always been roving, with no evidence of visual function, and visual evoked potentials demonstrated absent cortical responses at 6 months of age. Bilateral optic atrophy was noted at 2 years. Hearing appears to be normal. Echocardiography revealed mild non-obstructive left ventricular hypertrophy. Poor feeding was present from birth, and from 5 years he has been fed by gastrostomy tube. He has had persistent hepatomegaly with normal liver transaminases and no signs of liver failure or cholestasis. He has had severe scoliosis from 5 years, treated with a corset. He was treated with riboflavin, uridine, creatine, lipoic acid, dichloroacetate and thiamine, without any obvious clinical response. He is currently 10 years old.

All samples were taken after informed patient/parental consent, and the study was approved by the local Ethics Committee.

BN-PAGE analysis

Assembled respiratory chain complexes were detected using BN-PAGE, performed as described previously (25). Samples were obtained from $1-2 \times 10^6$ cultured fibroblasts and mitochondrial-enriched pellets were produced by subcellular fractionation using differential centrifugation. The protease inhibitors pepstatin, leupeptin and phenylmethylsulphonyl

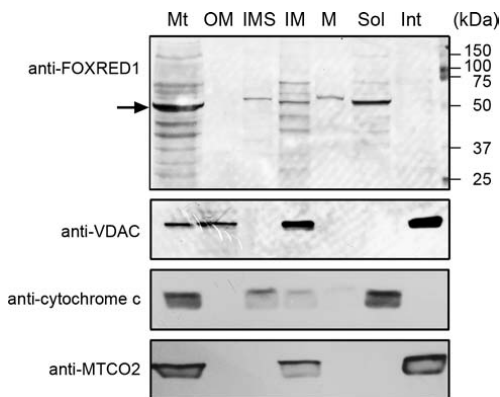


Figure 7. Submitochondrial fractionation. The ~53 kDa *FOXRED1* protein (indicated by the arrow) shows a clear mitochondrial localization; more specifically, it is contained within the soluble fraction and associated with the IM. The slightly larger band detected in the IMS and the M may represent an immature polypeptide containing a mitochondrial targeting sequence, which is then cleaved to release the mature protein. The smaller mature protein then associates with the IM to achieve its fully functional state. Antibodies against mitochondrial proteins were used to test the purity of the fractions: anti-VDAC for the OM (and IM), anti-cytochrome *c* for the IMS (also visible as associated with the IM) and anti-MTCO2 for the IM. Key: MT, whole mitochondria; OM, outer membrane; IMS, intermembrane space; M, matrix; SOL, soluble fraction; INT, integral proteins fraction.

fluoride were added to all homogenization, centrifugation and storage buffers. Mitochondrial protein fractions were solubilized with *n*-dodecyl-beta-D-maltoside, and 15–20 μ l of the sample was loaded and run into 4–12% polyacrylamide gels, electrotransferred to Hybond-P membrane (GE healthcare) and probed with antibodies to subunit NDUFB6 (Mitosciences, OR, USA). The secondary antibody was goat anti-mouse conjugated to horseradish peroxidase (Dako). Equal loading was confirmed by reprobing blots with anti-SDHA and anti-MTCO2 antibodies (Mitosciences).

Genetic studies

Whole genome-wide SNP genotyping was performed in the Iranian-Jewish proband and his unaffected siblings using the GeneChip Human Mapping 10K Xba Array (Affymetrix). We assumed an autosomal recessive model, and the output data were analysed assuming more than 30 consecutive homozygous SNPs as being significant. Five regions of significant homozygosity were observed in the patient but not his unaffected siblings, and these were further confirmed by microsatellite analysis. Microsatellites were selected using the Ensembl Human Genome Browser and PCR reactions were carried out using 5' fluorescently labelled forward primers (primer sequences available upon request). After PCR amplification, the labelled DNA fragments were diluted 1/10–1/18 and then run together with the ET550-R size standard (final concentration 1/20, Amersham Biosciences) at 10 000 V for 75 min on an ABI MegaBACE™ cycle sequencer (Applied Biosystems), according to the manufacturer's

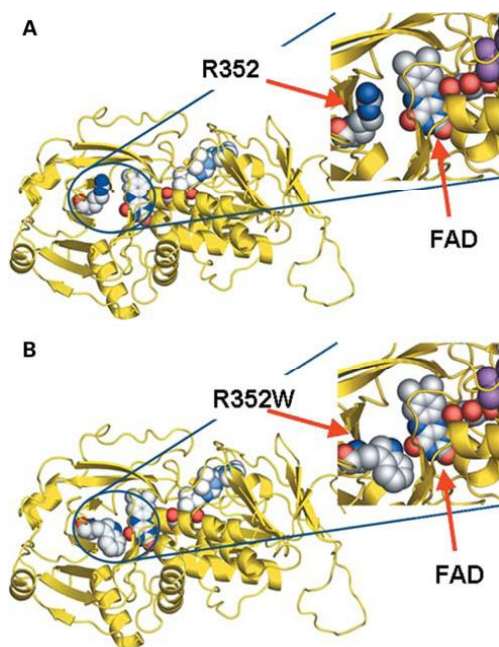


Figure 8. *FOXRED1* protein modelling. Model of the *FOXRED1* protein based on the *Bacillus* monomeric sarcosine oxidase structure (PDB code: 2gb0). (A) The model with residue R352 and the FAD moiety shown in space-filling representation. Inset is a close-up of the relation between R352 and the FAD. (B) The model of the R352W mutant. The observed mutation to tryptophan [R352W] hypothetically visualized in (B)] could potentially place the mutant amino acid sidechain within contact distance of the FAD and interfere with binding.

instructions. Samples were denatured at 95°C for 2 min and placed on ice before loading. Sample injection was at 3000 V for 45 s. The data were analyzed using Genetic Profiler software v2.2 (Amersham Biosciences). The genes within the candidate regions were prioritized by bioinformatic analyses, including integration with the MitoCarta catalogue (11).

DNA sequence analysis

Eleven genes were sequenced by cycle sequencing (Big Dye v3.1 Terminator System) and analysis on MegaBACE™ (Supplementary Material, Table S2). Primer sequences for *FOXRED1* are given in Supplementary Material, Table S3; primer sequences for the other 10 genes are available upon request. *FOXRED1* exon 9 was amplified and sequenced using primers: forward: 5'-CCATGCTGTTTCTGCAGTTC-3'; reverse: 5'-GCCAAAAGCCTGATTGTTTC-3'. RFLP analysis was used to confirm the mutation: *MspI* (NewEngland Biolabs) cut the 245 bp wild-type amplicon into two fragments of 121 and 124 bp. The mutation c.1054C>T abolished the restriction site, leaving the 245 bp amplicon uncut. Two hundred and sixty eight pan-ethnic control alleles were screened for the c.1054C>T mutation in *FOXRED1*. The

Table 1. Complex I assembly factors associated with disease

Gene	Synonym(s)	Number of patients (families)	Age at onset	Age at death	Clinical features	MRI features	Maximum blood lactate, mM (reference <2)	Residual complex I activity	References
<i>NDUFA1</i>	CIA30	1 (1)	11mo	Alive at 20y	Cardioencephalomyopathy (HCM, WPW, cortical visual failure, RP)	NS	10	30% fb ^b	(7)
<i>NDUFA2</i>	NDUFA12, B17.2L, Mimetin	1 (1)	12mo	13y	Progressive encephalopathy	Symmetrical lesions in mammillothalamic tracts, SN/ML, MLF, spinothalamic tracts and cerebellum	Normal (CSF lactate 4.2 mM)	38% m ^a	(8)
		2 (2)	20mo; 8mo	2y; 21mo	Progressive encephalopathy	Symmetrical lesions in mammillothalamic tracts, SN/ML, MLF and spinothalamic tracts	Normal (CSF lactate 2.6 mM)	24–36% m ^a , 53% fb ^b	(35)
		1 (1)	3mo	1y	LS	Bilateral symmetrical lesions in thalamus, cerebral peduncles, brainstem and spinal cord	5	21–23% fb ^b	(36)
		1 (1)	Ante-natal (IUGR)	14mo	Encephalomyopathy, dysmorphism, hepatopathy (NB contiguous gene deletion involving two other genes, <i>ELOVL7</i> and <i>ERCC8</i>)	Normal (CT)	3.4	45% fb ^b	(37)
<i>NDUFA3</i>	C3orf60	5 (3)	Neonate (N=4)	3–4mo	Lethal neonatal disease	Normal	27	26–40% m ^a , 18–39% fb ^b	(9)
<i>NDUFA4</i>	C6orf66, HRPAP20	5 (1)	3mo Neonate	6mo 2–5d (N=3); alive at 16mo; alive at 7y	Myoclonic seizures Infantile encephalomyopathy	Diffuse leukomalacia Severe atrophy of cerebellum, cerebellum, basal ganglia, pons and medulla	NS 38	33% fb ^b 0–21% m ^a	(10)
<i>C8ORF38</i>		2 (1)	7–10mo	34mo; alive at 22mo	LS	LS	Persistently elevated	36% m ^a , 20% f ^a ; 14% fb ^b	(11)
<i>C20ORF7</i>		1 (1)	Ante-natal (IUGR)	7d	Dysmorphism, lethal neonatal disease	Agensis of corpus callosum (ultrasound)	16.5	25% m ^a , 4% f ^a , 25% fb ^b	(12)
		3 (1)	3y	36y; alive at 29y; alive at 23y	LS	Progressive atrophy and high signal affecting caudate nuclei and putamina	Normal (CSF lactate 5 mM)	36% m; 6% pbmc	(38)
<i>FOXRED1</i>		1 (1)	Neonate	Alive at 10y		Delayed myelination, ventricular dilatation and abnormal signal in thalami and basal ganglia	6.8	7% m ^a	This report

CT, computed tomography; d, days; fb, fibroblast; HCM, hypertrophic cardiomyopathy; IUGR, intrauterine growth retardation; l, liver; LS, Leigh syndrome; m, muscle; ML, medial lemniscus; MLF, medial longitudinal fasciculus; mo, months; MRI, magnetic resonance imaging; NS, not stated; pbmc, peripheral blood mononuclear cell; RP, pigmentary retinopathy; SN, substantia nigra; WPW, Wolff–Parkinson–White syndrome; y, year.
^aPercent normal control.
^bPercent lowest control.

FOXRED1 gene was also sequenced in 24 other patients with isolated complex I deficiency who did not have a genetic diagnosis.

Western blot analysis

Western blot analysis was performed as described elsewhere (25) on whole cell lysates (pre- and post-transduction), probing with anti-FOXRED1 antibody (Abnova, Taipei, Taiwan), and anti-NDUFA9 and anti-MTCO2 antibodies (Mitosciences). The secondary antibody was goat anti-mouse conjugated to horseradish peroxidase (Invitrogen). The analysis was performed at baseline and between days 15 and 20 after cell viral transduction. Densitometry measurements were carried out using Alpha Ease FC software (Alpha Innotech/Cell Biosciences, Santa Clara, CA, USA).

Mitochondrial complex I and complex IV dipstick assay

Activities of complexes I and IV were determined in whole cell lysates of patient and control fibroblasts with the Mitochondrial Dipstick Assay kit, performed according to the manufacturer's instructions (Mitosciences). Thirty micrograms of proteins were allowed to wick up laterally through the dipstick membrane, the dipsticks were transferred into the appropriate (complex I or complex IV) enzyme substrate buffer and enzyme activities were calculated by measuring the optical density of precipitating, colorimetric enzyme reaction products using the ImageJ[®] program. Standard curves were constructed from multiple determinations of complex activities in cultured human fibroblast extracts; complex I R^2 0.94–0.98 ($n = 3$) and complex IV R^2 0.91–0.92 ($n = 3$). All measurements were done in triplicate and the results expressed as the complex I/complex IV activity ratio for each sample and compared with the fibroblast control range. All measurements were performed at baseline and between days 15 and 20 after cell viral transduction.

Preparation of lentiviral vectors

A synthetic codon-optimized *FOXRED1* gene was designed to include a Kozak sequence (to increase translational initiation) and two STOP codons (to ensure efficient termination) and was generated by assembly of synthetic oligonucleotides (Genart, Regensburg). The gene was then subcloned into a lentiviral vector (26) and expression linked to eGFP through an internal ribosomal entry sequence. This vector utilizes a strong retroviral promoter element derived from the spleen focus-forming virus and a mutated woodchuck post-translational regulatory element. Vector stocks were pseudotyped with the vesicular stomatitis virus envelope as described previously (27). Vector stocks of pGIPZ, a commercially available lentiviral vector system expressing puromycin/eGFP markers and shRNAi against *FOXRED1* or scrambled shRNAi controls (Open Biosystems), were prepared in a similar manner for knock-down experiments. Vector stocks were titred by fluorescence-activated cell sorting (FACS) following dilutional transduction of a fixed number of 293T cells, and stored at -80°C until required.

Complementation studies

Patient fibroblasts were cultured in DMEM and transduced with the lentiviral vector expressing eGFP alone or in combination with *FOXRED1*. Transduced cells were enriched for eGFP expression by FACS and expanded for functional studies.

RNA interference studies

Silencing the *FOXRED1* gene in control fibroblasts was achieved by transducing the cells with the pGIPZ shRNAmir vector. Stably transduced clones were selected in $1\ \mu\text{g/ml}$ puromycin (Gibco-Invitrogen). *FOXRED1*-silenced fibroblasts died within 20 days of culture following viral transduction.

Submitochondrial fractionation

Mitochondria from cultured HeLa S3 cells were isolated by differential centrifugation as reported previously (28). To sub-fractionate mitochondria, the swell–shrink procedure was used as described (29), except that the IMS was further purified by extraction in 10 mM Hepes-NaOH (pH 7.4), 0.5 mM EDTA, 125 mM sucrose and 0.5% (v/v) Triton X-100 on ice for 30 min, followed by centrifugation at 160 000g, 4°C for 1 h. To distinguish soluble and peripheral membrane proteins from integral membrane proteins, mitochondria were extracted with the alkaline carbonate method (30).

Purity of the subfractionated mitochondrial compartments was tested by probing with antibodies to detect a specific marker for each submitochondrial fraction: VDAC (~ 30 kDa; Calbiochem, 86–173/016, clone 31HL) was used as an OM marker, cytochrome *c* (~ 12 kDa; BD Pharmingen, 556433) for the IMS and MTCO2 (26 kDa; Mitosciences, MS405, clone 12C4-F12) for the IM.

Protein modelling

PSI-BLAST (14) searches against the PDB resulted in several sarcosine oxidase hits. The model was generated using the Bacillus structure 2gb0 (15). Manual alignment editing was used to improve agreement with the secondary structure prediction generated by PSIPRED (16). The model was generated using MODELLER (31) with intermediate refinement (library schedule 1, 300 refinement cycles, three repeats, maximum PDF value $1e - 06$); all non-protein atoms were inherited. Sidechain packing was re-optimized using SCWRL3 (32). All images were generated using PyMOL (33).

mRNA coexpression analysis

mRNA expression across 61 mouse tissues was performed using the GNF1M tissue atlas (34). The mouse tissue atlas contained probes corresponding to 909 distinct MitoCarta genes, including *Foxred1*. The mouse tissue atlas was used since probes targeting *FOXRED1* were not present on the human GNF tissue atlas. Expression values were normalized across tissues based on the Z-score. The Pearson pairwise correlation was calculated for each gene pair, and this correlation matrix was clustered hierarchically using the R hclust function.

AUTHORS CONTRIBUTIONS

S.R. was the overall study principal investigator who conceived the study and obtained financial support. S.R., E.F. and A.J.D. designed and oversaw the study, interpreted the results and drafted and synthesized the manuscript. J.-W.T. performed the BN-PAGE and western blot studies. A.T.P. performed the homozygosity mapping. M.I.S. modelled the human wild-type and mutated FOXRED1 protein. T.H. and W.Q. assisted in the lentiviral transduction. P.R. helped with acquisition and analysis of sequence data. S.E.C. and V.K.M. investigated the bioinformatics profiles of candidate genes within homozygous regions. M.B.-G. co-supervised the homozygosity mapping and revised the manuscript.

SUPPLEMENTARY MATERIAL

Supplementary Material is available at *HMG* online.

ACKNOWLEDGEMENTS

We thank Dr Stefan Wiemann for permission to publish the mitochondrial localization images of FOXRED1, and Dr Amanda Heslegrave and Kerra Pearce for technical assistance. We thank Professor Robert Taylor for providing DNA samples from additional patients with complex I deficiency.

Conflict of Interest statement. None declared.

FUNDING

This work was supported by the UK Medical Research Council (G0200335 to S.R. and career development fellowship to M.I.S.), the Child Health Research Appeal Trust, Jeans 4 Genes, Climb and Leukaemia and Lymphoma research.

REFERENCES

- Efremov, R.G., Baradaran, R. and Sazanov, L.A. (2010) The architecture of respiratory complex I. *Nature*, **465**, 441–445.
- Rahman, S. and Hanna, M.G. (2009) Diagnosis and therapy in neuromuscular disorders: diagnosis and new treatments in mitochondrial diseases. *J. Neurol. Neurosurg. Psychiatry*, **80**, 943–953.
- Kirby, D.M., Crawford, M., Cleary, M.A., Dahl, H.H., Dennett, X. and Thorburn, D.R. (1999) Respiratory chain complex I deficiency: an underdiagnosed energy generation disorder. *Neurology*, **52**, 1255–1264.
- Thorburn, D.R., Sugiana, C., Salemi, R., Kirby, D.M., Worgan, L., Ohtake, A. and Ryan, M.T. (2004) Biochemical and molecular diagnosis of mitochondrial respiratory chain disorders. *Biochim. Biophys. Acta*, **1659**, 121–128.
- Lazarou, M., Thorburn, D.R., Ryan, M.T. and McKenzie, M. (2009) Assembly of mitochondrial complex I and defects in disease. *Biochim. Biophys. Acta*, **1793**, 78–88.
- Hoefs, S.J., Dieteren, C.E., Distelmaier, F., Janssen, R.J., Epplen, A., Swarts, H.G., Forkink, M., Rodenburg, R.J., Nijtmans, L.G., Willems, P.H. *et al.* (2008) NDUFA2 complex I mutation leads to Leigh disease. *Am. J. Hum. Genet.*, **82**, 1306–1315.
- Dunning, C.J., McKenzie, M., Sugiana, C., Lazarou, M., Silke, J., Connelly, A., Fletcher, J.M., Kirby, D.M., Thorburn, D.R. and Ryan, M.T. (2007) Human CIA30 is involved in the early assembly of mitochondrial complex I and mutations in its gene cause disease. *EMBO J.*, **26**, 3227–3237.
- Ogilvie, I., Kennaway, N.G. and Shoubridge, E.A. (2005) A molecular chaperone for mitochondrial complex I assembly is mutated in a progressive encephalopathy. *J. Clin. Invest.*, **115**, 2784–2792.
- Saada, A., Vogel, R.O., Hoefs, S.J., van den Brand, M.A., Wessels, H.J., Willems, P.H., Venselaar, H., Shaq, A., Barghuti, F., Reish, O. *et al.* (2009) Mutations in NDUFAF3 (C3ORF60), encoding an NDUFAF4 (C6ORF66)-interacting complex I assembly protein, cause fatal neonatal mitochondrial disease. *Am. J. Hum. Genet.*, **84**, 718–727.
- Saada, A., Edvardson, S., Rapoport, M., Shaq, A., Amry, K., Miller, C., Lorberboum-Galski, H. and Elpeleg, O. (2008) C6ORF66 is an assembly factor of mitochondrial complex I. *Am. J. Hum. Genet.*, **82**, 32–38.
- Pagliarini, D.J., Calvo, S.E., Chang, B., Sheth, S.A., Vafai, S.B., Ong, S.E., Walford, G.A., Sugiana, C., Boneh, A., Chen, W.K. *et al.* (2008) A mitochondrial protein compendium elucidates complex I disease biology. *Cell*, **134**, 112–123.
- Sugiana, C., Pagliarini, D.J., McKenzie, M., Kirby, D.M., Salemi, R., Abu-Amero, K.K., Dahl, H.H., Hutchison, W.M., Vaschetto, K.A., Smith, S.M. *et al.* (2008) Mutation of C20orf7 disrupts complex I assembly and causes lethal neonatal mitochondrial disease. *Am. J. Hum. Genet.*, **83**, 468–478.
- Boeckmann, B., Bairoch, A., Apweiler, R., Blatter, M.C., Estreicher, A., Gasteiger, E., Martin, M.J., Michoud, K., O'Donovan, C., Phan, I. *et al.* (2003) The SWISS-PROT protein knowledgebase and its supplement TrEMBL in 2003. *Nucleic Acids Res.*, **31**, 365–370.
- Altschul, S.F., Madden, T.L., Schaffer, A.A., Zhang, J., Zhang, Z., Miller, W. and Lipman, D.J. (1997) Gapped BLAST and PSI-BLAST: a new generation of protein database search programs. *Nucleic Acids Res.*, **25**, 3389–3402.
- Trickey, P., Wagner, M.A., Jorns, M.S. and Mathews, F.S. (1999) Monomeric sarcosine oxidase: structure of a covalently flavinylated amine oxidizing enzyme. *Structure*, **7**, 331–345.
- Jones, D.T. (1999) Protein secondary structure prediction based on position-specific scoring matrices. *J. Mol. Biol.*, **292**, 195–202.
- Mehrle, A., Rosenfelder, H., Schupp, I., del, V.C., Arlt, D., Hahne, F., Bechtel, S., Simpson, J., Hofmann, O., Hide, W. *et al.* (2006) The LIFEdb database in 2006. *Nucleic Acids Res.*, **34**, D415–D418.
- Claros, M.G. and Vincens, P. (1996) Computational method to predict mitochondrially imported proteins and their targeting sequences. *Eur. J. Biochem.*, **241**, 779–786.
- Schmidt, O., Pfanner, N. and Meisinger, C. (2010) Mitochondrial protein import: from proteomics to functional mechanisms. *Nat. Rev. Mol. Cell Biol.*, **11**, 655–667.
- Carroll, J., Fearnley, I.M., Skehel, J.M., Shannon, R.J., Hirst, J. and Walker, J.E. (2006) Bovine complex I is a complex of 45 different subunits. *J. Biol. Chem.*, **281**, 32724–32727.
- Fontanesi, F., Soto, I.C., Horn, D. and Barrientos, A. (2006) Assembly of mitochondrial cytochrome c-oxidase, a complicated and highly regulated cellular process. *Am. J. Physiol. Cell Physiol.*, **291**, C1129–C1147.
- Rahman, S., Blok, R.B., Dahl, H.H., Danks, D.M., Kirby, D.M., Chow, C.W., Christodoulou, J. and Thorburn, D.R. (1996) Leigh syndrome: clinical features and biochemical and DNA abnormalities. *Ann. Neurol.*, **39**, 343–351.
- Loupaty, F.J., Clayton, P.T., Ruiter, J.P., Ofman, R., Ijlst, L., Brown, G.K., Thorburn, D.R., Harris, R.A., Duran, M., Desouza, C. *et al.* (2007) Mutations in the gene encoding 3-hydroxyisobutyryl-CoA hydrolase results in progressive infantile neurodegeneration. *Am. J. Hum. Genet.*, **80**, 195–199.
- Ng, S.B., Buckingham, K.J., Lee, C., Bigham, A.W., Tabor, H.K., Dent, K.M., Huff, C.D., Shannon, P.T., Jabs, E.W., Nickerson, D.A. *et al.* (2010) Exome sequencing identifies the cause of a Mendelian disorder. *Nat. Genet.*, **42**, 30–35.
- Williams, S.L., Valnot, I., Rustin, P. and Taanman, J.W. (2004) Cytochrome c oxidase subassemblies in fibroblast cultures from patients carrying mutations in COX10, SCO1, or SURF1. *J. Biol. Chem.*, **279**, 7462–7469.
- Qasim, W., Mackey, T., Sinclair, J., Chatziandreou, I., Kinnon, C., Thrasher, A.J. and Gaspar, H.B. (2007) Lentiviral vectors for T-cell suicide gene therapy: preservation of T-cell effector function after cytokine-mediated transduction. *Mol. Ther.*, **15**, 355–360.
- Demaision, C., Parsley, K., Brouns, G., Scherr, M., Battmer, K., Kinnon, C., Grez, M. and Thrasher, A.J. (2002) High-level transduction and gene expression in hematopoietic repopulating cells using a human immunodeficiency [correction of immunodeficiency] virus type 1-based

- lentiviral vector containing an internal spleen focus forming virus promoter. *Hum. Gene Ther.*, **13**, 803–813.
28. Rickwood, D., Wilson, M.T. and Darley-Usmar, V.M. (1987) In Darley-Usmar, V.M., Rickwood, D. and Wilson, M.T. (eds), *Mitochondria: a practical approach*, IRL Press Ltd, p. 6.
 29. Zhang, L., Shimoji, M., Thomas, B., Moore, D.J., Yu, S.W., Marupudi, N.I., Torp, R., Torgner, I.A., Ottersen, O.P., Dawson, T.M. and Dawson, V.L. (2005) Mitochondrial localization of the Parkinson's disease related protein DJ-1: implications for pathogenesis. *Hum. Mol. Genet.*, **14**, 2063–2073.
 30. Fujiki, Y., Hubbard, A.L., Fowler, S. and Lazarow, P.B. (1982) Isolation of intracellular membranes by means of sodium carbonate treatment: application to endoplasmic reticulum. *J. Cell Biol.*, **93**, 97–102.
 31. Sali, A. and Blundell, T.L. (1993) Comparative protein modelling by satisfaction of spatial restraints. *J. Mol. Biol.*, **234**, 779–815.
 32. Canutescu, A.A., Shelenkov, A.A. and Dunbrack, R.L. Jr. (2003) A graph-theory algorithm for rapid protein side-chain prediction. *Protein Sci.*, **12**, 2001–2014.
 33. DeLano, W.L. (2002) *The PyMOL Molecular Graphics System*. DeLano Scientific, San Carlos, CA, USA. <http://www.pymol.org>. Accessed November 2007.
 34. Su, A.I., Wiltshire, T., Batalov, S., Lapp, H., Ching, K.A., Block, D., Zhang, J., Soden, R., Hayakawa, M., Kreiman, G. *et al.* (2004) A gene atlas of the mouse and human protein-encoding transcriptomes. *Proc. Natl Acad. Sci. USA*, **101**, 6062–6067.
 35. Barghuti, F., Elian, K., Gomori, J.M., Shaag, A., Edvardson, S., Saada, A. and Elpeleg, O. (2008) The unique neuroradiology of complex I deficiency due to NDUFA12L defect. *Mol. Genet. Metab.*, **94**, 78–82.
 36. Hoefs, S.J., Dieteren, C.E., Rodenburg, R.J., Naess, K., Bruhn, H., Wibom, R., Wagena, E., Willems, P.H., Smeitink, J.A., Nijtmans, L.G. *et al.* (2009) Baculovirus complementation restores a novel NDUFAF2 mutation causing complex I deficiency. *Hum. Mutat.*, **30**, E728–E736.
 37. Janssen, R.J., Distelmaier, F., Smeets, R., Wijnhoven, T., Ostergaard, E., Jaspers, N.G., Raams, A., Kemp, S., Rodenburg, R.J., Willems, P.H. *et al.* (2009) Contiguous gene deletion of ELOVL7, ERCC8 and NDUFAF2 in a patient with a fatal multisystem disorder. *Hum. Mol. Genet.*, **18**, 3365–3374.
 38. Gerards, M., Sluiter, W., van den Bosch, B.J., de, W.E., Calis, C.M., Frentzen, M., Akbari, H., Schoonderwoerd, K., Scholte, H.R., Jongbloed, R.J. *et al.* (2010) Defective complex I assembly due to C20orf7 mutations as a new cause of Leigh syndrome. *J. Med. Genet.*, **47**, 507–512.

ORIGINAL ARTICLE

Mutations in the mitochondrial complex I assembly factor *NDUFAF1* cause fatal infantile hypertrophic cardiomyopathy

Elisa Fassone,^{1,2} Jan-Willem Taanman,³ Iain P Hargreaves,⁴ Neil J Sebire,⁵ Maureen A Cleary,⁶ Michael Burch,⁷ Shamima Rahman^{1,6,8}

► An additional table is published online only. To view this file please visit the journal online (<http://jmg.bmj.com>).

¹Mitochondrial Research Group, Clinical and Molecular Genetics Unit, UCL Institute of Child Health, London, UK

²Dino Ferrari Centre, Department of Neurological Sciences, University of Milan, IRCCS Foundation Cà Granda, Ospedale Maggiore, Milan, Italy

³Department of Clinical Neurosciences, Institute of Neurology, University College London, London, UK

⁴Neurometabolic Unit, National Hospital for Neurology, Queen Square, London, UK

⁵Histopathology Unit, Great Ormond Street Hospital, London, UK

⁶Metabolic Unit, Great Ormond Street Hospital, London, UK

⁷Cardiology Unit, Great Ormond Street Hospital, London, UK

⁸MRC Centre for Neuromuscular Diseases, National Hospital for Neurology, London, UK

Correspondence to

Dr Shamima Rahman, Clinical and Molecular Genetics Unit, UCL Institute of Child Health, 30 Guilford Street, London WC1N 1EH, UK; s.rahman@ich.ucl.ac.uk

Received 13 July 2011

Revised 3 August 2011

Accepted 11 August 2011

ABSTRACT

Background Hypertrophic cardiomyopathy (HCM) is frequently fatal in infancy. Mitochondrial disease causing infantile HCM is characterised by extreme biochemical and genetic heterogeneity, but deficiency of respiratory chain complex I is observed relatively frequently. Identification of the precise genetic basis has prognostic implications for the likelihood of neurological involvement.

Objective The authors' objective is to report two heterozygous missense mutations in the *NDUFAF1* gene as a cause of fatal infantile HCM in a patient with isolated complex I deficiency.

Methods The authors investigated a cohort of 30 paediatric patients with complex I deficiency using biochemical and genetic approaches. The patients were clinically heterogeneous; phenotypes included HCM, Leigh syndrome, other encephalomyopathies and multisystem disease. Complex I assembly was evaluated using Blue Native polyacrylamide gel electrophoresis.

Results Sequence analysis of *NDUFAF1* revealed compound heterozygous missense mutations (c.631C>T;p.Arg211Cys and c.733G>A;p.Gly245Arg) in one patient with fatal infantile HCM. These changes were absent in 240 ethnically matched control alleles. No *NDUFAF1* mutations were observed in the remaining patients. Functional studies demonstrated a severe reduction in *NDUFAF1* protein in Western blots of patient fibroblasts and accumulation of abnormal complex I assembly intermediates on Blue Native polyacrylamide gel electrophoresis.

Conclusions The authors report a case of fatal infantile HCM caused by missense mutations in *NDUFAF1* associated with complex I misassembly. Establishing a genetic diagnosis in mitochondrial cardiomyopathy is challenging and achieved in only a minority of cases because of complex genetics. A precise genetic diagnosis is important to provide accurate prognostic and genetic counselling advice regarding recurrence risks and to guide future reproductive options.

INTRODUCTION

Cardiomyopathy is a rare but potentially devastating disorder of the heart muscle with an incidence of 1.13 cases per 100 000 children per year in the USA.¹ Hypertrophic cardiomyopathy (HCM) accounts for ~6% of cases listed for paediatric heart transplantation.² More than two-thirds of children do not have a known diagnosis at the time

of clinical presentation with cardiomyopathy. The differential diagnosis includes viral illness, genetic defects of sarcomeric proteins³ and inherited metabolic diseases.⁴ Approximately 9% of paediatric HCM cases are caused by an inborn error of metabolism,⁵ including lysosomal storage disorders, fat oxidation defects and mitochondrial respiratory chain enzyme deficiencies (the largest subgroup, representing over half of metabolic HCM cases).⁴ Diagnosis rests on clinical characterisation, family history, echocardiographic appearances and laboratory investigations, including tissue biopsy.

Identification of the precise genetic basis of HCM yields essential prognostic information. The likelihood of progressive neurological disease is critically important, since many centres would consider this a contraindication to cardiac transplantation. Disorders of the mitochondrion are characterised by extreme genetic heterogeneity, with multiple possible modes of inheritance related to the bigenomic (mitochondrial and nuclear) inheritance of this dynamic subcellular organelle.⁶ Mitochondrial disease can theoretically arise from the mutation of any of the >1500 components of the mitochondrial proteome,⁷ although, so far, only ~80 nuclear genes have been proven to cause mitochondrial dysfunction,⁸ in addition to the 37 mitochondrially encoded genes.

Mitochondrial complex I (NADH:ubiquinone oxidoreductase; EC 1.6.5.3) is the largest enzyme in the respiratory chain, with essential functions in electron transfer and proton pumping. Complex I generates ~40% of the proton motive force that is eventually harnessed by ATP synthase (complex V) to synthesise ATP from ADP and inorganic phosphate.^{9 10} Human complex I consists of 38 different nuclear-encoded structural proteins, 7 mitochondrial DNA (mtDNA)-encoded structural proteins, 1 flavin mononucleotide moiety and 8 iron–sulphur clusters, all of which are assembled together in an intricate process that remains incompletely understood.¹¹ Complex I deficiency is the most commonly observed biochemical defect in childhood-onset mitochondrial disease and is genetically heterogeneous. Fewer than half of cases appear to be caused by mutations in structural subunits of the enzyme, and mutations in assembly factors are thought to account for the majority of cases.¹² Mutations in nine different assembly factors (*NDUFAF1*,¹³ *NDUFAF2*,¹⁴ *NDUFAF3*,¹⁵ *NDUFAF4*,¹⁶ *C8orf38*,⁷ *C20orf7*,¹⁷ *FOXRED1*,¹² *NUBL18* and *ACAD9*¹⁸) have been associated with human complex I deficiency to date.

Mitochondrial disease

Here, we used a combined biochemical and genetic approach to identify compound heterozygous missense mutations in *NDUFAF1* as a novel cause of complex-I-deficient fatal infantile HCM. *NDUFAF1* encodes a protein previously known as CIA30 that is essential for the correct assembly of complex I, although its precise function remains unclear.^{11 20 21}

PATIENTS AND METHODS

Clinical data

The patient, the first child of healthy unrelated French parents, was born at 37 weeks of gestation weighing 3.17 kg. The neonatal period was unremarkable, and early developmental milestones were normal. She was first presented to medical attention at 6 months with an episode of respiratory-syncytial-virus-positive bronchiolitis, which was managed conservatively with nasogastric tube feeding. Following discharge, she became more unwell, with pallor, poor feeding, sweating and weight loss of 380 g. At 6.5 months, she presented to the emergency department in cardiogenic shock (O₂ saturation of 90%, heart rate of 180 beats/min and hepatomegaly palpable at 5 cm below the inferior costal margin). Initial blood gas values revealed metabolic acidosis (pH 6.86; base deficit, 22 mmol/l). Before retrieval to the regional cardiac intensive care unit, she was intubated and ventilated; given intraosseous volume replacement, antibiotics and bicarbonate; and started on dopamine infusion.

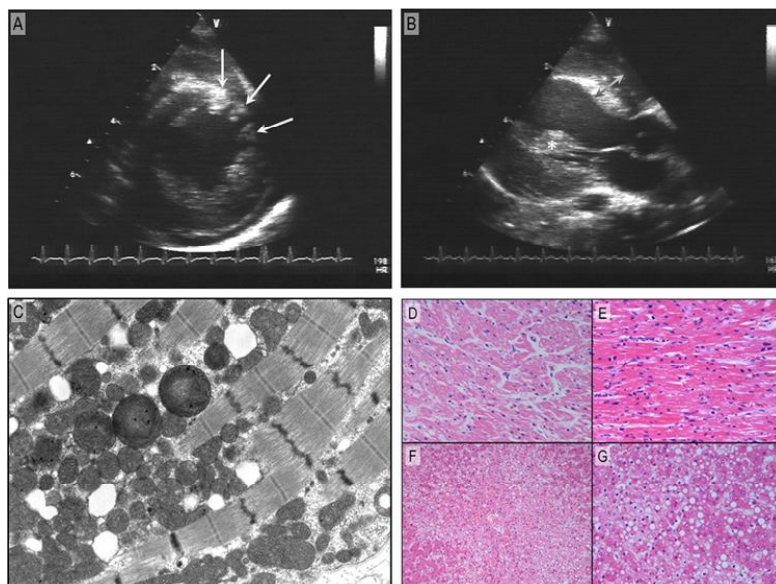
Echocardiogram (figure 1A,B) demonstrated pericardial effusion, biventricular hypertrophy and mild to moderate left ventricular (LV) dysfunction (fractional shortening, 25%). Both atria were enlarged, and there was evidence of diastolic impairment. Apical views showed trabeculation suggestive of non-compaction of the left ventricle (NCLV). Coronary artery anatomy was normal. Despite positive pressure ventilation and inotropic support with dopamine and adrenaline, she remained hypotensive and acidotic (pH 7.2; base deficit, 19 mmol/l), with an elevated blood lactate level (9 mmol/l; reference, <2 mmol/l). The acidosis did not improve, and cardiac function continued to deteriorate. Veno-arterial extracorporeal membrane oxygenation

(ECMO) was commenced on day 2 of her critical illness. Subsequently, balloon atrial septostomy was performed to decompress the left atrium, and pericardiocentesis was undertaken. Lactic acidosis persisted on full ECMO support (flow, 165%), despite the patient being warm and well perfused. Haemofiltration was therefore commenced via the ECMO circuit on the following day, with a reduction in blood lactate levels to 2–7 mmol/l. ECMO support was successfully weaned and stopped after 9 days. Continuous veno-venous haemofiltration was continued further for 6 days.

The combination of echocardiographic appearances and persistent lactic acidosis on full ECMO support led to the suspicion of an inborn error of metabolism. Urine organic acid analysis demonstrated marked excretion of lactate, pyruvate, ketones and Krebs cycle intermediates (fumarate, malate and 2-oxoglutarate), as well as moderately increased levels of glutarate and 3-hydroxyglutarate. This profile was consistent with, although not diagnostic of, a mitochondrial respiratory chain disorder. Plasma acylcarnitine analysis revealed moderately elevated hydroxybutyrylcarnitine but no other abnormalities. Cranial ultrasound results were normal, and electroencephalographic findings were consistent with a sedated critically unwell infant.

Muscle biopsy showed no ragged-red or cytochrome-c-oxidase-negative fibres, but there was increased lipid deposition. Electron microscopy demonstrated accumulation of enlarged and abnormal mitochondria (figure 1C). Spectrophotometric analysis of respiratory chain enzyme activities revealed severe isolated deficiency of complex I in skeletal muscle, with 25% residual activity compared to the lowest control (patient complex I activity, 0.026; reference range, 0.104–0.268 (ratio to citrate synthase activity)). The activities of complexes II+III and IV were normal. Forty-eight hours after continuous veno-venous haemofiltration was stopped, blood lactate levels rose to 17–18 mmol/l despite maximal medical treatment for low cardiac output, including inotropes, cooling, sedation and muscle relaxation. Cardiac reserve was minimal. On day 24 of her critical illness, she had cardiorespiratory arrest requiring two

Figure 1 Short-axis echocardiography showing ventricular hypertrophy with trabeculations (indicated by the arrows) suggestive of NCLV and posterior pericardial effusion (A). Long-axis echocardiography showing ventricular hypertrophy, thickened LV papillary muscles (indicated by the asterisk), unusual speckled appearance of the myocardium and bright subendocardium, particularly in the septum of the left ventricle (septum indicated by the double arrow) (B). Ultrastructural examination of muscle demonstrates accumulation of enlarged and abnormal mitochondria, which show electron-dense cristae forming concentric arrays (C). LV myocardium showing myocardial hypertrophy without evidence of disarray but with cytoplasmic clearing and occasional small round eosinophilic inclusions, which represent giant mitochondria (D, E). Photomicrographs demonstrating a liver with marked zonal perivenular macrovesicular steatosis (F,G). NCLV, non-compaction of the left ventricle; LV, left ventricular.



doses of epinephrine. Output was briefly re-established, but she died later that night.

Postmortem examination revealed an enlarged globular heart (weight, 93 g; weight expected for age, 34 g). Sections from the myocardium showed myocardial hypertrophy without evidence of disarray, but with foci of myofibre loss and replacement fibrosis, focal haemorrhage and hemosiderin deposition within the centres of the LV papillary muscles, and a mild degree of LV endocardial fibrosis (figure 1D,E). There was no myocarditis. Liver histology revealed marked zonal macrovesicular steatosis (figure 1F,G). Respiratory chain enzyme activities in the liver were normal (complex I, 0.207; reference range, 0.054–0.221).

Patient cohort

We investigated a cohort of 30 paediatric patients with complex I deficiency using biochemical and genetic approaches. These patients were clinically heterogeneous: phenotypes included Leigh syndrome, other encephalomyopathies, HCM, isolated myopathy and multisystem disease. mtDNA analysis revealed pathogenic mutations in 10 cases (33%). Complex I assembly in the remaining cases was investigated using Blue Native polyacrylamide gel electrophoresis (BN-PAGE). A candidate gene approach was used to search for assembly factor mutations in patients accumulating abnormal complex I subassemblies on BN-PAGE analysis. *NDUFS4* was also screened since mutations in this subunit are known to disrupt complex I assembly.

Genetic analyses

All samples were taken after informed patient/parental consent had been obtained, and the study was approved by the local ethics committee. Total DNA was extracted from the muscle of the patient and from the blood of the parents and control subjects. The entire mtDNA, exons and flanking intronic regions of the nuclear genes *NDUFS4*, *FOXRED1* and *NDUFAF1* (GenBank accession numbers NM_002495, NM_017547 and NM_016013.2, respectively) were amplified using specific primers (sequences available on request). Direct sequencing was performed using the BigDye® Terminator v1.1 Cycle Sequencing Kit (Applied Biosystems). Total RNA was extracted from cultured skin fibroblasts from the patient using the RNeasy Tissue Kit (Qiagen). Complementary DNA was synthesised, and the full-length transcript was amplified and sequenced.

In vitro studies of mutant *NDUFAF1*

Complex I activity of fibroblasts was measured with a microplate assay kit according to the manufacturer's instructions, and

the results were normalised to complex IV activity assayed using the same microplate method (MitoSciences, Eugene, Oregon, USA). All measurements were performed in triplicate.

Expression of *NDUFAF1* was assessed in mitoplasts derived from patient and control fibroblasts and 143B206 ρ^0 cells lacking mitochondrially encoded proteins²² with Western blot analysis, as previously described,²⁵ using a monoclonal anti-*NDUFAF1* antibody (Novus Biologicals, Cambridge, UK). A monoclonal anti-SDHA antibody (MitoSciences) was used as a loading control. Levels of mtDNA and nuclear-encoded subunits of complex I were investigated using antibodies to ND1 (a kind gift from Dr A Lombès) and *NDUFA9* (MitoSciences), respectively.

The effect of the *NDUFAF1* mutations on complex I holoenzyme assembly was investigated in patient and control mitoplasts isolated from fibroblasts, performed as previously described, using BN-PAGE.^{12–24} Complex I assembly was assessed using antibodies to the ND1, *NDUFB6* and *NDUFA9* subunits; the other mitochondrial enzyme complexes were probed with antibodies to SDHA (complex II), *UQCRC2* (complex III) and *ATP5A1* (complex V) (MitoSciences). No cardiac or skeletal muscle samples remained for use in functional studies.

RESULTS

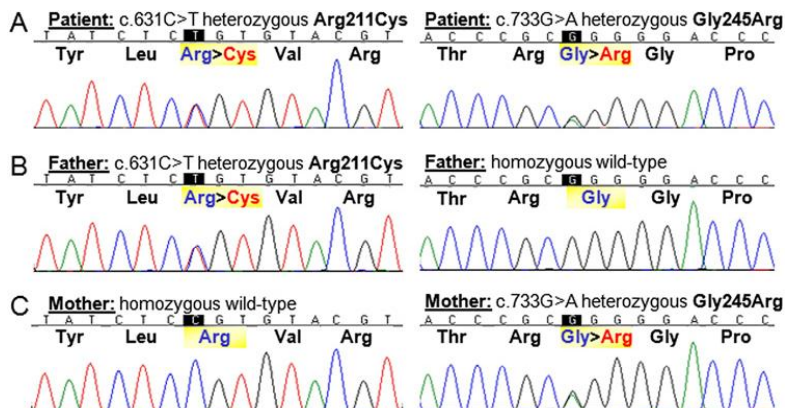
Identification of mutations in *NDUFAF1*

Sequence analysis of *NDUFAF1* revealed two heterozygous missense mutations in exon 2 in the patient: c.631C>T; p.Arg211Cys and c.733G>A; p.Gly245Arg (figure 2A), which were also confirmed in complementary DNA. Each parent was heterozygous for one of these mutations (figure 2B,C), confirming that they were on separate alleles (ie, in *trans*) in the patient. Phylogenetic analysis demonstrated that Arg211 and Gly245 are highly conserved amino acids (figure 3). These changes were absent in 240 ethnically matched control alleles and also in 1094 control individuals genotyped in the 1000 Genomes cohort (<http://www.1000genomes.org>). No *NDUFAF1* mutations were observed in the remainder of the patient cohort. In the patient, no mutations in the mtDNA or in *NDUFS4* or *FOXRED1* (two nuclear genes previously associated with complex-I-deficient cardiomyopathy) were observed.

Functional characterisation of the *NDUFAF1* mutations

Patient fibroblasts showed ~57% residual complex I activity compared to three age-matched normal controls (figure 4). *NDUFAF1* protein levels were severely reduced in patient mitoplasts compared to three controls and ρ^0 cells on Western

Figure 2 Sequencing of exon 2 of the *NDUFAF1* gene revealed two compound heterozygous mutations, c.631C>T; Arg211Cys and c.733G>A; Gly245Arg, in the patient (A). Her father is heterozygous for the c.631C>T; Arg211Cys mutation and homozygous wild type for the second variant (B), while her mother is heterozygous for the c.733G>A; Gly245Arg mutation and homozygous wild type for the first mutation (C).



Mitochondrial disease

Figure 3 The amino acid residues affected by the missense mutations in exon 2 are 33 amino acids apart within the NDUFAF1 protein and are highly conserved from humans to the nematode *Caenorhabditis elegans* and fungi.

	c.631 C>T Arg211Cys	c.733 G>A Gly245Arg
Homo sapiens	YDWSQENTL Y LRV R GDGR E W M VN I KEDT D EFQRTN Q MY S YEM F TRGG E Y W Q E V K I P E	YDWSQENTL Y LRV R GDGR E W M VN I KEDT D EFQRTN Q MY S YEM F TRGG E Y W Q E V K I P E
Hs mutated protein	YDWSQENTL Y LRV R GDGR E W M VN I KEDT D EFQRTN Q MY S YEM F TRGG E Y W Q E V K I P E	YDWSQENTL Y LRV R GDGR E W M VN I KEDT D EFQRTN Q MY S YEM F TRGG E Y W Q E V K I P E
<i>Pan troglodytes</i>	YDWSQENTL Y LRV R GDGR E W M VN I KEDT D EFQRTN Q MY S YEM F TRGG E Y W Q E V K I P E	YDWSQENTL Y LRV R GDGR E W M VN I KEDT D EFQRTN Q MY S YEM F TRGG E Y W Q E V K I P E
<i>Mus musculus</i>	YDWSQENTL Y LRV R GDGR E W M VN I KEDT D EFQRTN Q MY S YEM F TRGG E Y W Q E V K I P E	YDWSQENTL Y LRV R GDGR E W M VN I KEDT D EFQRTN Q MY S YEM F TRGG E Y W Q E V K I P E
<i>Rattus norvegicus</i>	YDWSQENTL Y LRV R GDGR E W M VN I KEDT D EFQRTN Q MY S YEM F TRGG E Y W Q E V K I P E	YDWSQENTL Y LRV R GDGR E W M VN I KEDT D EFQRTN Q MY S YEM F TRGG E Y W Q E V K I P E
<i>Bos taurus</i>	YDWSQENTL Y LRV R GDGR E W M VN I KEDT D EFQRTN Q MY S YEM F TRGG E Y W Q E V K I P E	YDWSQENTL Y LRV R GDGR E W M VN I KEDT D EFQRTN Q MY S YEM F TRGG E Y W Q E V K I P E
<i>Canis familiaris</i>	YDWSQENTL Y LRV R GDGR E W M VN I KEDT D EFQRTN Q MY S YEM F TRGG E Y W Q E V K I P E	YDWSQENTL Y LRV R GDGR E W M VN I KEDT D EFQRTN Q MY S YEM F TRGG E Y W Q E V K I P E
<i>Gallus gallus</i>	YDWSQENTL Y LRV R GDGR E W M VN I KEDT D EFQRTN Q MY S YEM F TRGG E Y W Q E V K I P E	YDWSQENTL Y LRV R GDGR E W M VN I KEDT D EFQRTN Q MY S YEM F TRGG E Y W Q E V K I P E
<i>Danio rerio</i>	YDWSQENTL Y LRV R GDGR E W M VN I KEDT D EFQRTN Q MY S YEM F TRGG E Y W Q E V K I P E	YDWSQENTL Y LRV R GDGR E W M VN I KEDT D EFQRTN Q MY S YEM F TRGG E Y W Q E V K I P E
<i>Anopheles gambiae</i>	YDWSQENTL Y LRV R GDGR E W M VN I KEDT D EFQRTN Q MY S YEM F TRGG E Y W Q E V K I P E	YDWSQENTL Y LRV R GDGR E W M VN I KEDT D EFQRTN Q MY S YEM F TRGG E Y W Q E V K I P E
<i>Drosophila melanogaster</i>	YDWSQENTL Y LRV R GDGR E W M VN I KEDT D EFQRTN Q MY S YEM F TRGG E Y W Q E V K I P E	YDWSQENTL Y LRV R GDGR E W M VN I KEDT D EFQRTN Q MY S YEM F TRGG E Y W Q E V K I P E
<i>Caenorhabditis elegans</i>	SK R R N S H L L K V R G D G R S Y K I M H S PL S M D E T W G D S R S H P L H T R G G E Y W Q E V K I P E	SK R R N S H L L K V R G D G R S Y K I M H S PL S M D E T W G D S R S H P L H T R G G E Y W Q E V K I P E
<i>Yarrowia lipolytica</i>	W N W E O R H E L R V R G D R R K E V N V S A T P --- L A S D L W Q H R L E I O T P G E W E T W V I E I	W N W E O R H E L R V R G D R R K E V N V S A T P --- L A S D L W Q H R L E I O T P G E W E T W V I E I
<i>Neurospora crassa</i>	W D I D E P A Y L A M R V R T D A R S Y E V N V R T E S V --- V P L D L H Q H R L E V K K P G W E T W V I K I	W D I D E P A Y L A M R V R T D A R S Y E V N V R T E S V --- V P L D L H Q H R L E V K K P G W E T W V I K I

blot analysis (figure 5A). Levels of the mitochondrially encoded complex I core subunit ND1 were normal in the patient, whereas levels of the nuclear-encoded membrane arm subunit NDUFA9 were reduced.

BN-PAGE analysis demonstrated a severe reduction in the ~980 kDa complex I holoenzyme in the patient, with all complex I subunit antibodies used (figure 5B). In contrast, the levels of complex II, complex III and complex V holoenzymes appeared to be normal. Distinctive complex I subassemblies, corresponding to ~400 and ~460 kDa, were observed in the patient when probing against ND1 (figure 5B). These were not seen in any of the control samples. In contrast, a physiological subassembly of ~600 kDa was only present in control samples (figure 5B). No signal was detected in the patient sample when probing against NDUFAF1, suggesting that the very low level of residual NDUFAF1 protein in the patient is not able to efficiently bind the nascent complex I, leaving it stalled at an early assembly stage.^{11–13} Further physiological subassemblies were observed in the controls when probing against NDUFAF1: a doublet at ~460 kDa, corresponding to the NDUFAF1 entry point in the complex I assembly process,¹¹ and two other larger subassemblies of >600 kDa. Interestingly, ρ^0 cells did not contain any fully assembled complex I holoenzyme, as expected; however, when probing against NDUFAF1, we saw a very small subassembly of ~80 kDa, together with a less visible band at ~205 kDa, indicating that the complex I assembly process in these cells lacking mitochondrially encoded subunits, presumably containing only a few nuclear-encoded subunits, is disrupted at an extremely early stage.

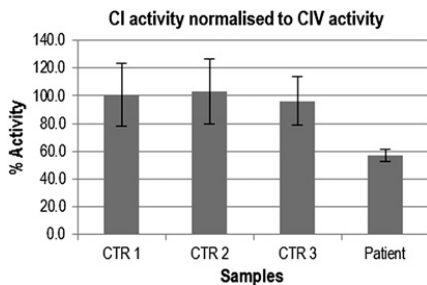


Figure 4 Complex I activity was measured in patient and CTR fibroblasts using the microplate assay kit. All measurements were performed in triplicate and expressed as ratio to complex IV activity assayed with the same method. The residual complex I activity in the patient was ~57% of the CTR mean in cultured skin fibroblasts (compared to 25% of the lowest CTR in skeletal muscle, as measured by spectrophotometric assay; data not shown). CTR, control.

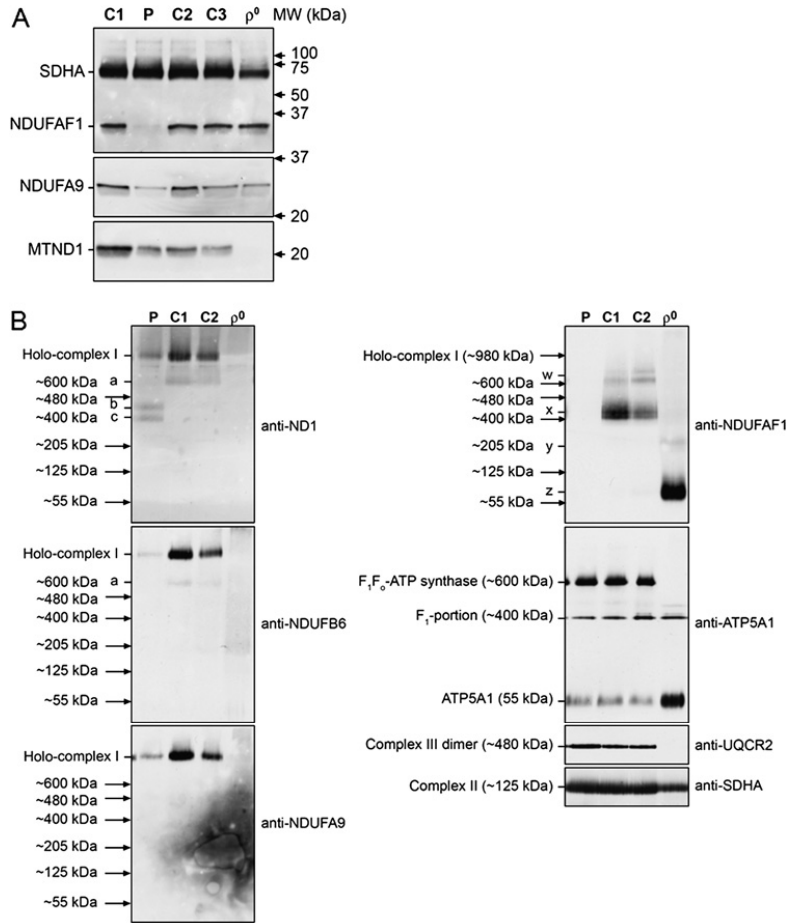
DISCUSSION

We employed a combined biochemical and genetic approach, using BN-PAGE to identify patients accumulating abnormal complex I assembly intermediates in cultured skin fibroblasts, followed by candidate gene sequencing of known complex I assembly factors to identify compound heterozygous missense mutations in *NDUFAF1* as a novel cause of fatal infantile HCM. We observed *NDUFAF1* mutations in one of our cohort of 30 paediatric patients with isolated complex I deficiency associated with heterogeneous clinical phenotypes. The affected patient was a 7-month-old infant who was previously well and developing normally prior to the onset of her cardiac symptoms. The pathogenicity of the *NDUFAF1* mutations is supported by several lines of evidence. The healthy parents were each heterozygous for one of the missense mutations observed in their daughter, and these mutations were not present in 120 control subjects and 1094 individuals genotyped for the 1000 Genomes Project. The affected amino acid residues are highly phylogenetically conserved, from fungi (*Neurospora crassa* and *Yarrowia lipolytica*) to humans in the case of Arg211Cys, and from nematodes to humans in the case of Gly245Arg (figure 3). Finally, functional studies demonstrated a severe reduction in the steady-state levels of NDUFAF1 protein in Western blots of patient fibroblasts, with accumulation of abnormal complex I assembly intermediates on BN-PAGE analysis similar to those seen in the only other patient previously reported to have complex I deficiency caused by *NDUFAF1* mutations.¹³ Our report confirms NDUFAF1 as a bona fide assembly factor of complex I, mutations of which cause isolated complex I deficiency.

Recent x-ray crystallographic studies have demonstrated the complex I holoenzyme to be an L-shaped macromolecule composed of four functional modules: the N module is responsible for NADH oxidation, the Q module is responsible for ubiquinone reduction, and the proximal P_F and distal P_D modules are responsible for proton translocation.^{9–10} Assembly of complex I has been extensively studied in the fungus *N crassa* and in human cells^{11–15–25–26}; these studies, together with the phylogenetic profiling work of Pagliarini *et al*,⁷ have led to the identification of 24 putative complex I assembly factors (supplementary table 1 online). Sixteen of these have already been associated with human disease, including nine complex I deficiency syndromes and one mitochondrial disorder with multiple respiratory chain deficiencies.^{12–18–27–28} Interestingly, mutations in seven of these putative complex I assembly factors have been linked to non-mitochondrial diseases such as peroxisomal disorders, organic acidemias and a ketone body utilisation defect (supplementary table 1 online). It is not clear whether reduced complex I activity may be involved in the pathogenesis of any of these disorders. While the precise

Figure 5 Western blot analysis demonstrated a severe reduction in NDUFAF1 protein levels in P mitoplasts compared to C mitoplasts isolated from fibroblasts; normal staining of SDHA confirmed equal loading of all samples. Levels of ND1 (a core subunit assembled early into the nascent complex I enzyme) were normal, whereas levels of NDUFA9 (a membrane arm subunit that was incorporated later) were reduced in patients. As expected, ρ^0 cells lacked mitochondrially encoded ND1 but had normal levels of all nuclear-encoded proteins analysed (A). BN-PAGE of mitoplasts isolated from P and C fibroblasts and ρ^0 cells. Complex I was detected using antibodies to the ND1, NDUFB6 and NDUFA9 subunits. Levels of the ~980 kDa complex I holoenzyme were severely reduced in P mitoplasts. In contrast, levels of complexes II, III and V, detected with antibodies to SDHA, UQCRC2 and ATP5A1, respectively, were the same in the P and C lanes, confirming equal loading of the samples. The signals of these antibodies were used as molecular weight markers. Abnormal complex I assembly intermediates of ~400 kDa (c) and ~460 kDa (b) were seen to accumulate in the patient—but a physiological subassembly at ~600 kDa (a) present in controls was not seen in the patient—when probing against ND1 (top left). No NDUFAF1 signal could be detected in the P sample (top right), confirming the findings of Western blot analysis. Probing against NDUFAF1 revealed further physiological subassemblies in C cells: a doublet at ~460 kDa (x) and two subassemblies at >600 kDa (w).

These were not observed in P mitoplasts. No fully assembled complex I holoenzyme was observed in ρ^0 cells, as expected; however, when probing against NDUFAF1, we saw a very small subassembly of ~80 kDa (z) and a less visible band at ~205 kDa (y) (B). BN-PAGE, Blue Native polyacrylamide gel electrophoresis. P, patient; C, control.



mechanism of complex I assembly is still debated, a consensus view of a dynamic multidirectional process that includes the possibility of direct subunit exchange into pre-existing mature complex I has recently been proposed.¹¹

NDUFAF1 was initially identified as the human homologue of CIA30, one of the first two complex I assembly factors identified in *N. crassa*,²⁵ and was demonstrated to be a ubiquitously expressed, mitochondrially targeted protein.^{20–21} NDUFAF1 is a protein of 327 amino acids and ~37.7 kDa and contains no predicted transmembrane domains. Ryan *et al.*²⁹ described its N-terminally processed mitochondrial targeting signal, and Dunning *et al.*¹⁵ showed that NDUFAF1 peripherally associates with the matrix face of the mitochondrial inner membrane. A role for NDUFAF1 in complex I assembly is also supported by RNA interference experiments, which showed disrupted complex I assembly in HeLa cells,²¹ and by recent studies of the testicular nuclear receptor (TR4)^{-/-} knockout mouse model.³⁰ TR4 is a member of the nuclear receptor superfamily of transcription factors and appears to regulate complex I activity by binding to hormone response elements in the *NDUFAF1*

promoter sequence. TR4^{-/-} mice had a ragged-red fibre myopathy associated with complex I deficiency and reduced *NDUFAF1* gene expression. Furthermore, lentiviral over-expression of *NDUFAF1* was able to restore complex I activity and ATP generation to control levels in primary fibroblasts from TR4^{-/-} mice.

The precise function of NDUFAF1 remains obscure; this is also true for all currently known complex I assembly factors. NDUFAF1 appears to be involved at an intermediate stage of complex I assembly, in contrast to C20orf7, NDUFAF3 and NDUFAF4, which are needed early in the assembly process, and to NDUFAF2, which has a role in the late stages.¹¹ Tandem affinity purification experiments demonstrated that NDUFAF1 copurifies with two other putative complex I assembly factors, ECSIT and ACAD9.^{26–27} Interestingly, *ACAD9* mutations have recently been reported to cause complex-I-deficient HCM, including a fatal infantile phenotype similar to that of our patient with *NDUFAF1* mutations.^{19,27} Possible functions of the various putative complex I assembly factors/chaperones include iron-sulphur cluster synthesis (eg, NUBPL), translational

Mitochondrial disease

coactivation of complex I subunits (as has been suggested for C20orf7 for ND1) and direction of nuclear-encoded complex I subunits to the correct intramitochondrial compartment (ie, to the matrix side of the enzyme or to the intermembrane space).¹¹

Clinical recognition of mitochondrial heart disease can be difficult in the absence of multisystem features or a clear family history. The presence of lactic acidosis in a patient with heart failure usually reflects inadequate tissue oxygenation and perfusion rather than primary mitochondrial dysfunction, but persistence of lactic acidosis despite adequate ventilatory and circulatory support, as in the present case, should arouse suspicion of an underlying mitochondrial disorder. Echocardiographic features may also be helpful. Metabolic investigations in this infant were pursued because of the ventricular hypertrophy associated with poor systolic function, quite unlike the briskly contracting ventricles in HCM associated with sarcomeric protein abnormalities. There was also increased trabeculation suggestive of, but not definitive for, NCLV. The latter is a rare genetic cardiomyopathy that is characterised by hypertrabeculation of the left ventricle and appears to be an arrest of normal myocardial development.³¹ NCLV is frequently caused by mitochondrial disease, including mtDNA mutations and Barth syndrome.^{32 33}

Mitochondrial cardiomyopathy is clinically and biochemically heterogeneous. Establishing a genetic diagnosis is challenging and achieved in only a minority of cases because of complex genetics, including bigenomic inheritance, and is guided by biochemical findings in biopsied tissue, which may show an isolated deficiency of one respiratory chain enzyme complex (most commonly complex I or complex IV) or a combined defect affecting multiple enzymes. In the case of cardiomyopathy, inaccessibility of the affected tissue poses further difficulties: endomyocardial biopsy has associated risks and does not provide sufficient tissue for conventional assays of mitochondrial respiratory chain function. For this reason, we and others use skeletal muscle for diagnostic purposes, accepting that this potentially lowers the diagnostic success rate since the mitochondrial biochemical defect may be limited to cardiac muscle.⁴ Demonstration of isolated complex I deficiency in the skeletal muscle from our patient led to screening of candidate genes. Complex I deficiency is genetically heterogeneous and may arise from mutations in the 45 structural subunits of the enzyme (including 7 mtDNA-encoded subunits and 38 nuclear-encoded subunits) or in any of the known and putative assembly factors.^{7 12 18 19} We first screened the entire mtDNA in our patient and subsequently performed systematic analysis of candidate nuclear genes previously reported to be associated with mitochondrial cardiomyopathy, eventually leading to the identification of compound heterozygous missense mutations in *NDUFAP1*.

The reported modes of inheritance of mitochondrial heart disease include autosomal recessive (representing the majority), X linked (eg, *NDUFA1* and *TAZ* mutations), maternal (mtDNA point mutations) and sporadic (large-scale mtDNA rearrangements). A precise genetic diagnosis is important to provide parents with accurate prognostic and genetic counselling advice regarding recurrence risks and to guide future reproductive options. In this case, the parents had a successful pregnancy with donor egg in vitro fertilisation, resulting in a healthy child. Although subsequent demonstration of normal mtDNA sequence in the patient's skeletal muscle indicated that maternal inheritance was extremely unlikely, the parents opted for further donor egg in vitro fertilisation procedures, unfortunately without success. Identification of the underlying nuclear gene

mutations allows these parents the option of prenatal or preimplantation genetic diagnosis for future pregnancies.

Cardiac muscle has a high energy requirement. Energy deficiency appears to be a common pathogenic mechanism in HCM: by directly affecting mitochondrial energy production (respiratory chain defects), by altering energy sensing (deficiency of AMP-activated kinase) or by increasing sarcomeric energy utilisation (sarcomeric protein mutations).⁵ However, cardiomyopathy is not an invariant feature of mitochondrial respiratory chain deficiency. For mtDNA-related disease, where mutations are present in multiple copies, this conundrum may be explained by tissue segregation and threshold effects, with a critical mutation load being required for biochemical expression. Other explanations are required for the phenotypic variation in nuclear gene defects causing mitochondrial disease³⁴—for example, cardiomyopathy is not an invariant feature of mitochondrial disease caused by complex I assembly factor defects,¹² suggesting differential importance of the various complex I assembly factors within the heart and possibly additional tissue-specific roles for these molecular chaperones. A relatively high expression of *NDUFAP1* in cardiac tissues supports a specific role for this assembly factor in heart mitochondria.²⁰ In addition, mitochondria play critical roles in intracellular calcium homeostasis, generation of reactive oxygen species (especially at complex I) and control of apoptosis; disruption of these functions is likely to contribute to HCM pathogenesis.

It is interesting to note that our case and the previously reported case with *NDUFAP1* mutations had cardiomyopathy apparently triggered by viral illnesses, at 6 months in our case and at 15 months in the previous case.¹⁵ *NDUFAP1* has recently been implicated in immune pathways, including T cell activation,^{35 36} and we speculate that this may explain why viral infection triggered decompensation and development of HCM in both patients with *NDUFAP1* mutations. In marked contrast to our patient, the previously reported case showed normalised cardiac function, other than recurrent episodes of supraventricular tachycardia related to Wolff–Parkinson–White syndrome.¹⁵ His subsequent clinical course was characterized by multisystem problems, including developmental delay, mild cognitive impairment, cortical visual dysfunction, pigmentary retinopathy, kyphoscoliosis, osteoporosis and pubertal delay, with survival until the age of at least 21 years (age at time of report). Phenotypic heterogeneity is a phenomenon that is increasingly being recognised in nuclear-encoded mitochondrial disorders.^{34 37} Environmental factors, including age at exposure to first metabolic stress, severity of first metabolic stress (ie, viral infection) and autoimmune phenomena,³⁸ may have contributed to the differential severity of the phenotypes in the two *NDUFAP1*-deficient cases. The reasons for the apparent reversal of cardiomyopathy in the case reported by Dunning *et al* are unclear. Improvement of mitochondrial disease symptoms has been reported with mutations in mitochondrial and nuclear genes, although the molecular mechanisms underlying this are not understood at present.^{39 40} The rapidly expanding knowledge of the molecular basis of mitochondrial disease will hopefully lead to a greater understanding of these issues in the future.

Acknowledgements We are extremely grateful to the parents, who gave their consent and full support to this study.

Funding SR is supported by the Great Ormond Street Hospital Children's Charity. This project received grant funding from the Great Ormond Street Hospital/UCL Institute of Child Health Science Development Initiative and was made possible by a British–Italian partnership grant from the British Council.

Competing interests None.

Ethics approval Ethics approval was provided by the Great Ormond Street Hospital/Institute of Child Health research ethics committee.

Contributors EF performed genetic analyses; EF and JW performed functional analyses of the mutant protein; IPH assayed mitochondrial enzymes; NJS collated histological information; MAC and MB collected clinical data; EF and SR cowrote the manuscript; SR devised the study and obtained funding; and all authors reviewed and revised the manuscript.

Provenance and peer review Not commissioned; externally peer reviewed.

REFERENCES

- Wilkinson JD, Landy DC, Colan SD, Towbin JA, Sleeper LA, Orav EJ, Cox GF, Canter CE, Hsu DT, Webber SA, Lipshultz SE. The pediatric cardiomyopathy registry and heart failure: key results from the first 15 years. *Heart Fail Clin* 2010;**6**:401–13, vii.
- Gajarski R, Natfel DC, Pahl E, Alejos J, Pearce FB, Kirkin JK, Zamberlan M, Dipchand AL. Outcomes of pediatric patients with hypertrophic cardiomyopathy listed for transplant. *J Heart Lung Transplant* 2009;**28**:1329–34.
- Watkins H, Ashrafian H, Redwood C. Inherited cardiomyopathies. *N Engl J Med* 2011;**364**:1643–56.
- Bonnet D, de Lonlay P, Gautier I, Rustin P, Rotig A, Kachaner J, Acar P, LeBidois J, Munnich A, Sidi D. Efficiency of metabolic screening in childhood cardiomyopathies. *Eur Heart J* 1998;**19**:790–3.
- Colan SD, Lipshultz SE, Lowe AM, Sleeper LA, Messere J, Cox GF, Lurie PR, Orav EJ, Towbin JA. Epidemiology and cause-specific outcome of hypertrophic cardiomyopathy in children: findings from the Pediatric Cardiomyopathy Registry. *Circulation* 2007;**115**:773–81.
- Rahman S, Hanna MG. Diagnosis and therapy in neuromuscular disorders: diagnosis and new treatments in mitochondrial diseases. *J Neural Neurosurg Psychiatry* 2009;**80**:943–53.
- Pagliarini DJ, Calvo SE, Chang B, Sheth SA, Vafai SB, Ong SE, Walford GA, Sugiana C, Boneh A, Chen VK, Hill DE, Vidal M, Evans JG, Thorburn DR, Carr SA, Mootha VK. A mitochondrial protein compendium elucidates complex I disease biology. *Cell* 2008;**134**:112–23.
- Tucker EJ, Compton AG, Thorburn DR. Recent advances in the genetics of mitochondrial encephalopathies. *Curr Neurol Neurosci Rep* 2010;**10**:277–85.
- Hunte C, Zickermann V, Brandt U. Functional modules and structural basis of conformational coupling in mitochondrial complex I. *Science* 2010;**329**:448–51.
- Eftremov RG, Baradaran R, Sazanov LA. The architecture of respiratory complex I. *Nature* 2010;**465**:441–5.
- McKenzie M, Ryan MT. Assembly factors of human mitochondrial complex I and their defects in disease. *IUBMB Life* 2010;**62**:497–502.
- Fassone E, Duncan AJ, Taanman JW, Pagnamenta AT, Sadowski MI, Holand T, Qasim W, Rutland P, Calvo SE, Mootha VK, Bitner-Grindzicz M, Rahman S. FOXRED1, encoding an FAD-dependent oxidoreductase complex-I-specific molecular chaperone, is mutated in infantile-onset mitochondrial encephalopathy. *Hum Mol Genet* 2010;**19**:4837–47.
- Dunning CJ, McKenzie M, Sugiana C, Lazarou M, Silke J, Connelly A, Fletcher JM, Kirby DM, Thorburn DR, Ryan MT. Human CIA30 is involved in the early assembly of mitochondrial complex I and mutations in its gene cause disease. *EMBO J* 2007;**26**:3227–37.
- Ogilvie I, Kennaway NG, Shoubridge EA. A molecular chaperone for mitochondrial complex I assembly is mutated in a progressive encephalopathy. *J Clin Invest* 2005;**115**:2784–92.
- Saada A, Vogel RO, Hoefs SJ, van den Brand MA, Wessels HJ, Willems PH, Venselaar H, Shaag A, Barghuti F, Reish O, Shohat M, Huynen MA, Smeitink JA, van den Heuvel LP, Nijtmans LG. Mutations in NDUFAF3 (C3ORF60), encoding an NDUFAF4 (C6ORF66)-interacting complex I assembly protein, cause fatal neonatal mitochondrial disease. *Am J Hum Genet* 2009;**84**:718–27.
- Saada A, Edwardson S, Rapoport M, Shaag A, Amry K, Miller C, Lorberbaum-Galski H, Elpeleg O. C6ORF66 is an assembly factor of mitochondrial complex I. *Am J Hum Genet* 2008;**82**:32–8.
- Sugiana C, Pagliarini DJ, McKenzie M, Kirby DM, Salemi R, bu-Amero KK, Dahl HH, Hutchison WM, Vascotto KA, Smith SM, Newbold RF, Christodoulou J, Calvo S, Mootha VK, Ryan MT, Thorburn DR. Mutation of C20orf7 disrupts complex I assembly and causes lethal neonatal mitochondrial disease. *Am J Hum Genet* 2008;**83**:468–78.
- Calvo SE, Tucker EJ, Compton AG, Kirby DM, Crawford G, Burt NP, Rivas M, Guiducci C, Bruno DL, Goldberger OA, Redman MC, Wilshire E, Wilson CJ, Altschuler D, Gabriel SB, Daly MJ, Thorburn DR, Mootha VK. High-throughput, pooled sequencing identifies mutations in NUBPL and FOXRED1 in human complex I deficiency. *Nat Genet* 2010;**42**:851–8.
- Haack TB, Danhauser K, Haberberger B, Hoser J, Strecker V, Boehm D, Uziel G, Lamantea E, Invernizzi F, Poulton J, Rolinski B, Iuso A, Biskup S, Schmidt T, Mewes HW, Wittig I, Meitinger T, Zeviani M, Prokisch H. Exome sequencing identifies ACAD9 mutations as a cause of complex I deficiency. *Nat Genet* 2010;**42**:1131–4.
- Janssen R, Smeitink J, Smeets R, van Den HL. CIA30 complex I assembly factor: a candidate for human complex I deficiency? *Hum Genet* 2002;**110**:264–70.
- Vogel RO, Janssen RJ, Ugalde C, Grovenstein M, Huijbens RJ, Visch HJ, van den Heuvel LP, Willems PH, Zeviani M, Smeitink JA, Nijtmans LG. Human mitochondrial complex I assembly is mediated by NDUFAF1. *FEBS J* 2005;**272**:5317–26.
- King MP, Attardi G. Human cells lacking mtDNA: repopulation with exogenous mitochondria by complementation. *Science* 1989;**246**:500–3.
- Williams SL, Valnot I, Rustin P, Taanman JW. Cytochrome c oxidase subassemblies in fibroblast cultures from patients carrying mutations in COX10, SCO1, or SURF1. *J Biol Chem* 2004;**279**:7462–9.
- Schagger H, Bentlage H, Ruitenbeek W, Pfeiffer K, Rotter S, Rother C, Bottcher-Purkl A, Lodemann E. Electrophoretic separation of multiprotein complexes from blood platelets and cell lines: technique for the analysis of diseases with defects in oxidative phosphorylation. *Electrophoresis* 1996;**17**:709–14.
- Kuffner R, Rohr A, Schmiede A, Krull C, Schulte U. Involvement of two novel chaperones in the assembly of mitochondrial NADH:ubiquinone oxidoreductase (complex I). *J Mol Biol* 1998;**283**:409–17.
- Vogel RO, Janssen RJ, van den Brand MA, Dieteren CE, Verkaart S, Koopman WJ, Willems PH, Pluk W, van den Heuvel LP, Smeitink JA, Nijtmans LG. Cytosolic signaling protein Escit also localizes to mitochondria where it interacts with chaperone NDUFAF1 and functions in complex I assembly. *Genes Dev* 2007;**21**:615–24.
- Nouws J, Nijtmans L, Houten SM, van den Brand M, Huynen M, Venselaar H, Hoefs S, Gloerich J, Kronick J, Hutchin T, Willems P, Rodenburg R, Wanders R, van den Heuvel L, Smeitink J, Vogel RO. Acyl-CoA dehydrogenase 9 is required for the biogenesis of oxidative phosphorylation complex I. *Cell Metab* 2010;**12**:283–94.
- Ghezzi D, Sevrioukova I, Invernizzi F, Lamperti C, Mora M, D'Adamo P, Novara F, Zuffardi O, Uziel G, Zeviani M. Severe X-linked mitochondrial encephalomyopathy associated with a mutation in apoptosis-inducing factor. *Am J Hum Genet* 2010;**86**:639–49.
- Ryan MT, Voos W, Pfanner N. Assaying protein import into mitochondria. *Methods Cell Biol* 2001;**65**:189–215.
- Liu S, Lee YF, Chou S, Uno H, Li G, Brookes P, Massett MP, Wu Q, Chen LM, Chang C. Mice lacking TR4 nuclear receptor develop mitochondrial myopathy with deficiency in complex I. *Mol Endocrinol* 2011;**25**:1301–10.
- Captur G, Nihoyannopoulos P. Left ventricular non-compaction: genetic heterogeneity, diagnosis and clinical course. *Int J Cardiol* 2010;**140**:145–53.
- Tang S, Batra A, Zhang Y, Ebenroth ES, Huang T. Left ventricular noncompaction is associated with mutations in the mitochondrial genome. *Mitochondrion* 2010;**10**:350–7.
- Bleyl SB, Mumford BR, Thompson V, Carey JC, Psyher TJ, Chin TK, Ward K. Neonatal, lethal noncompaction of the left ventricular myocardium is allelic with Barth syndrome. *Am J Hum Genet* 1997;**61**:868–72.
- Pagnamenta AT, Hargreaves IP, Duncan AJ, Taanman JW, Heales SJ, Land JM, Bitner-Grindzicz M, Leonard JV, Rahman S. Phenotypic variability of mitochondrial disease caused by a nuclear mutation in complex II. *Mol Genet Metab* 2006;**89**:214–21.
- Kaminski MM, Sauer SW, Klemke CD, Suss D, Okun JG, Krammer PH, Gulow K. Mitochondrial reactive oxygen species control T cell activation by regulating IL-2 and IL-4 expression: mechanism of ciprofloxacin-mediated immunosuppression. *J Immunol* 2010;**184**:4827–41.
- West AP, Brodsky IE, Rahner C, Woo DK, Erdjument-Bromage H, Tempst P, Walsh MC, Choi Y, Shadel GS, Ghosh S. TLR signalling augments macrophage bactericidal activity through mitochondrial ROS. *Nature* 2011;**472**:476–80.
- Smeitink JA, Elpeleg O, Antonika H, Diepstra H, Saada A, Smits P, Sasarman F, Vriend G, Jacob-Hirsch J, Shaag A, Rechavi G, Welling B, Horst J, Rodenburg RJ, van den Heuvel B, Shoubridge EA. Distinct clinical phenotypes associated with a mutation in the mitochondrial translation elongation factor EFTs. *Am J Hum Genet* 2006;**79**:869–77.
- Ono H, Nakamura H, Matsuzaki M. A NADH dehydrogenase ubiquinone flavoprotein is decreased in patients with dilated cardiomyopathy. *Intern Med* 2010;**49**:2039–42.
- Horvath R, Kemp JP, Tuppen HA, Hudson G, Oldfors A, Marie SK, Moslemi AR, Servidei S, Holme E, Shanske S, Kollberg G, Jayakar P, Pyle A, Marks HM, Holinski-Feder E, Scavina M, Walter MC, Coku J, Gunther-Scholz A, Smith PM, McFarland R, Chrzanoska-Lightowlers ZM, Lightowlers RN, Hirano M, Lochmuller H, Taylor RW, Chinnery PF, Tulinius M, DiMauro S. Molecular basis of infantile reversible cytochrome c oxidase deficiency myopathy. *Brain* 2009;**132**:3165–74.
- Zeharia A, Shaag A, Pappo O, Mager-Heckel AM, Saada A, Benat M, Karicheva O, Mandel H, Ofek N, Segel R, Marom D, Rotig A, Tarassov I, Elpeleg O. Acute infantile liver failure due to mutations in the TRMU gene. *Am J Hum Genet* 2009;**85**:401–7.



Mutations in the mitochondrial complex I assembly factor NDUFAF1 cause fatal infantile hypertrophic cardiomyopathy

Elisa Fassone, Jan-Willem Taanman, Iain P Hargreaves, et al.

J Med Genet 2011 48: 691-697

doi: 10.1136/jmedgenet-2011-100340

Updated information and services can be found at:

<http://jmg.bmj.com/content/48/10/691.full.html>

These include:

References

This article cites 40 articles, 11 of which can be accessed free at:

<http://jmg.bmj.com/content/48/10/691.full.html#ref-list-1>

Email alerting service

Receive free email alerts when new articles cite this article. Sign up in the box at the top right corner of the online article.

Topic Collections

Articles on similar topics can be found in the following collections

[Cardiomyopathy](#) (69 articles)
[Genetic screening / counselling](#) (688 articles)
[Immunology \(including allergy\)](#) (476 articles)
[Metabolic disorders](#) (268 articles)
[Molecular genetics](#) (1043 articles)
[Muscle disease](#) (115 articles)
[Neuromuscular disease](#) (210 articles)

Notes

To request permissions go to:

<http://group.bmj.com/group/rights-licensing/permissions>

To order reprints go to:

<http://journals.bmj.com/cgi/reprintform>

To subscribe to BMJ go to:

<http://group.bmj.com/subscribe/>